SISSA
Scuola
Internazionale
Superiore di
Studi Avanzati

Neuroscience Area – PhD course in

Molecular Biology

Distinct tau fibril types and their role in prion diseases

Candidate:

Luigi Celauro

Advisor:

Prof. Giuseppe Legname

Academic Year 2021-22

ABSTRACT

Neurodegenerative diseases are often characterized by the co-deposition of different amyloidogenic proteins, normally defining distinct proteinopathies.

An interesting example is represented by prion diseases, in which the presence of PrPSc plaques is often accompanied by aggregates of the tau protein, normally implicated in another class of diseases called tauopathies. How this copresence of amyloidogenic proteins can influence the progression of prion disease is still a matter of debate.

Recently, the cellular form of the prion protein, PrP^{C}, has been investigated as a possible receptor of amyloidogenic proteins, since its binding activity with Aβ, tau and α-synuclein has been proved and it has been linked to several neurotoxic behaviours exerted by these proteins.

In our previous paper we showed that PrP^{C} acts as a receptor for tau K18 amyloid fibrils and that the exposure of cultured cells to these fibrils causes an increased PrP^{C} retention at the plasma membrane. Interestingly, tau K18 fibril administration reduced PrP^{Sc} levels in chronically prion-infected cells, probably by an impairment of PrP^{C} conversion due to the fibril binding.

To deepen this aspect, we decided to exploit, together with tau K18, also another construct of tau containing the sequence forming the core of Alzheimer's disease tau filaments *in vivo*. Our results suggest that, despite differing for six amino acids only, these two constructs form different tau fibril types *in vitro*. However, their effect on PrP^{Sc} reduction was comparable and probably based on the binding to PrP^{C} at the plasma membrane, inhibiting the conversion event. Moreover, both amyloid fibrils were able to hinder the earlier phases of prion infection, slowing down prion replication and making cells less prone to be infected.

Our results suggest PrP^{C} as a receptor for different tau fibril types and point out a role of tau amyloid fibrils in preventing the prion conversion event at the base of the pathology. These findings may help disentangle the mutual relationship between amyloidogenic proteins that often show co-deposition.

LIST OF ABBREVIATIONS

2-D: two-dimensional
3-D: three-dimensional
3-MA: 3-methyladenine
AD: Alzheimer's disease
AGD: argyrophilic grain disease
APP: amyloid precursor protein
ARTAG: aging-related tau astrogliopathy
Aβ: amyloid β
BCA: bicinchoninic acid assay
BSE: bovine spongiform encephalopathy
CBD: corticobasal degeneration
CIE: clathrin-independent endocytosis
CJD: Creutzfeldt-Jakob disease
CME: clathrin-mediated endocytosis
CNS: central nervous system
CSF: cerebrospinal fluid
CWD: chronic wasting disease
DLB: dementia with Lewy bodies
EEG: electroencephalogram
ESCRT: endosomal sorting complex required for transport
FBD: familial British dementia
fCJD: familial Creutzfeldt-Jakob disease
FDD: familial Danish dementia
FFI: fatal familial insomnia
FTD: frontotemporal dementia
FTLD-tau: frontotemporal lobar degeneration-tau
GAG: glycosaminoglycan
GGT: globular glial tauopathy
GPI: glycosylphosphatidylinositol
GPT: GGT-PSP-Tau fold
GSS: Gerstmann-Sträussler-Scheinker
HS: heparan sulfate
HSPGs: heparan sulfate proteoglycans
ILVs: intraluminal vesicles
KO: knockout
LBs: Lewy bodies
LR: laminin receptor
LRP: laminin receptor precursor
LRP1: low-density lipoprotein receptor-related protein 1
LTD: long-term depression
LTP: long-term potentiation
MAP: microtubule associated protein
MBDs: microtubule binding domains
MCI: mild cognitive impairment
MEM: minimal essential medium
MRI: magnetic resonance imaging

MSA: multiple system atrophy
MTT: 3-(4,5-dimethylthiazol-2-yl)-2,5-diphenyltetrazolium bromide
MVBs: multivesicular bodies
NFT: neurofibrillary tangle
PART: primary age-related tauopathy
PCR: polymerase chain reaction
PD: Parkinson's disease
PFA: paraformaldehyde
PHFs: paired helical filaments
PI3K: phosphoinositide 3-kinase
PiD: Pick's disease
PK: proteinase K
PNS: peripheral nervous system
PSP: progressive supranuclear palsy
PSWC: pseudoperiodic sharp wave complexes
RF-cloning: restriction-free cloning
RT-QuIC: real-time quaking-induced conversion
sCJD: sporadic Creutzfeldt-Jakob disease
SDS-PAGE: sodium dodecyl sulphate-polyacrylamide gel electrophoresis
SEC: size-exclusion chromatography
SFs: straight filaments
TEM: transmission electron microscopy
ThT: thioflavin T
TME: transmissible mink encephalopathy
TNTs: tunnelling nanotubes
vCJD: variant Creutzfeldt-Jakob disease
VPS: vacuolar protein sorting
WB: western blot

TABLE OF CONTENTS

ABSTRACT 2

LIST OF ABBREVIATIONS 3

INTRODUCTION 8

1.1. Neurodegenerative diseases 8

1.2. Prions and prion-like diseases 8

1.3. Human prion diseases 10
1.3.1. Sporadic prion diseases 12
1.3.2. Genetic prion diseases 12
1.3.3. Acquired prion diseases 13
1.3.4. Diagnosis 14
1.3.5. Prion strains 15

1.4. Cellular prion protein 17
1.4.1. PrP^{C} expression and functions 18
1.4.2. PrP^{C} as amyloid receptor 18
1.4.2.1. PrP^{C} as PrP^{Sc} receptor 18
1.4.2.2. PrP^{C} as Aβ receptor 19
1.4.2.3. PrP^{C} as tau receptor 19
1.4.2.4. PrP^{C} as α-synuclein receptor 20
1.4.3. PrP^{C} intracellular trafficking 21
1.4.4. PrP^{C} intercellular trafficking 22
1.4.5. PrP^{C} to PrP^{Sc} conversion 23
1.4.6. PrP^{Sc} intracellular trafficking 23
1.4.7. PrP^{Sc} intercellular trafficking 24

1.5. Tauopathies 26
1.5.1. 3R tauopathies 28
1.5.1.1. Pick's disease 28
1.5.2. 4R tauopathies 28
1.5.2.1. Progressive supranuclear palsy 28
1.5.2.2. Corticobasal degeneration 28
1.5.2.3. Globular glial tauopathy 29
1.5.2.4. Argyrophilic grain disease 29
1.5.3. Mixed tauopathies: 4R+3R 29
1.5.3.1. Primary age-related tauopathy 29
1.5.3.2. Alzheimer's disease 30

1.6. Tau Protein 32
1.6.1. Tau expression and structure 32

1.6.2. Tau functions 34
1.6.3. Tau in pathologies 35
1.6.4. Tau aggregation and toxic species 36
1.6.5. Tau spreading 39
1.6.6. Tau strains 42

1.7. Prion diseases and tau pathology 44

AIM OF THE RESEARCH 46

MATERIALS AND METHODS 47

2.1. Tau 244-378 cloning 47

2.2. Tau expression and purification 48

2.3. Fibrillization of tau proteins 49

2.4. Transmission electron microscopy (TEM) analysis 49

2.5. Cell cultures 49

2.6. Tau K18 fluorophore-labelled fibrils 50

2.7. Tau fibril treatments 50

2.8. Analysis of internalized tau amyloids 50

2.9. Metabolic cell activity and cell count 51

2.10. ScN2a treatments 51

2.11. Western blotting 51

2.12. Proteinase K digestion 52

2.13. Immunofluorescence 52

2.14. *De novo* prion infection 53

RESULTS 54

3.1. Production and *in vitro* fibrillization of tau 244-378 54

3.2. Tau fibril effect on PrP^{Sc} 59

3.3. Tau fibril localization 62

3.4. Tau fibrils do not reduce PrP^{Sc} levels by entering cells 66

3.5. Tau fibrils hinder prion *de novo* infection 70

DISCUSSION AND CONCLUSIONS.....73

REFERENCES.....78

INTRODUCTION

1.1. Neurodegenerative diseases

According to the 2020 World Population ageing report of United Nations, “the world continues to experience an unprecedented and sustained change in the age structure of the global population, driven by increasing levels of life expectancy and decreasing levels of fertility”. In 2020, individuals 65 years of age or older were 727 million, with women representing the major part. This number is expected to more than double in 2050 worldwide, reaching 1.5 billion, with a share of the population of 16% and with all regions equally contributing [1].

Around 50 million people suffer from dementia worldwide and this number is predicted to increase up to 150 million by 2050 [2], together with the enormous social and economic cost linked to these pathologies. In 2020, the estimated global cost of dementia was 1.3 trillion US dollars and it is expected to more than double by 2050 [3].

Neurodegenerative diseases are a group of pathologies characterized by the reduction in the functionality of specific subsets of neurons and resulting in the degeneration of these cells and in the symptoms typical of these illnesses such as memory loss, speech impairments, movement problems and others. A common feature of so different pathologies is the aggregation and the deposition of normally soluble proteins that start becoming insoluble, enriched in beta sheets and that accumulate as fibers called “amyloid”. Protein aggregates are found either intracellularly or in the extracellular space of the central nervous system (CNS) cells and their deposition occurs in a disease- and protein-specific way. Differences in cells that accumulate amyloids and in cells that degenerate might be explained by seeing the accumulation of amyloids as the end point of a cascade, with the earlier stages more linked to the pathogenesis. The most peculiar neurodegenerative disease is prion disease, with unique features that, over the years, have attracted the attention of scientific and health authorities. Others neurodegenerative diseases sharing with prion diseases some clinical features have been termed as “prion-like”.

1.2. Prions and prion-like diseases

Prion diseases are characterized by the structural conversion of the cellular form of the prion protein, PrP^{C}, into the disease-causing form, PrP^{Sc} [4]. The misfolding event triggering this

conversion may result from the direct contact between PrP^C and the pathogenic PrP^{Sc}, which induces the native PrP^C to misfold in a process known as "templated conformation change" or "seeding" [5]. This induced conformational change has classified prion diseases as "infectious", meaning that the spontaneous transmission between individuals has happened outside of an experimental setting, despite most of the cases occur with unknown reason from the wild-type protein or through mutations in PrP^C sequence.

Other diseases, termed "prion-like", share with prions the induced conformational change that leads to the propagation of protein misfolding and to the cell-to-cell spreading of pathological proteins in specific anatomic regions. These diseases are classified as "not infectious", as the transmission between individuals has never been proved. According to the type of protein mainly found aggregated in the CNS of the patient, prion-like pathologies are classified as tauopathies, such as progressive supranuclear palsy (PSP), corticobasal degeneration (CBD) and others; α-synucleinopathies including Parkinson's disease (PD), dementia with Lewy bodies (DLB) and multiple system atrophy (MSA); TDP-43 proteinopathies; FUS/FET proteinopathies; trinucleotide repeat diseases and others. Alzheimer's disease (AD) is usually considered separately, as it shows both Amyloid β (Aβ) and tau accumulation [6].

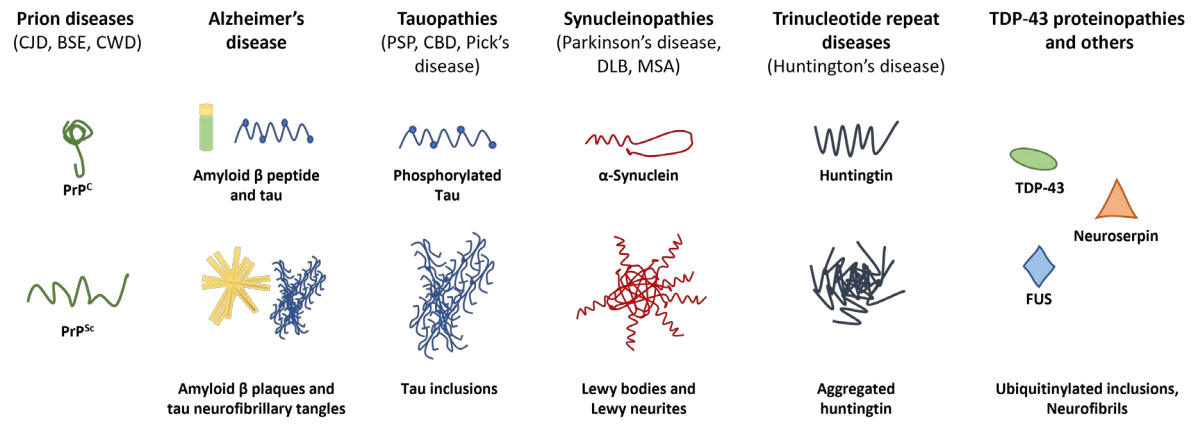

Figure 1. Prion and prion-like diseases. Schematic representation of the misfolded proteins and of the protein aggregates involved in the most common neurodegenerative diseases.

Especially in the aging brain, these proteinopathies show frequently co-occurrence with different combinations, making the classification harder.

Except for trinucleotide repeat diseases, arising from mutations causing the abnormal expansion of repetitive sequences, the sporadic cases of the other pathologies involve the wild-type proteins and, rarely, pathogenic missense or splicing mutations [5].

Even though associated with the same protein deposition, these diseases exhibit very different phenotypes and the age of onset, the cognitive decline, the location and extent of protein aggregates may vary significantly, even among individuals affected by the same pathology.

The mechanisms underlying the initial conversion of the normal soluble proteins into insoluble filamentous aggregates remain unknown.

For most of the aggregated proteins involved in these pathologies, the same templated conformation change, described originally for prions, has been documented. In the case of prion diseases, several factors can generate a peculiar PrP^{Sc}, which is able to imprint its unique conformation to the PrP^{C} molecules, thus generating distinct diseases propagating in individuals [7,8]. These unique conformations, or "strains", have been reported also for Aβ [9-11], tau [12-14] and α-synuclein [15-18], and they may provide an explanation for the existence of different tauopathies and synucleinopathies, that, even though showing the accumulation of the same protein, differ in the clinical symptoms, brain-region affected and cell types targeted.

In the case of prions, their propagation is linked to the transfer from an infected cell to a naïve one, suggesting that PrP^{Sc} can spread through connected cells or that it can be released in the extracellular environment and taken up by nearby cells. The intracerebral injection of brain extracts from AD patients induced the accumulation of Aβ deposits in mice [19], while Frost and colleagues demonstrated that tau fibrils added to the culture medium are taken up by cells and induce the fibrillization of endogenous cytoplasmic tau [20]. Moreover, healthy neurons transplanted into PD patients developed, years later, Lewy bodies (LBs) positive for α-synuclein, suggesting that the pathogenic form, in the host brain, induced the aggregation of the normal protein in the transplanted cells [21,22].

1.3. Human prion diseases

Prion diseases are a heterogeneous group of fatal and infectious pathologies that afflict mammals and cause neurodegeneration. Creutzfeldt-Jakob disease (CJD), Gerstmann-Sträussler-Scheinker syndrome (GSS) and fatal familial insomnia (FFI) characterize humans, but other examples of mammals' prion diseases are represented by scrapie in sheep, bovine spongiform encephalopathy (BSE) in cattle and chronic wasting disease (CWD) in cervids. Their unique features are linked to the ability of these diseases to be inherited, to be infectious or to arise spontaneously. In fact, the majority of prion diseases are classified as

sporadic and account for 85% of all the cases, while some forms are genetic (15%) and less than 1% are acquired [23]. Among the clinical symptoms there are dementia, insomnia, deviant behaviour, ataxia and paraplegia [24], while neuropathologically, poor or extensive atrophy and neuronal loss, vacuolation and spongiform changes, astrocytic gliosis and prion protein amyloid plaques deposition, the latter representing the only diagnostic marker [25]. The agent responsible for these diseases are prions, infectious proteins derived from the structural conversion of the cellular prion protein (PrP^{C}) to the disease-causing scrapie isoform (PrP^{Sc}) [4].

The first case of human prion diseases was reported in 1920 by Hans Creutzfeldt, who described in a patient "a peculiar focal illness of the central nervous system" [26]. The following year, Alfons Maria Jakob, neuropathologist in Hamburg, described other cases of patients who had developed loss of memory, behavioural changes, speech, and motor defects [27,28]. However, in the end, only two out of five cases described by Jakob met the criteria for the current diagnosis of prion diseases, and not even the Creutzfeldt's one. In 1957, another degenerative disease, kuru, was described by Daniel Carleton Gajdusek among natives of New Guinea [29,30] and, years later, it was linked to the consumption of the relatives' brains for ritualistic purposes. The experiments demonstrating the transmission of kuru to chimpanzees [31-33] won a Nobel Prize for Gajdusek in 1976 and, without any doubt, proved the infectious nature of this disease. In 1982, Stanley B. Prusiner coined the term "prion", standing for "proteinaceous infectious particle", to describe the protein-containing infectious agent responsible for prion disease [34] and, in 1997, won the Nobel Prize for his studies. Prusiner and his group supported the prion hypothesis by isolating the infectious protein particle from infected animals and inactivating it by methods known to disrupt proteins [35,36].

As mentioned before, in humans, around 85% of all cases are sporadic CJD (sCJD), in which the conversion of PrP^{C} to PrP^{Sc} is considered to occur spontaneously. From 10% to 15% of all cases are genetic (familial mostly) and linked to mutations in the gene encoding for the prion protein, *PRNP,* making it more prone to change conformation into PrP^{Sc}. The less frequent and most known cases are acquired, in which PrP^{Sc} is transmitted to an individual causing his/her endogenous PrP^{C} to misfold.

1.3.1. Sporadic prion diseases

Sporadic prion diseases include sCJD and the recently identified variably protease-sensitive prionopathy, characterized by the presence of an insoluble PrP, more sensitive to protease digestion than normal prion diseases [37].

The usual onset of sCJD is between 55 and 75 years of age with around 85% of the patients dying within 1 year [38]. First developed symptoms are cognitive, and they vary among cases including altered sleep, vertigo, headache, and behavioural changes together with aphasia, apraxia, and visual disturbances [39]. The progression is rapid with the development of myoclonus, consisting in the involuntary and irregular twitching of muscles. Neuropathologically, neuronal loss, gliosis and vacuolation in the cell body are observed and the deposition of PrP^{Sc} may be revealed by immunocytochemistry and proteinase K (PK) digestion followed by Western Blot (WB) analysis [40]. The diagnosis is usually performed with magnetic resonance imaging (MRI) and electroencephalogram (EEG). Cerebrospinal fluid (CSF) analysis may detect the presence of 14-3-3 neural protein, normally released after rapid neuronal loss. To date, none of these methods is considered to be completely specific [41]. Interestingly, the rate of homozygosity of polymorphism at codon 129 of human *PRNP* gene, resulting in the substitution of valine with methionine, is higher in sCJD patients, suggesting this as a factor predisposing to the development of the disease [42].

1.3.2. Genetic prion diseases

Genetic prion diseases are usually divided in three subcategories: familial Creutzfeldt-Jakob disease (fCJD), GSS and FFI, all associated to mutations in the *PRNP* gene encoding for the prion protein. There are now at least 40 different known mutations in the PrP encoding gene, causing alterations in the number of repeats in the N-terminal portion of PrP and point mutations in the C-terminus [43]. Four point mutations at codons 102, 178, 200 and 210 and insertions of five or six octapeptide repeats account for 95% of the cases [41]. All these factors are thought to make the cellular prion protein, PrP^{C}, more prone to convert into PrP^{Sc} [40]. fCJD is typically presented as a progressive dementia, with an earlier age of onset and protracted clinical course than sCJD, and characterized by ataxia and other motor symptoms, typically manifested between 30 and 55 years of age. Several other mutations result in different phenotypes and in the use of distinct names. GSS is usually a slow progressive disease arising at the age of 50, albeit earlier onset cases have been reported [44]. Many PrP^{Sc}-positive deposits are found throughout the brain and also cases of neurofibrillary tangles presence, typical of

Alzheimer's disease, have been reported [45]. Fatal familial insomnia is a very rare prion disease usually manifested at 40 years of age and characterized by a long-lasting insomnia followed by motor and cognitive symptoms [23]. The neuronal loss usually occurs within the thalamus. FFI was originally associated to a mutation at codon 178, found later also in familial Creutzfeldt-Jakob disease; this mutation, together with the polymorphism at codon 129, might produce two altered conformations of the prion protein and two distinct disease phenotypes [46].

1.3.3. Acquired prion diseases

The acquired forms of prion diseases usually derive from the accidental transmission of PrP^{Sc}, which causes the endogenous PrP^{C} to misfold and to trigger the disease.

As mentioned before, Kuru was the first acquired prion disease identified and linked to the endocannibalism practice, now almost totally eradicated.

Variant Creutzfeldt-Jakob disease (vCJD) is the only known prion disease able to be transmitted directly from animals, affected by BSE, to humans. It is thought that BSE epidemics, also known as "mad cow disease", raised especially in United Kingdom due to the practice of feeding sheep products, some of which contaminated with prions, to cattle. Some of the food products, derived from the infected cattle, were consumed by humans who developed the disease, that had its peak in 1992-1993 [23]. This pathology is characterized by the onset of psychiatric symptoms, preceding by months the canonical neurological ones, and by an earlier age of onset and a longer disease duration [47]. Almost all reported cases so far are homozygous for methionine at codon 129 of *PRNP* gene. Moreover, this form of prion diseases differs from the others for the presence of PrP^{Sc}, not only in the CNS, but also in the lymphoreticular system, maybe because acquired through oral or blood product exposure [23]. Some cases of vCJD, acquired from blood transfusion, were also reported in UK [48].

Prions were reported also to be transmitted iatrogenically, through infected corneal transplants, human growth hormone extracted from cadavers, dura mater transplants and contaminated neurosurgical instruments, albeit their incidence has now declined since the introduction of recombinant human growth hormone, synthetic dura mater grafts and appropriate sterilizing procedures [23]. The homozygosity at codon 129 seems to predispose to iatrogenic CJD [49]. Interestingly, Aβ accumulation was also found in the brain of patients who died for iatrogenic prion disease caused by the exposure to infected human growth hormone;

whether this effect is linked to Aβ transmission or to its synthesis and accumulation triggered by prion pathogenesis needs to be clarified [50,51].

1.3.4. Diagnosis

Diagnosis of prion diseases is performed through clinical and molecular methods.

EEG analysis was largely used for the detection of periodic or pseudoperiodic sharp wave complexes (PSWC) in the advanced stages of the disease, but its reliability has been questioned for being able to detect only some subtypes of the pathology [52].

MRI signal abnormalities are another important tool in the detection of prion diseases, also before the onset of clinical symptoms. These alterations become usually more extensive with the progression of the disease, evidencing dilatation of ventricles and cortical thinning [38].

Cerebrospinal fluid (CSF) analysis, to detect markers linked to brain injury, may help in the diagnosis. However, the detection of one of these proteins, 14-3-3, may result ambiguous due to the release of high amount of this neural protein in the CSF also in non-prion related disorders [53]. Total tau protein content is also used as a CSF marker for prion diseases, showing high specificity especially when combined with the 14-3-3 test [54,55], although concerns have emerged regarding sample preparation and it is thought that MRI analysis should always support the interpretation of the results [56].

In 2010, a new technique for the *in vitro* detection of a very small amount of PrP^{Sc}, called real-time quaking-induced conversion (RT-QuIC), has been developed [57]. This assay uses recombinant PrP as substrate, seeded with the PrP^{Sc} present in the specimen, and intermittent cycles of shaking, that favour the conversion of the substrate into PrP^{Sc}. The conversion event is monitored by the fluorescence emission of the Thioflavin T (ThT), a specific dye that binds to the forming β-sheets [57]. This test revealed a sensitivity greater than 80% and 100% specificity, albeit in a small group of cases [57].

The sequencing of the gene encoding for PrP, *PRNP*, is usually performed to exclude prion diseases caused by genetic mutations. Moreover, methionine homozygosity at codon 129 constitutes a risk factor for the development of prion diseases, being overrepresented in sCJD and vCJD patients [53,58,59]. Finally, insertions/deletions of repeats in the octapeptide region are considered pathogenic, because of the increase in the formation of protease resistant PrP [55].

The two isoforms of PrP, PrP^{C} and PrP^{Sc}, share the same identical aminoacidic sequences, but the conformational change of the secondary structure makes PrP^{Sc} richer in β-sheets and partially resistant to proteolysis. Consequently, PrP^{C} is completely digested upon PK

treatment, while PrP^{Sc} proteolysis results in the removal of the N-terminal amino acids and in the appearance of the distinct bands corresponding to the di-, mono- and un-glycosylated forms of PrP^{Sc} in WB.

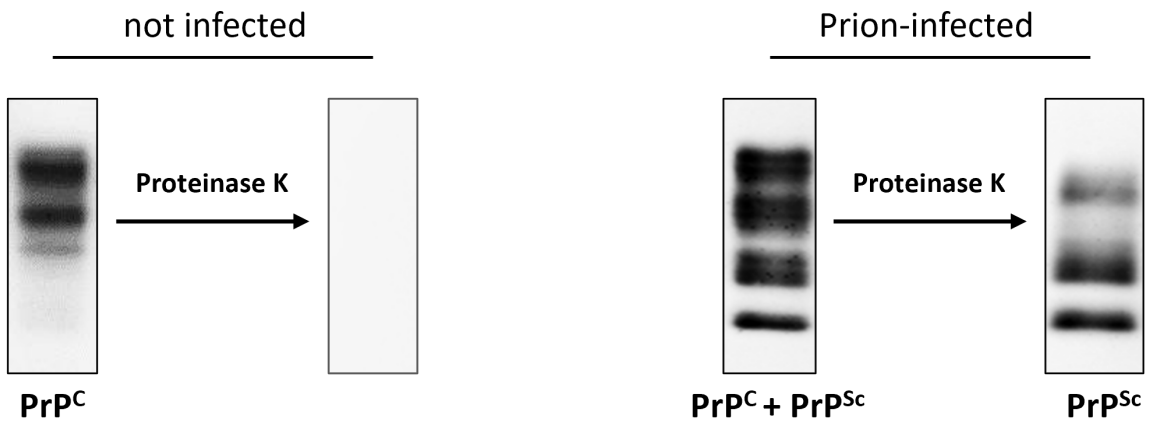

Figure 2. WB banding pattern of not infected and prion-infected samples. In not infected samples (left panel), proteinase K completely digests PrP^{C} resulting in no signal coming from the membrane after the incubation with anti-PrP antibody. In prion-infected samples (right panel), both PrP^{C} and PrP^{Sc} are present, and the digestion with proteinase K results in the appearance of three bands corresponding to the PK-resistant core of PrP^{Sc}.

Size, mobility and abundance of bands are used to distinguish different PrP^{Sc} associated to specific diseases [53].

Finally, immunohistochemistry is used to localize and to reveal the morphology of PrP^{Sc} deposits in different regions of the brain.

The two methods mentioned above, together with the genetic screening, represent to date the only tools for a definitive diagnosis of prion diseases [55].

1.3.5. Prion strains

Prions are characterized by the existence of "strains", described as infectious particles that, when transmitted to identical hosts, produce distinct prion disease phenotypes, including incubation times, specific neuronal target, and lesion profiles [60]. Usually, the existence of strains is linked to differences in the nucleic acid of pathogens, but in the case of PrP^{Sc}, a protein-only infectious particle, this property must be explained by other factors. The idea that different strains result from PrP itself is supported by differences in the biochemical properties of two prion strains, responsible for the transmissible mink encephalopathy (TME). Differences following PK digestion [61] and in the resistance to denaturing agents and

proteolysis [62] suggest the existence of distinct conformations. Even though a strain can only be identified after experiments evaluating the characteristics associated with its transmission, biochemical analyses are useful to evaluate differences in the glycosylation pattern or in the size of the PK resistant fragments. Transmission of prion diseases between different mammalian species may be restricted by the so called “species barrier”, when prions isolated from one species result less infectious when inoculated in other species, with longer incubation time and reduced attack rate. Usually, the first inoculation of prions from species A to species B results in not all inoculated animals developing the disease and in variable incubation periods when compared to the inoculation within the same species. The second passage to further animals of species B, instead, resembles the one within the same species, with all animals developing the disease with consistent incubation periods [63]. This peculiar effect is thought to reside in PrP primary and 3-D structure differences between the donor and the acceptor species, affecting the efficiency of the protein-protein interaction at the base of prion conversion.

Among animal prion diseases, strains derived from hamster prions (Sc237and 263K), mouse-adapted BSE prions (301C and 301V) and mouse-adapted scrapie prions (RML, ME7, 139A, and 79A) are used to study human prion diseases [64]. RML prions, for example, derive from scrapie prions that have been adapted into mouse by repetitive passages. Distinct human prion strains, differing in their biochemical and neuropathological patterns, as well as in their transmission properties, have been identified in CJD, kuru and FFI. These strains differ in their banding pattern on WB upon PK digestion, suggesting different human PrP^{Sc} conformations. PrP^{Sc} fragment sizes and the ratios of the three PrP glycoforms are maintained when passed in transgenic mice expressing human PrP and result in murine prions with the same fragment sizes and glycoform ratios as the original inoculum [65]. Furthermore, vCJD prions differ in their glycoform pattern when compared to classical CJD, but they resemble the ones observed in cattle BSE and BSE when transmitted to other species [65].

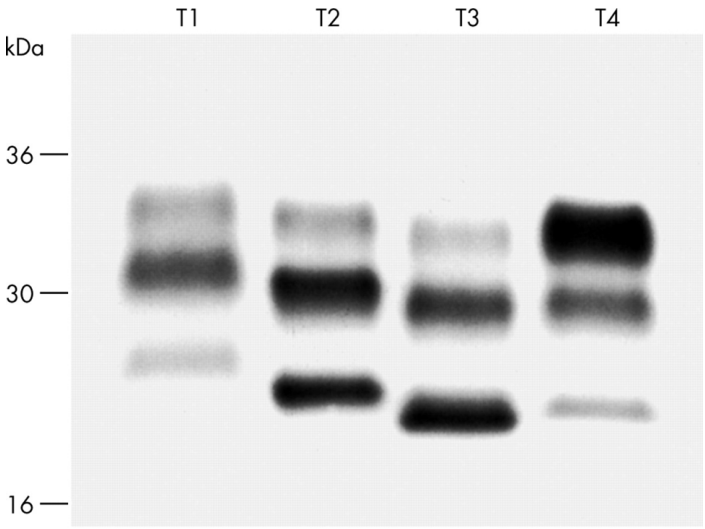

Figure 3. Molecular strains of human prion diseases [63]**.** WB of brain homogenates after treatment with PK showing different molecular and glycoform ratios. T1-T3: sporadic or iatrogenic CJD, T4: vCJD.

1.4. Cellular prion protein

The human cellular form of the prion protein is encoded by the *PRNP* gene, located in the short arm of chromosome 20 and consisting of two exons, with the second one containing the full coding sequence. In mice, the *Prnp* gene is located in chromosome 2 and the last exon of three encodes for the protein [66].

The precursor protein of 253 amino acids is synthetized in the endoplasmic reticulum and there it is modified with the removal of the C-terminal signal peptide, the attachment of the glycosylphosphatidylinositol (GPI)-anchor, the formation of the disulfide bond between Cys179 and Cys214 and the N-linked glycosylation at Asn181 and Asn197 [67-69]. The protein is subsequently modified in the Golgi network, with the refinement of the glycans attached to the asparagines, giving rise to four different protein isoforms: the un-glycosylated one, two mono-glycosylated forms and the di-glycosylated one, with both asparagines occupied by glycans [70]. The GPI-anchored mature protein of 208 amino acids is attached to the extracellular part of the plasma membrane [71], and it is characterized by an N-terminal disordered domain, with four octa-repeats regions where divalent cations bind [72], and a C-terminal globular domain, consisting of three α-helices, a three stranded antiparallel β-sheet and the GPI-anchor [73,74]. During its trafficking, PrP^{C} undergoes several endoproteolytic processes, with both physiological and pathological functions [75]. The α-cleavage, which occurs at position 111/112 of the human sequence, produces a N1 fragment of 11 kDa with neuroprotective effects [76] and a C1 fragment of 16 kDa, which cannot be converted into PrP^{Sc} and therefore considered as inhibiting the misfolding event [77]. The β-cleavage, occurring at

residues 90/91 of the human sequence, results in the formation of a 9 kDa N2 fragment and a 18-20 kDa C2 fragment, related to prion infection [78,79].

The endoproteolytic cleavage, close to the GPI-anchor, produces an almost full length PrP protein called "shed PrP", present in CSF and blood, shown to bind protein oligomers and fibrils, inhibiting their neurotoxic effects [80].

1.4.1. PrP^C expression and functions

PrP^C is already present during embryogenesis, but its highest level of expression in the CNS is reached during adulthood [81]. Its expression was also seen in skeletal and cardiac tissues, lymphoid organs, lung, gut, spleen, ovary and testis [82]. Despite its ubiquitous expression, mouse models lacking PrP^C do not present significant defects [83]. The most evident phenotype of *Prnp* knocked out mice is the resistance to PrP^{Sc} infection [84]. Other roles are the involvement in circadian rhythms [85], neurogenesis and neuronal differentiation [86], hippocampal synaptic plasticity [87], and myelin formation and maintenance in peripheral nervous system (PNS) [88]. PrP^C is expressed also outside of the CNS and it was found in cells of the immune system [89], suggesting its role in the immunological system [90].

1.4.2. PrP^C as amyloid receptor

Several lines of research have focused on the identification of putative cellular receptors responsible of or assisting the detrimental effects exerted by circulating amyloid species involved in neurodegenerative diseases. Recently, because of its already demonstrated ability to transduce PrP^{Sc} toxicity, PrP^C has been largely studied as a possible binding partner of several amyloid species.

1.4.2.1. PrP^C as PrP^{Sc} receptor

Prion infectivity resides in its ability to take contacts and convert PrP^C, which has now been identified as the main factor essential for prion replication. As previously mentioned, the most evident phenotype of PrP^C knocked out mice is their resistance to PrP^{Sc} infection [84]. In addition of being resistant to prions, PrP^C knockout (KO) mice are not damaged by exogenous PrP^{Sc}, as demonstrated by a study in which grafts overexpressing PrP^C accumulate prions that show no toxicity to their surrounding PrP^C KO tissues [91]. Moreover, arresting the propagation of PrP^{Sc}, by depleting the PrP^C neuronal pool, prevents prions neurotoxicity, despite the extraneuronal PrP^{Sc} accumulation [92]. Besides the toxicity induced by prion infection, another

study pointed out the possible role of PrP^C in mediating PrP^{Sc} toxicity without any prion replication. In this work, the expression of PrP^C of different species, and so less prone to be converted by PrP^{Sc} due to the species barrier, led anyway to neurotoxic signals, independently of prion replication [93].

1.4.2.2. PrP^C as Aβ receptor

Aβ pathology, as well as the one of other prion-like proteins, comprises many different proteopathic species with distinct structural properties and neuropathological features [94,95]. It is now widely accepted that small (oligomers) and large (protofibrils) Aβ aggregates, rather than monomers, are responsible for the effect on neural physiology [96], and that this heterogeneity could be responsible for the different clinical manifestation [97]. The binding between PrP^C and Aβ oligomers was demonstrated using Aβ-42 synthetic oligomers, which show nanomolar binding affinity to PrP^C. In addition, the long-term potentiation (LTP) blockage, induced by these amyloid species, was absent in PrP null mice [98]. This effect was reverted by preventing the binding using anti-PrP specific antibodies. Seemingly, Freir and colleagues showed that two antibodies targeting residues 93-102 and 143-153 of the prion protein blocked the inhibition of LTP mediated by Aβ, both *in vitro* and *in vivo* [99]. Significant apoptotic phenotypes were observed in SH-SY5Y, when transiently transfected to express PrP^C and cultivated with Chinese hamster ovary cell line (CHO-7PA2) secreting toxic Aβ species [93].

Besides several other studies suggested PrP^C as a mediator of Aβ neurotoxic effects [100-103], some works described Aβ-mediated impairments that do not depend on PrP^C [104-106]. These apparently controversial results may derive from the use of heterogeneous Aβ amyloid preparations, obtained by *in vitro* aggregation of the monomers or from the culture medium of specific cell lines or from AD affected brains. Being the pathological Aβ not a single molecule, it is unlikely that PrP^C could transduce all the pathological toxic effects of these so heterogeneous entities.

1.4.2.3. PrP^C as tau receptor

Tau is a microtubule-binding protein regulating microtubule assembly and stability and it is expressed in the CNS as six different isoforms due to alternative splicing. Tau protein is neuropathologically involved in tauopathies, a class of neurodegenerative diseases characterized by the accumulation of insoluble tau inclusions, called neurofibrillary tangles

(NFTs), accumulating in neurons and glia [107]. However, transgenic mice expressing wild-type or mutant human tau suggest that NFTs are not sufficient for neurodegeneration [108,109], and their formation may exert protective functions, sequestering toxic monomeric or oligomeric tau species. Therefore, soluble oligomers, rather than insoluble aggregates, are suggested to be the toxic species, despite the difficulties in their characterization and the heterogeneity of oligomer preparations.

Full-length recombinant tau was reported to bind recombinant PrP^C in its octapeptide domain [110]. In another study, the toxic effects exerted by extracellular tau species were prevented by the administration of anti-PrP 6D11 antibody [111], and similar results were obtained by Ondrejcak and colleagues, who showed the prevention of LTP inhibition induced by both recombinant and brain-derived tau, using anti-PrP antibodies [112]. Recently, soluble aggregates of tau were shown to bind PrP^C *in vitro* and their detrimental effects on LTP and neurites were prevented by PrP^C ablation or using anti-PrP antibodies [100]. Moreover, the *in vivo* effect of tau on long-term depression (LTD) was investigated in rats, where the hippocampal injection of soluble tau aggregates increased the threshold for LTD induction in a PrP^C-dependent manner. Interestingly, tau soluble aggregates completely blocked the Aβ-facilitated LTD, indicating that the cellular prion protein could mediate a range of different and sometimes opposing actions, following the interaction with distinct amyloid proteins [113]. Our previous work investigated the interplay between recombinant tau K18 amyloid fibrils, directly administered to the culture medium of N2a cells, and PrP^C. We were able to find an interaction of the prion protein with tau fibrils, prevented by the treatment with anti-PrP antibodies, and an increased uptake of tau fibrils in cells expressing PrP^C compared to the ones knocked-out for the protein. Interestingly, the exposure of prion-infected cells to these amyloids induced a decrease in PrP^{Sc} levels, probably because of a direct binding between PrP^C and tau, that hinders the conversion event [114].

1.4.2.4. PrP^C as α-synuclein receptor

α-synuclein is, in its monomeric state, an intrinsically disordered protein of 140 amino acids localized in the pre-synaptic terminals. Although its localization may suggest a role in the regulation of neurotransmitter release, synaptic function and plasticity, α-synuclein functions remain unknown [115,116]. α-synuclein monomers can aggregate forming oligomers and fibrillar conglomerates, linked to cytotoxicity [117]. In the aggregation process, α-synuclein interacts with other proteins giving rise to LBs, neuronal intracellular inclusions constituted mainly by

α-synuclein fibrillar aggregates [118]. Abnormal cytoplasmic α-synuclein inclusions characterize α-synucleinopathies, a class of neurodegenerative diseases that includes PD, DLB and MSA.
Although not mandatory for their transport, the expression of PrP^C promotes α-synuclein fibril spreading in the brain of injected mice, together with the formation of LB-like aggregates. Moreover, the overexpression of PrP^C in HEK293 cells enhances the binding of α-synuclein fibrils to the plasma membrane [119]. Same data were confirmed by Aulić and colleagues both *in vitro* and *in vivo* and, interestingly, the authors reported an effect of α-synuclein fibrils in the reduction of PrP^{Sc} [120]. The interaction with α-synuclein fibrils is prevented by the expression of a mutant form of PrP^C lacking its central domain [119], while the detrimental effects of α-synuclein oligomers are abolished by pre-treating hippocampal slices with anti-PrP 6D11 antibody [121].
In contrast, in another paper, the authors found no binding between α-synuclein oligomers and PrP^C, and comparable α-synuclein-mediated toxicity between $PRNP^{+/+}$ and $PRNP^{0/0}$ mice [122]. As for Aβ, the characterization of different preparations of α-synuclein oligomers/fibrils is extremely important to assess the contribution of PrP^C in synucleinopathies.

1.4.3. PrP^C intracellular trafficking

The cellular prion protein continuously transits from the extracellular plasma membrane to the endocytic compartments [123]. From early endosomes, PrP^C can be recycled back to the plasma membrane or degraded in the endolysosomal compartments [124]. Its association to lipid rafts [125], enriched in cholesterol and sphingolipids, starts when the immature PrP^C precursor resides in the ER [126]. PrP^C routing involves either clathrin-dependent and -independent pathways. GPI-anchored proteins, such as PrP^C, are not able to physically interact with the adaptor proteins responsible for the clathrin-mediated endocytosis (CME), because of the lack of intracellular aminoacidic sequences. However, their internalization can be mediated through the interaction with other partners [127]. CME of PrP^C requires its N-terminal aminoacidic sequence, from position 23 to 107 of the mouse sequence [128], and this could imply the association with the extracellular domain of a transmembrane protein that contains a coated pit internalization signal [129]. PrP^C interaction with laminin receptor precursor (LRP) and the 67-kDa laminin receptor (LR), resulting in its internalization via clathrin-coated pits, has been documented [130]. Moreover, PrP^C interacts with the transmembrane low-density lipoprotein receptor-related protein 1 (LRP1), and this binding allows the internalization via a clathrin-dependent mechanism [131]. Controversial data on the

involvement of clathrin in PrP^C internalization were obtained in Neuro2a (N2a) cells, where the downregulation of clathrin has no effect on PrP^C uptake [132].The protein is then targeted to early endosomes through the Ras-related protein Rab5 [133], and Dynamin may play a role in the PrP^C internalization pathway.

PrP^C internalization may also rely on caveolae, plasma membrane pits formed by the assembly of cytoplasmic proteins on a caveolin platform [134], which move PrP^C to late endocytic multivesicular bodies (MVBs) and lysosomes rather than to the recycling compartments [135]. PrP^C octarepeats region was shown to interact with Caveolin-1, a 22kDa protein organizing several caveolar functions [136]. Among clathrin-independent endocytosis (CIE) mechanisms, copper binding to the N-terminal region of PrP^C promotes its endocytosis through a pathway regulated by flotillin and Fyn kinase [137].

1.4.4. PrP^C intercellular trafficking

Apart from being present on the plasma membrane, PrP^C was found in MVBs [138], specialized endosomes containing intraluminal vesicles (ILVs), whose content can be degraded in lysosomes or released in the extracellular space after the fusion with the plasma membrane [139]. *Prnp*-null mice exhibit reduced MVBs formation and exosome release [140], suggesting an important role of PrP in exosome metabolism.

PrP^C overexpression was connected to the formation of tunnelling nanotubes (TNTs), cytoplasmic extensions connecting distant cells [141], where the protein transits probably by surface continuity or by vesicular transport [142].

Normally, the endosomal sorting complex required for transport (ESCRT) is involved in MVBs biogenesis, targeting cargoes to the ILVs, and its alteration affects PrP^C trafficking and localization [143]. Moreover, the dysregulation of vacuolar protein sorting (VPS) proteins, implicated in ESCRT pathway, affects PrP^C localization. The downregulation of Vps35 and Vps28 respectively blocks and increases PrP^C internalization [144], while the expression of a Vps4 dominant-negative isoform accumulates PrP^C at the limiting membrane of endosomes [143].

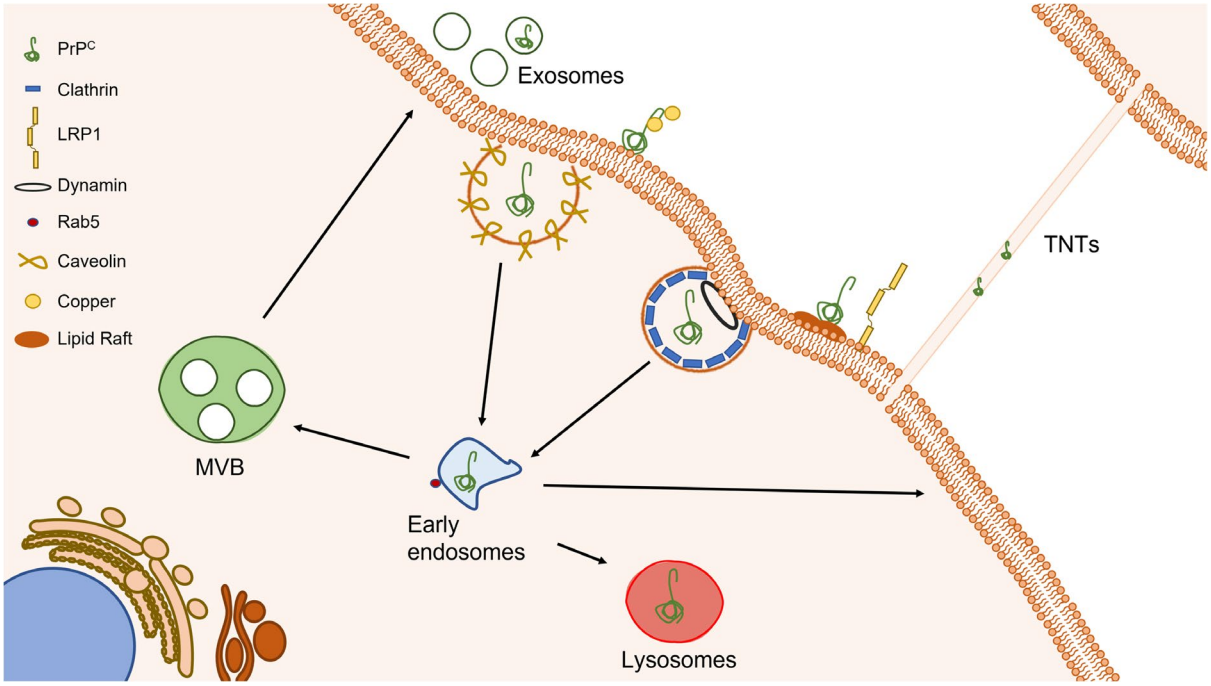

Figure 4. PrP^{C} intra- and intercellular trafficking. PrP^{C} internalization can be mediated by the interaction with clathrin, caveolin or other adaptor proteins such as LRP1. From the early endosomes, the protein can be recycled back to the plasma membrane or, alternatively, PrP^{C} can be delivered to lysosomes for degradation or directed to the extracellular space through exosomes and TNTs.

1.4.5. PrP^{C} to PrP^{Sc} conversion

Prion diseases are characterized by the pathological conformational change of PrP^{C} into PrP^{Sc} and the consequent accumulation of the latter in the CNS [145]. In this transition, a portion of PrP^{C} α-helices and coil structures is converted into β-sheets, which make PrP^{Sc} structurally different from its counterpart [146]. This change in the structure is accompanied by different physical-chemical properties of PrP^{Sc}, such as the resistance of its C-terminal fragment to PK degradation and the insolubility in non-denaturing detergents [34]. Therefore, PK digestion and WB are routinely performed to assess PrP^{Sc} presence. After PK digestion, PrP^{Sc} resistant fragments (PrP 27-30) show a lower molecular weight and maintain the characteristic three-band pattern corresponding to the di-, mono- and un-glycosylated forms, while PrP^{C} is completely digested (Fig. 2).

1.4.6. PrP^{Sc} intracellular trafficking

The conversion of PrP^{C} to PrP^{Sc} seems to require from minutes to hours after the first exposure [147,148]. Although, together with PrP^{C}, PrP^{Sc} was found localized at the plasma membrane, it seems to reside primarily in the intracellular compartments [149,150]. After being

endocytosed, PrP^{Sc} is recycled to the plasma membrane or, alternatively, sent to the Golgi apparatus via the retromer pathway, to be degraded in lysosomes [151].

MVBs have been proposed as an important site for prion conversion since, by preventing their maturation, PrP^{Sc} accumulation is reduced [152].

PrP^{Sc} internalization pathways were thought to be the same as PrP^{C}, but their identification is still controversial. For instance, clathrin- and caveolae-mediated endocytosis pathways slightly control prion uptake but remain fundamental for the establishment of the infection [153].

LRP/LR may represent an important receptor for prions, as their uptake is reduced upon the administration of an antibody targeting LRP/LR [154]. Moreover, BSE prions in vCJD seem to be internalized by LRP/LR in gut enterocytes [155].

LRP1 represents another prion receptor, which after binding, targets PrP^{Sc} to lysosomes rather than to the plasma membrane [156].

Heparan sulfate (HS) is a glycosaminoglycan (GAG) related to heparin and covalently attached to a range of core proteins to form HS-proteoglycans (HSPGs) [157]. The treatment with heparinase and chlorate, inhibitors of sulfation, strongly reduces PrP^{Sc} rods binding and uptake [158]. Furthermore, the binding of PrP^{Sc} to Chinese Hamster Ovary (CHO) cell membranes could be reduced by heparin treatment [159], suggesting an involvement of HS in prion uptake.

Macropinocytosis, a non-selective process responsible for the delivery of cargoes to late endosomal and lysosomal compartments, was shown to be involved in the uptake of fibrillar prions [160]. Whether macropinocytosis mediates prion uptake or the establishment of an efficient infection remains to be clarified, since the treatment with amiloride, an inhibitor of macropinocytosis, does not influence PrP^{Sc} uptake in ROV cells [161], while in N2a cells the inhibition of this pathway was sufficient to prevent PrP^{C} conversion in its pathological counterpart [162].

Murine neurons infected with prions internalize PrP^{Sc} by vesicles positive for late endosomal and lysosomal markers but not by early endocytic, synaptic, or raft-derived vesicles [163]. Interestingly, PrP^{C} seems not involved in the uptake process of PrP^{Sc}, since exogenous PrP^{Sc} has been found in the extremities of neurites either in WT or PrP KO cells [163].

1.4.7. PrP^{Sc} intercellular trafficking

PrP^{Sc} is proposed to spread among cells through direct contact, TNTs, and exosomes.

Previous works demonstrated that prion-infected cells are efficiently able to transmit their infectivity to neighbouring naïve cells by direct contact [164,165].

TNTs represent another way of PrP^{Sc} spreading in neuronal CAD cells [142], and astrocytes may contribute to this process, through the involvement of different intercellular connections delivering PrP^{Sc} to neurons [166]. Inside TNTs, PrP^{Sc} moves in endolysosomal vesicles [142,166], but the escaping mechanism leading to PrP^{Sc} interaction with PrP^{C} needs to be clarified. Both the number of TNTs and the amount of released vesicles are increased following prion infection, boosting PrP^{Sc} spreading in a positive feedback loop [166].

Being, as well as PrP^{C}, a GPI-anchor protein residing in lipid rafts, PrP^{Sc} can be incorporated into exosomes [167]. The treatment with monensin, which stimulates the release of exosomes, is accompanied by an increased prion infectivity [168], and PrP^{Sc} enriched exosomes are infectious when challenged in mice [138,169]. Moreover, the amount of infectivity associated with the exosomal pathway was seen to be prion strain-dependent in RK13 cells [170]. Prion infection could also modify the exosomal population, which shows different structural characteristics compared to the ones of the uninfected cells [167]. In addition, exosomes might not represent the only population of vesicles involved in prion spreading, as showed in N2a cells, where PrP^{Sc} was found associated to plasma membrane-derived microvesicles, resulted to be infectious both *in vitro* and *in vivo* [171]. Detectable levels of infectivity were also found in lower-speed vesicle preparations, consistent with PrP^{Sc} association with larger vesicles [138]. Interfering with the ESCRT machinery strongly affects the association of prions with exosomes [172], albeit ESCRT-independent pathways for the delivery of cargoes into exosomes have been described, such as the one requiring ceramide, a sphingolipid abundant in rafts, produced by the neutral sphingomyelinase (nSMase) pathway [173]. The treatment of prion-infected cells with the nSMase2 inhibitor GW4869 was found to hinder PrP^{Sc} targeting into exosomes [174].

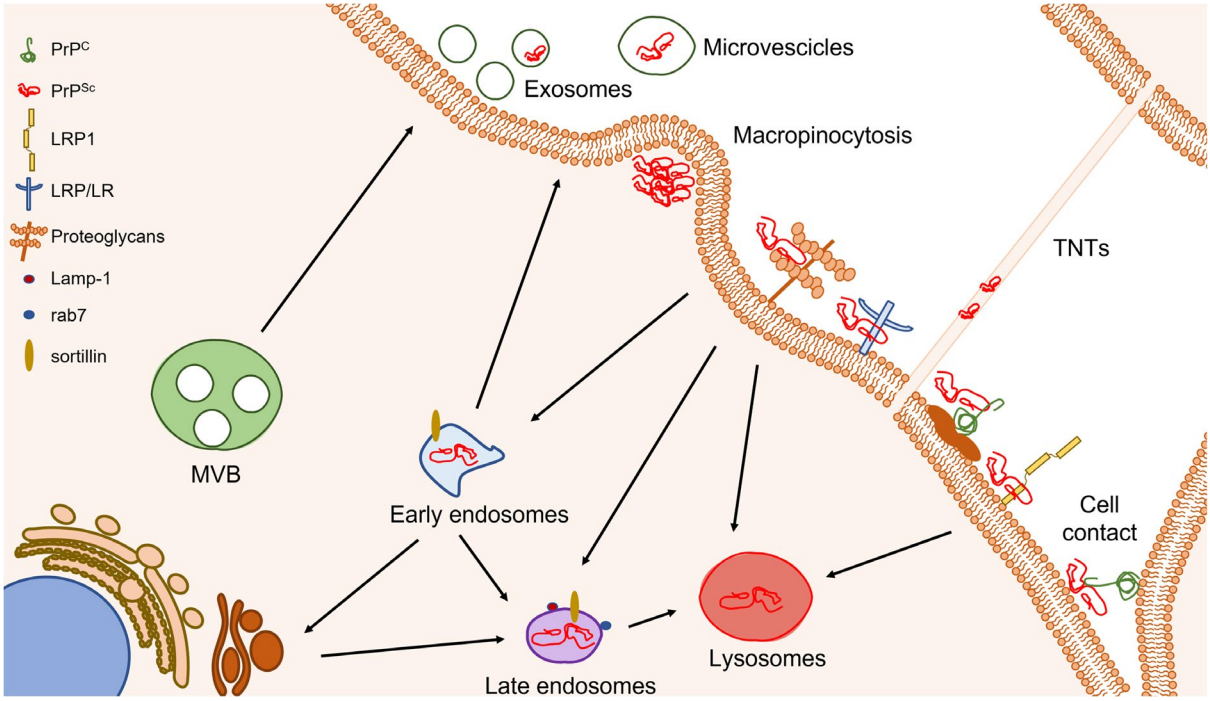

Figure 5. PrP^{Sc} intra- and intercellular trafficking. During prion infection, PrP^{Sc} is internalized through the interaction with several binding partners. In the cytoplasm, PrP^{Sc} is mainly found in endosomal vesicles positive for Lamp-1 and rab7. From there, PrP^{Sc} is sent to lysosomes for degradation or directed to the extracellular environment through exosomes and TNTs, contributing to the propagation of the infection.

1.5. Tauopathies

Neurodegenerative diseases characterized by the deposition of misfolded tau in the brain are collectively known as tauopathies. To date, more than 26 different tauopathies have been identified [175]. Disorders in which the accumulation of tau is the predominant feature are called primary tauopathies, distinguished from the ones in which tau deposition is secondary to other events, known as secondary tauopathies. The nomenclature of primary tauopathies overlaps with the classification of Frontotemporal Lobar Degeneration-Tau (FTLD-Tau). Alzheimer's disease belongs to the secondary tauopathies because triggered by Aβ accumulation [176].

Clinically, patients develop features of frontotemporal dementia (FTD), and secondary symptoms can vary according to the anatomic area, cell types involved, and specific tau isoforms deposited [177].

Tau is a microtubule binding protein playing an important role in microtubule polymerization and in promoting axonal transport and neuronal integrity [178]. In the adult human brain, six different tau isoforms are expressed, deriving from the alternative splicing of exons 2, 3 and 10 and differing for the presence of 3 (3R) or 4 (4R) microtubule binding domains (MBDs) [179].

In normal conditions, the ratio between 3R/4R isoforms is almost 1:1 and the dysregulation of this equilibrium, with the over-representation of a class over the other, may drive tau pathology [180]. Specific *MAPT* mutations can disrupt this equilibrium leading to tauopathies [181]. Most of the mutations occur in exons 9-13, and the ones residing in intron 10 and some in exon 10 affect its alternative splicing, increasing the ratio of 4R tau isoforms [182]. In all patients' brains with mutations affecting the splicing, insoluble tau levels comprise predominantly, but not exclusively, the isoform that is over-represented [183]. Moreover, two haplotypes of tau exist, H1 and H2, differing from each other for a 900 kb sequence inversion and for a 238 bp deletion in H2, upstream to the exon 10 [184]. In addition, a number of single-nucleotide polymorphisms in H1 was seen to produce several sub-variants, some of which associated with an increased risk of tauopathies, such as CBD and PSP [185], also because of an increased expression of 4R tau [186]. In addition, tau protein in tauopathies results abnormally hyperphosphorylated, decreasing its binding affinity to microtubules and promoting its self-aggregation [187]. According to the composition of the aggregates, tauopathies are classified in 3R, 4R or mixed 3R+4R. Following this classification, 3R tauopathies (60 and 64 kDa bands in WB of sarkosyl-insoluble fractions) comprise Pick's disease (PiD), 4R tauopathies (64 and 68 kDa bands) include PSP, CBD, globular glial tauopathy (GGT) and argyrophilic grain disease (AGD); mixed tauopathies are primary age-related tauopathy (PART) and AD, the latter as a secondary tauopathy (Fig. 6) [176]. Mutations in the *MAPT* gene, encoding for tau, are associated with FTLD [182]. Recently, a new classification based on the structure of the tau filament found in the pathologies has been proposed [188].

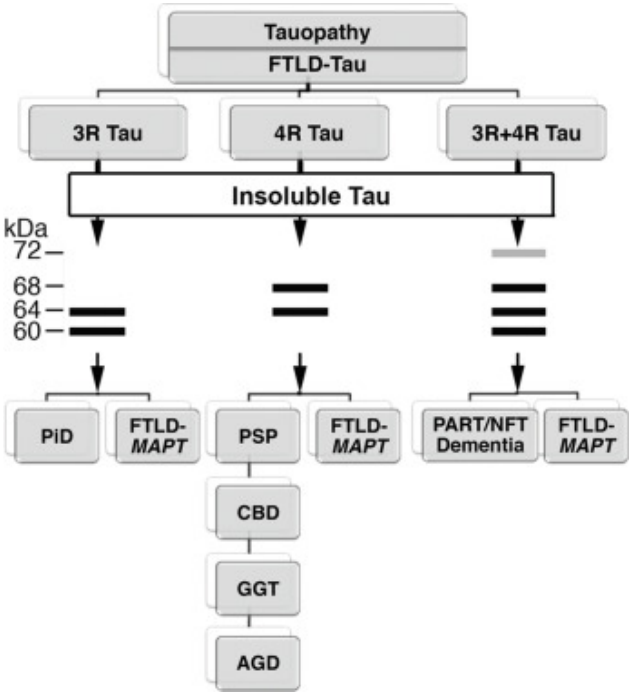

Figure 6. Molecular classification of tauopathies (Frontotemporal Lobar Degeneration (FTLD)-Tau) and WB patterns of insoluble tau [176]**.** 3R tauopathies (PiD, Pick's disease) are characterized by the presence of aggregated 3R tau isoforms (60 and 64 kDa bands). 4R tauopathies (PSP, progressive supranuclear palsy; CBD, corticobasal degeneration; GGT, globular glia tauopathy; AGD, argyrophilic grain disease) present the aggregation of 4R tau isoforms (64 and 68 kDa bands). Mixed tauopathies include primary age-related tauopathy (PART) and present either 3R and 4R aggregated tau isoforms (60, 64 and 68 kDa bands). Mutations in tau gene *MAPT* are associated with FTLD (FTLD-*MAPT*).

1.5.1. 3R tauopathies

1.5.1.1. Pick's disease

This pathology was firstly characterized by Arnold Pick, who described a severe atrophy of the frontal, temporal and parietal lobes [189]. Significant neuronal loss, gliosis and round intraneuronal inclusions called Pick's bodies, composed of filamentous 3R tau, are observed. Straight tau filaments are predominantly present in the hippocampus and in frontal and temporal cortices [190]. Tau pathology is also found as round Pick body-like inclusions in both oligodendroglia and astrocytes [191]. PiD is the only tauopathy predominantly associated with 3R tau inclusions.

1.5.2. 4R tauopathies

1.5.2.1. Progressive supranuclear palsy

PSP is characterized by atrophy in the subthalamic nucleus and pons, and by a depigmentation of the substantia nigra [192]. Intraneuronal tau pathology consists of NFTs and globular inclusions composed of 4R tau and associated with tufted astrocytes, with tau-positive inclusions forming densely packed fibrils that form tufts in the proximal processes surrounding astrocytic nuclei [193]. In oligodendrocytes, tau inclusions, called coiled bodies, surround the nucleus [194].

1.5.2.2. Corticobasal degeneration

In CBD, differently from PSP that affects the hindbrain areas, neuronal loss and gliosis occur in the frontoparietal cortex and extend to the frontal and superior temporal lobes [195]. Moreover, astrocytic inclusions have different morphology compared to the ones found in PSP, with plaques in CBD that might be involved earlier than neuronal accumulation [196] and

that represent a diagnostic criteria for CBD patients. Ballooned neurons have also been found in CBD, with an higher density compared to PSP, and with deposits composed of pre-tangles and not NFTs [197].

1.5.2.3. Globular glial tauopathy

GGT is characterized by tau pathology mainly consisting of 4R tau in oligodendrocytes and astrocytes [198]. Differently from PSP, GGT is characterized by globular oligodendrocytic and astrocytic inclusions [199], while neuronal tau pathology is mostly present as diffuse cytoplasmic globular or small tangle-like pathology [200]. Three subtypes have been documented according to the localization of tau aggregates. In type I, the globular inclusions in oligodendrocytes, located in the frontotemporal regions, lead to behavioural symptoms. In type II, the motor cortex and the corticospinal tract are affected with a consequent impairment of movement. Type III combines the features of the previous categories with higher burden and smaller size of astrocytic inclusions [201].

1.5.2.4. Argyrophilic grain disease

AGD is neuropathologically characterized by argyrophilic and 4R-tau immunoreactive grains, small spindle-shaped lesions in neuronal processes and, in particular, in dendrites and dendritic spines [202]. The immunostaining for p62 and ubiquitin is also helpful to detect grains. These grains are usually deposited in the transentorhinal and entorhinal cortices, the CA1 region of the hippocampus, the presubiculum, the neighbouring temporal cortex, the orbitofrontal cortex, and the insular cortex [203]. Oligodendritic coiled bodies and neuronal pretangles are also observed, while granular/fuzzy astrocytes are constantly present in the amygdala [201].

1.5.3. Mixed tauopathies: 4R+3R

1.5.3.1. Primary age-related tauopathy

PART usually shows AD-like NFTs with few or no Aβ plaques. In contrast to AD, NFTs are exclusively found in temporal lobes, basal forebrain, brainstem and olfactory bulb [204]. When associated with dementia, the term NFT (or tangle-only) dementia is also used [205]. In some cases, it is uncertain whether a progression towards AD will be seen and it is still under debate whether PART represents a distinct pathology or an early stage of AD [206]. Neurofibrillary

degeneration and ghost tangles restricted to the hippocampus and medial temporal lobe are seen [205].

1.5.3.2. Alzheimer's disease

AD is classified as a secondary tauopathy because of the formation of intracellular NFTs in the presence of extracellular amyloid plaques mainly formed by the amyloid β peptide in a fibrillar form. In contrast to FTLD-tau, AD affects people over the age of 75 and its symptoms are linked to dementia rather than changes in behaviour [203]. This is the most common form of dementia, thought to represent the 60-70% of all cases and afflicting 44 million people worldwide [207]. AD is usually manifested with short-term memory difficulties, but problems in expressive speech, visuospatial processing and executive functions may also occur [208]. The severity of the cognitive impairment in AD varies. The earliest symptomatic stages are usually referred as mild cognitive impairment (MCI), with the functional capacities relatively preserved, while a cognitive impairment compromising independence and affecting daily life is defined as dementia. A gradual onset and an ongoing progression of dementia usually characterize AD [208], albeit the starting point can precede of many years the clinical symptoms [209]. Age is the most important risk factor in developing AD, raising in individuals aged 65 years or more.

Sporadic AD represents the most common form, but a small percentage, less than 1% of the cases, is linked to autosomal dominant mutations in the gene encoding for the amyloid precursor protein (APP) and in the genes encoding for presenilin-1 and 2, forming the catalytic subunits of the γ-secretase complex [210]. Mutations in these genes are associated with an earlier age of onset [211]. Moreover, *APOE* polymorphism is the most important genetic risk factor for AD. The heterozygosity in the *APOE* ε4 increases the risk for dementia by 3-4 times, while the homozygosity by 12-15 times, when compared to *APOE* ε3 [212]. It is thought that the three ApoE isoforms may alter Aβ aggregation in the brain, with ApoE4 slowing its clearance [213]. Moreover, apart from exerting its effect on Aβ, APOE polymorphisms may affect directly tau pathogenesis, as demonstrated by an increased risk of PSP onset, which does not feature Aβ pathology [214], and by the influence on tau pathology in animal models, independently from Aβ [215]. Other risk factors may be represented by metabolic features such as diabetes mellitus, hypertension, obesity, and lifestyle such as alcohol abuse, smoking, low physical activity, and social isolation [208]. Aβ peptides derive from the cleavage of APP, a single transmembrane protein enriched in synapses, by β- and γ-secretase in the so called

"amyloidogenic pathway" [216], and then are secreted in the extracellular space. A peptide of 40 amino acids (Aβ-40) is the prevalent species secreted, while a longer fragment, Aβ-42, is less abundant [217]. Aβ-42 has a high propensity to aggregate and it is detected in the majority of extracellular amyloid plaques [218]. Mutations in *APP* or *PSEN1/2* may affect APP processing resulting in the alteration of Aβ42/Aβ40 ratio [217].

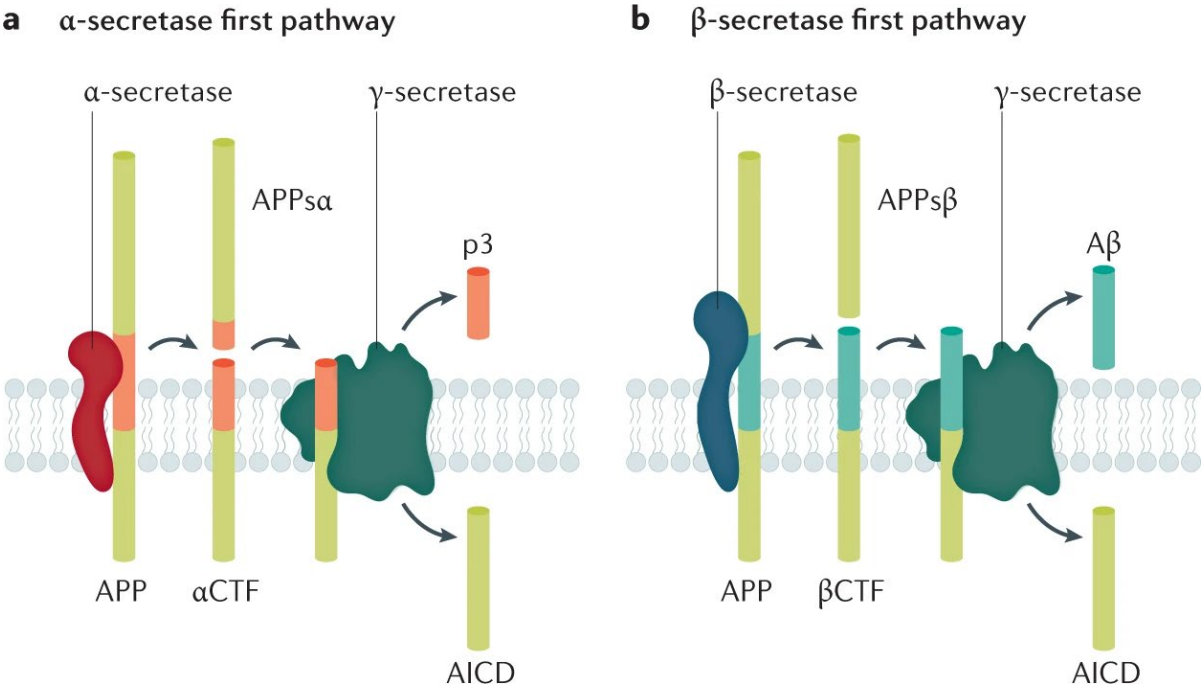

Figure 7. APP cleavage [208]**.** In the non-amyloidogenic pathway (left), APP is cleaved by α-secretase and the subsequent cleavage by γ-secretase originates the extracellular p3 peptide and the intracellular AICD fragment. In the amyloidogenic pathway (right), the subsequent cleavages by β- and γ-secretase produce AICD and the aggregation prone Aβ peptide.

Together with extracellular Aβ plaques, AD is characterized by the deposition of tau as intraneuronal NFTs, neuropil threads and dystrophic neurites (degenerated axons and dendrites containing tau and surrounding Aβ plaques) [208]. The deposition of all 3R and 4R six tau isoforms characterizes AD pathology. Tau aggregation may start following its phosphorylation. In the healthy brain, 2-3 residues of tau are phosphorylated. In contrast, in AD, its phosphorylation status is from 3- to 4- fold higher than normal brain, and hyperphosphorylated tau was seen to represent the main component of tau aggregates in AD brain [219]. This abnormal hyperphosphorylation seems to precede tau accumulation in AD neurons, since hyperphosphorylated tau has been found also in the absence of tangles both in AD and in normal aged brains [220]. The triggering event of this hyperphosphorylation is still

unclear, but it might be caused by conformational changes in tau protein that make it a better substrate for phosphorylation or a worse substrate for dephosphorylation [221].

Tangles are mainly formed by paired helical filaments (PHFs), formed by a twisted double-helical ribbon of subunits. Less abundant are straight filaments (SFs), differing from PHFs for the absence of width modulation [222]. Both PHFs and SFs show a similar C-shaped morphological unit that differs in the arrangement in the two types of filament [222]. Recently, Fitzpatrick and colleagues provided the first high-resolution structure of PHFs and SFs by cryogenic electron microscopy (cryo-EM) [223]. The link between Aβ and tau pathology is not well understood and even though Aβ accumulation has been considered the key factor driving tau accumulation following the so called "amyloid hypothesis" [224], other studies suggested an independent tau pathological role in AD [225-227].

1.6. Tau Protein

Tau protein represents, together with MAP1 and MAP2, the major microtubule associated protein (MAP) in a mature neuron [228]. Even though it has been discovered more than 40 years ago as an essential protein for microtubule assembly [178], tau research interest has grown since it was recognized as the main component of PHFs in AD [229,230].

1.6.1. Tau expression and structure

Human tau protein is encoded by the *MAPT* gene located on the long arm of chromosome 17 and containing 16 exons, although exons 0 and 14 are transcribed but not translated [231]. Tau pre-RNA splicing varies according to the neuronal type and its maturation stage [107]. The protein is transcribed from a 6 kb mRNA that generates 6 different isoforms, ranging from 37 to 46 kDa, due to the alternative splicing of exons 2, 3 and 10 [179,232]. Exons 2 and 3 encode for 29 amino acids inserts in the N-terminus of the protein and exon 3 is not transcribed when exon 2 is missing. Exons 4A, 6 and 8 are exclusively transcribed in the PNS. Exons 9-12 encode for 30-31 amino acids repeats forming the MBDs of tau, with the second repeats encoded by exon 10. Accordingly, the alternative splicing produces six different isoforms characterized by the presence of 0, 1 or 2 N-terminal inserts (0N, 1N or 2N) and by the presence of 3 (3R) or 4 (4R) MBDs [232].

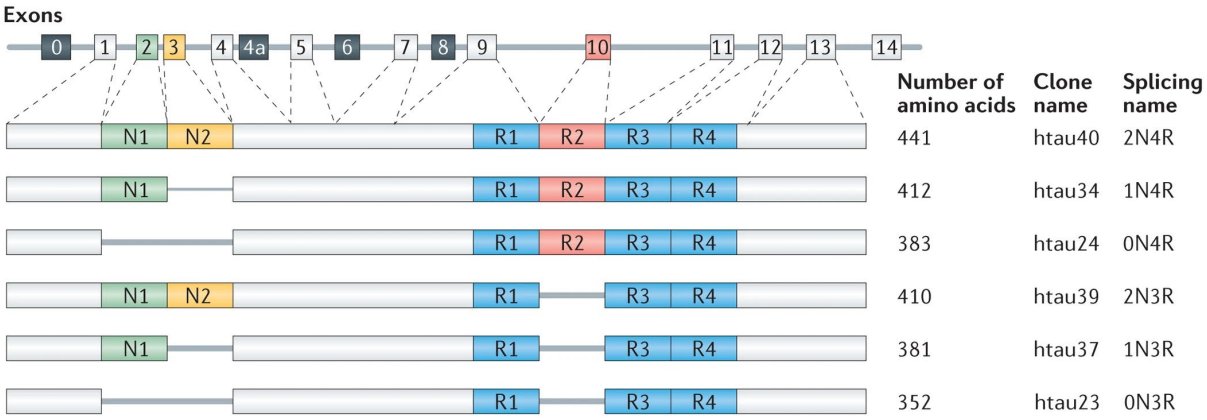

Figure 8. Tau encoding gene, *MAPT,* contains 16 exons [107]. Exons 1, 4, 5, 7, 9, 11, 12 and 13 are constitutive whereas the others can be alternatively spliced. The product of exons 2, 3 and 10 alternative splicing is six different isoforms characterized by the presence of two or three repeats constituting the MBDs and by zero, one or two N-terminal insertions.

Tau expression is finely regulated during development and in the adult human brain all six isoforms are expressed, whereas only the 0N3R is expressed in the fetal brain [179]. In the healthy human brain, the ratio between 3R and 4R isoforms is almost 1:1, although this ratio can differ in some regions [233]. Despite being used as a model for tauopathies investigations, mice tau expression differs from the human one. The adult mouse brain expresses only the isoforms with 4 MBDs and, even though being similar between N1 and the C-terminus, human and mouse tau proteins differ significantly at the N-terminus [107].

Tau is hydrophilic, very stable under acidic conditions and high temperatures. Moreover, tau is a basic protein, but the aminoacidic distribution gives to the protein an asymmetry of charges that is important for the binding to microtubules, the interaction with other partners, the internal folding, and the aggregation [107]. Although tau is natively unfolded, it can adopt a "paperclip" like structure, where the C-terminus folds over the MBDs and the N-terminus folds back over the C-terminus [234]. This structure may protect tau from aggregation. Four different domains can be distinguished: the N-terminal acidic projection domain, that goes from amino acid 1 to 150 and includes the two N-terminal inserts, the proline-rich domain (aa 151-243), the MBDs (aa 244-369), separated by flanking regions and constituting the structure by which tau binds and stabilizes microtubules, and the C-terminal tail, from amino acid 370 to 441 [235]. In contrast to the other regions, the second and third MBDs have a higher propensity to form an ordered β-sheet structure [236]. Although not binding to microtubules, the N-terminal region was seen to influence the attachment [237], and truncated constructs, lacking the N-terminal part, show altered microtubule interactions [238]. The N-terminal inserts

have unclear functions, but they seem to influence tau sub-cellular localization [239]. The proline-rich domain of tau contains seven Pro-X-X-Pro (PXXP) motifs, constituting a potential binding site for Src homology-3 (SH3)-containing proteins [232]. The regions flanking the MBDs regulate the interaction with microtubules [240]. The proline-rich and the MBDs play a role in the interaction of tau with other neurodegenerative-associated proteins such as α-synuclein, 14-3-3 and FUS, suggesting a role of tau in other diseases where these proteins are deposited [232]. Finally, tau C-terminal region function remains elusive, but it was suggested that it might play a role in influencing tau interaction with other partners [241].

1.6.2. Tau functions

In the developed neurons, tau is mainly located in axons where its affinity to microtubules is higher than in dendrites [242]. Here, tau protein stabilizes microtubules, promotes microtubule assembly and regulates their dynamics, allowing the reorganization of cytoskeleton [107]. Moreover, as discussed before, the different isoforms of tau can have different sub-cellular localizations and, consequently, the altered splicing may disrupt microtubule stability. Tau knockout mice have also demonstrated important roles in neurogenesis and neuroplasticity [243,244]. The binding with α- and β-tubulin heterodimers occurs through residues interspersed throughout and around the MBDs of tau [245], and mutations in these residues may destabilize the microtubules and increase free-tau molecules, promoting their aggregation [180]. Tau can regulate axonal transport competing with kinesin and dynein motor proteins for binding to microtubules and affecting both anterograde and retrograde transport [246,247]. Furthermore, tau might be essential for axonal elongation and maturation, since its knockdown inhibits neurite formation in cultured rat neurons [248].

Tau was also observed in dendrites where it can be involved in synaptic plasticity [249]. Some works also reported a nuclear tau localization in neuronal and non-neuronal cells [250,251], where it seems to maintain the integrity of genomic DNA and cytoplasmic and nuclear RNA [252].

Despite the first studies in tau knockout mice revealed no significant phenotypes [253], recent studies suggested that tau may be involved in the regulation of neuronal activity, neurogenesis, iron export and LTD [107]. Other studies pointed out a role of tau in neurogenesis, albeit with opposite results [243,254]. Lei and colleagues linked the deficiency of tau with the intraneuronal iron accumulation due to an impaired interaction of APP with ferroportin. The iron accumulation was observed in brain regions where soluble tau levels were reduced, such

as the cortex in AD or the substantia nigra in PD, linking tau deficiency to neurodegeneration [255]. Finally, the interaction of tau with actin has been documented and was shown to be important for the cytoskeleton network; tau phosphorylation can impair the binding with actin, leading to alterations in the cytoskeleton organization [256].

1.6.3. Tau in pathologies

How tau is linked to pathologies and what is the triggering event leading to tau misfolding and aggregation are still a matter of debate.

Mutations in *MAPT* gene are linked to tau aggregation in hereditary tauopathies although the cause of aggregation in sporadic diseases is still unknown. So far, no *MAPT* mutations have been associated to AD [182]. *MAPT* mutations are classified as missense, modifying the sequence of tau, and splicing mutations, altering the ratio of the isoforms without affecting the sequence. Some missense mutations can also alter the alternative splicing.

Most of the missense mutations reduce the binding affinity of tau to microtubules, altering their structure and increasing the level of unbound free tau. In contrast, some mutations, such as Q336H and Q336R, were shown to promote microtubule assembly *in vitro* [257,258]. Moreover, R5H and R5L tau mutants fail to interact with the p150 subunit of the dynactin complex, suggesting a possible impairment of the axonal transport [259]. Some mutations, such as P301L and P301S, were shown to increase the aggregation propensity of tau [12,260] and to make it more prone to be seeded [261-263].

Splicing mutations alter the ratio between 3R and 4R isoforms and, due to the increased binding affinity of 4R tau to microtubules, can result in microtubule instability [181,264]. Most of the pathogenic mutations reside within or near intron and exon 10 and usually result in an increased inclusion of exon 10 (repeat R2) with a consequent over-production of 4R isoforms. Other mutations, such as Δ280K, have an opposite effect, resulting in the constitutive exclusion of exon 10 from tau transcripts [265].

The interaction of tau with microtubules is negatively regulated by phosphorylation [266]. Some of tau phosphorylation sites are hyperphosphorylated in AD and other tauopathies. Almost 85 putative phosphorylation sites have been identified, some of which in the MBDs, that, when phosphorylated, decrease tau binding to microtubules [267]. Interestingly, also the phosphorylation of regions outside of the MBDs may influence the binding of tau to microtubules [268]. The detached tau, besides resulting in the cytoskeleton destabilization, undergoes self-aggregation forming oligomers and aggregates [269]. Other sites were seen to

be critical and, when phosphorylated, tau is transformed into an inhibitory molecule that sequesters other proteins, normally associated with microtubules [270]. The hyperphosphorylation may not only affect tau aggregation but also its correct sorting [271]. Missense mutations in the tau sequence, as well as altering potential phosphorylation sites, were also shown to promote phosphorylation when compared to WT tau [270]. It is poorly understood which phosphorylation sites are involved in the disease pathogenesis and which are phosphorylated only after the formation of tau pathology. Mimicking tau permanent phosphorylation reproduces some of the aspects of AD pathology [187], while the phosphorylation in the proline-rich region induces tau propensity to self-aggregate [232,272]. Moreover, other mechanisms might be involved in the phosphorylated tau-induced pathology. Tau phosphorylation at Ser262 or Ser 356 affects its recognition by the C-terminus of the heat shock protein 70-interacting protein-heat shock protein 90 (CHIP-HSP90) complex, impairing tau proteasomal degradation [273]. Furthermore, tau injection into synaptic terminals disrupts synaptic transmission [274]. Finally, tau phosphorylation may alter the interaction with its binding partners, as demonstrated for the kinesin-associated protein JUN N-terminal kinase-interacting protein 1 (JIP1) [275] and Fyn [276].

1.6.4. Tau aggregation and toxic species

The aggregation of tau characterizes several neurodegenerative diseases and understanding the phenomenon by which a normally soluble and disordered protein can undergo conformational changes forming fibrillar structures could help disentangle the molecular aspects of these disorders. In solution, the high positive charges surrounding the aggregation-prone MBDs make tau protein soluble [277] . The addition of negatively-charged cofactors, such as heparin [278], changes in solvent conditions [279], specific patterns of post-translational modifications [280], truncations and mutations, can alter tau solubility and can induce its aggregation. Two short hexapeptide motifs, VQIINK and VQIVYK in R2 and R3, were shown to be essential for tau aggregation and highly prone to form β-structures [281,282]. Moreover, since the structure of PHFs was shown to be constituted by the MBD regions of tau [283] and tau fragments made of MBDs sequence, without N- and C-termini, are more prone to aggregation than full-length tau [284], different *in vitro* tau constructs have been exploited. Two of these, K18 and K19, represent the model for 4R and 3R tau isoforms respectively. Tau K18 is constituted by four MBDs and ranges from residue 244 to residue 372 while K19 is similar to K18, but lacks the second repeat [285]. Both constructs efficiently form *in vitro* filaments in the

presence of cofactors such as heparin [286,287]. Although these models have helped clarifying many aspects of tau pathology, their usefulness has now been questioned. In fact, the structure of tau filaments from the brain of AD patients has been recently solved through high resolution cryo-EM [223]. Both PHFs and SFs are formed by an ordered core of pairs of protofilaments with C-shaped subunits and comprising residues 306-378 of tau, but they differ in the symmetry of the protofilament packing. The disordered N- and C-termini form the fuzzy coat.

The same group reported also the cryo-EM structures of the tau filaments from PiD (3R) [288] and CTE [289] and CBD [290] (4R), all extending up to residue 380 of the human tau sequence and confirming the existence of distinct molecular conformers of assembled tau, that differ between diseases [291]. When compared to the widely used tau K18 and K19 constructs, the absence of the C-terminal residues involves the formation of different structures, not resembling the ones of *in vivo* filaments [223]. Moreover, the use of cofactors, such as heparin, should be considered, since it has been shown that heparin-induced amyloid filaments differ significantly from the *in vivo* ones, at least in tauopathies [292].

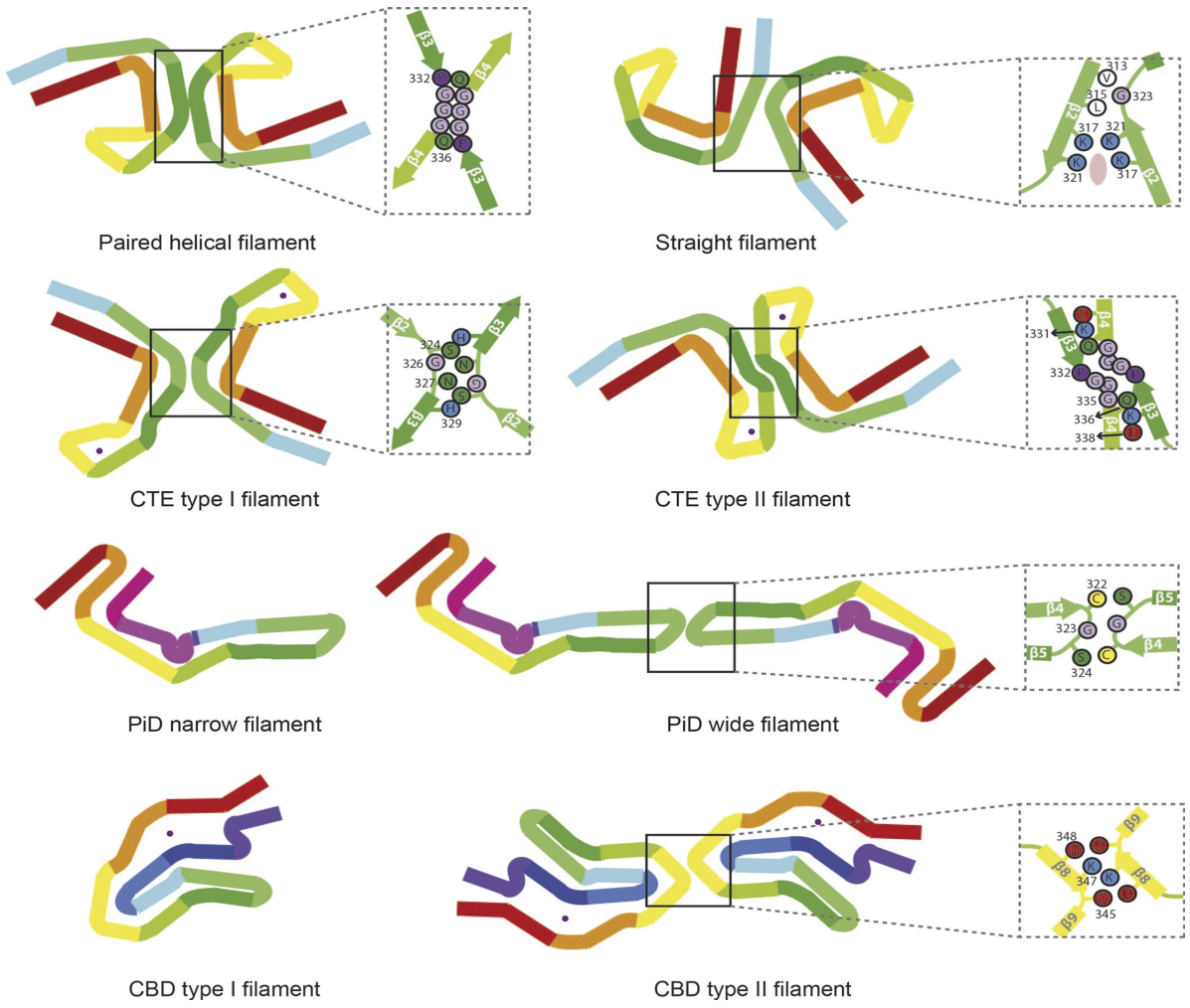

Figure 9. Tau filaments in diseases [291]. Each disease is characterized by two filament types. Two protofilaments are present in AD PHFs and SFs and in CTE type I and II filaments. Single or double protofilaments are seen in PiD and CBD.

The *in vitro* aggregation of tau seems to follow a nucleation-dependent mechanism. Following this process, tau monomer, in its paperclip conformation, needs to partially misfold in order to self-assemble and form an aggregation-competent nucleus [293]. This phase, known as "lag phase", can be accelerated by the addition of preformed fibrillar tau seeds or cofactor molecules and it is thought to represent the rate-limiting step in the aggregation process due to kinetic barriers [294]. Soluble tau monomers are then incorporated progressively into amyloid fibrils during the elongation phase, enabling the growth of the fibrils [295]. Secondary nucleation events and fragmentation of fibrils may contribute to further tau fibrillization. When the maximum number of monomers is incorporated into fibrils, the reaction reaches the plateau.

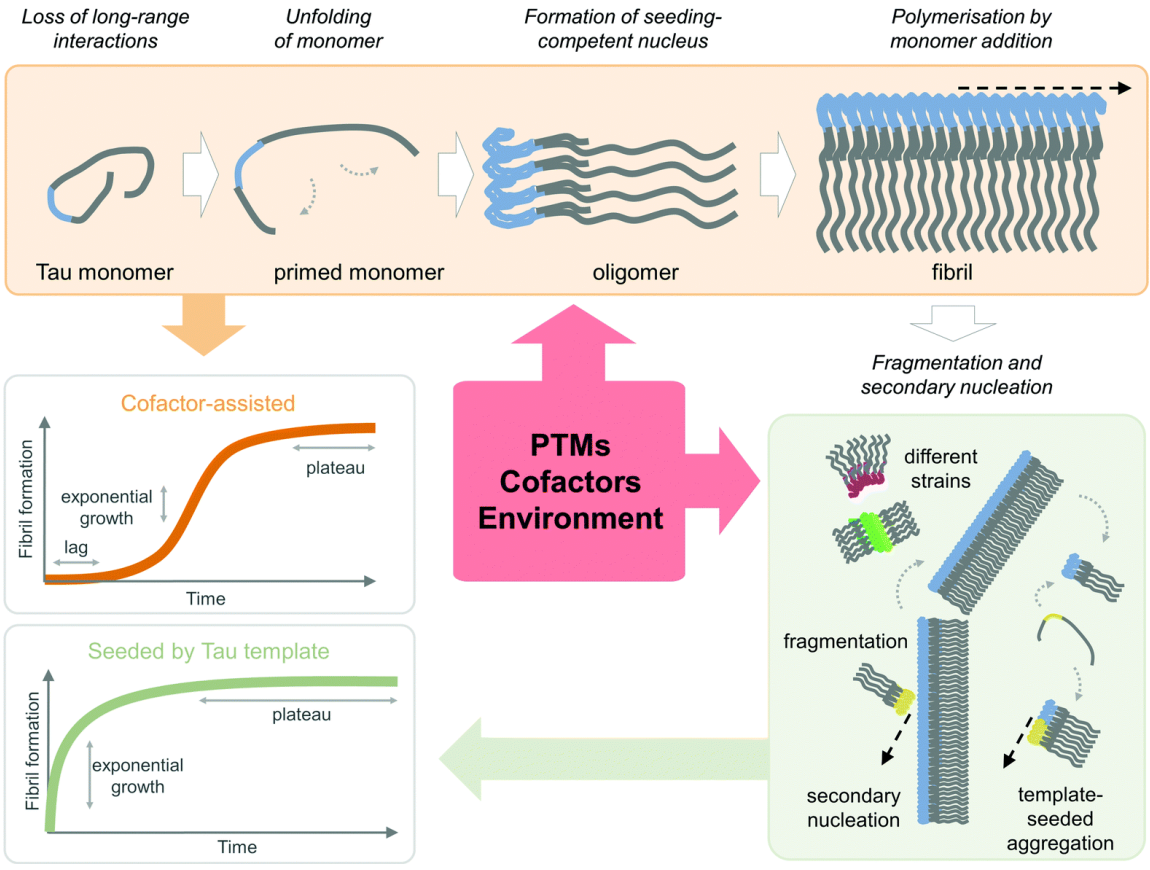

Figure 10. Tau *in vitro* fibrillization mechanism [277]. Tau aggregation is thought to start when the monomers lose their paperclip conformation and start to assemble forming seeding-competent nuclei, necessary for fibril polymerisation. Fragmentation and secondary nucleation can contribute to further tau aggregation. Several conditions such as post-translational modifications (PTMs) and cofactors can influence tau aggregation. Seeded tau fibrillization usually results in the loss of the lag phase and in an exponential curve kinetics.

The *in vivo* mechanism of tau aggregation remains unclear, but it may follow the same model. During amyloidogenesis, highly heterogeneous oligomeric tau species are formed and they are suggested to be converted into amyloid fibrils [296]. Oligomers are considered the most toxic species, thought to disrupt membranes integrity [297], to interact with other proteins [298], to cause mitochondrial and synaptic disfunctions [299] and to inhibit LTP [300]. NFTs formation may represent a protective response and, instead of being directly toxic, it might sequester toxic monomers or oligomers [301]. However, in the longer term, NFTs might compromise cell functions, sequestering other components and impairing axonal transport [107].

1.6.5. Tau spreading

According to the prion-like hypothesis of tau propagation, the pathology should initially start in one neuron. Then, pathological tau is released in the extracellular space to be internalized by another cell, where it can act as a seed for the misfolding of the intracellular tau.

In the extracellular environment, tau has been found both as free protein [302,303] and associated to extracellular vesicles (EVs) such as exosomes [304] and microvesicles [305]. Moreover, extracellular tau was observed either in its truncated monomeric forms [306], or as oligomers [307,308] and fibrillar aggregates [260,309], potentially contributing to the spreading of the pathology.

The internalization through a temperature-dependent process suggests an active process of endocytosis of both monomeric and aggregated tau species [20].

CME was seen to be involved in the uptake of monomeric tau but not of tau assemblies, that seem to follow a dynamin-dependent CIE [310]. The use of dynasore, a dynamin inhibitor, decreased tau propagation, suggesting an involvement of CME in tau uptake [311], even though dynamin activity is not exclusively linked to CME [312]. Moreover, the inhibition of clathrin function does not affect the uptake of tau aggregates or oligomers [313,314], as well as the one of recombinant fibrils [315].

Among CIE, the role of dynamin is still under debate, since some papers reported no role in the internalization of tau fibrils [315] or oligomers [314] while, in contrast, Wu and colleagues reported a decreased tau aggregate endocytosis following dynasore incubation [313]. Interestingly, the inhibition of actin polymerisation was seen to decrease the uptake of tau fibrils, suggesting a role of macropinocytosis in this process [315].

Tau uptake mechanisms were also suggested to occur through the interaction with other partners. The knockdown of LRP1 completely abolished the uptake of tau monomers and oligomers, while only partially reduced the one of fibrils [316]. The involvement of LRP1 in tau uptake was also assessed *in vivo,* where the LRP1 expression was found to mediate tau spreading throughout the brain [316].

HSPGs were also proposed to mediate tau uptake since the treatment with sodium chlorate, which prevents the sulfation of HSPGs, or with heparin, was shown to block the uptake of aggregated tau [315]. Furthermore, the co-injection of tau fibrils and heparin in mice significantly reduced tau internalization, confirming the role of HSPGs also *in vivo* [315]. Moreover, HSPGs seem to mediate the internalization of specific tau conformers, as demonstrated by a work in which the heparin administration highly affected the internalization of tau oligomers from AD brain, but not the one of PSP tau, that was only slightly affected [314]. Moreover, syndecans, belonging to HSPGs family, seem to mediate the specific uptake of tau fibrils in a lipid microdomain dependent pathway involving also flotillins [317].

Recently, an intensive area of study concerns the interaction between tau and other pathological proteins such as α-synuclein, Aβ and prions. For instance, the interaction with Aβ increases the uptake of tau in different cell models and this effect is in part dependent on HSPGs [318]. Moreover, the knockdown of the cellular prion protein caused a significant reduction in the uptake of tau fibrils, suggesting an interplay between these two proteins [114]. Both extracellular monomeric and fibrillar tau species activate the formation of TNTs, and tau fibrils were found inside these structures, facilitating their transfer between neurons [319]. The *in vivo* involvement of TNTs is currently unknown.

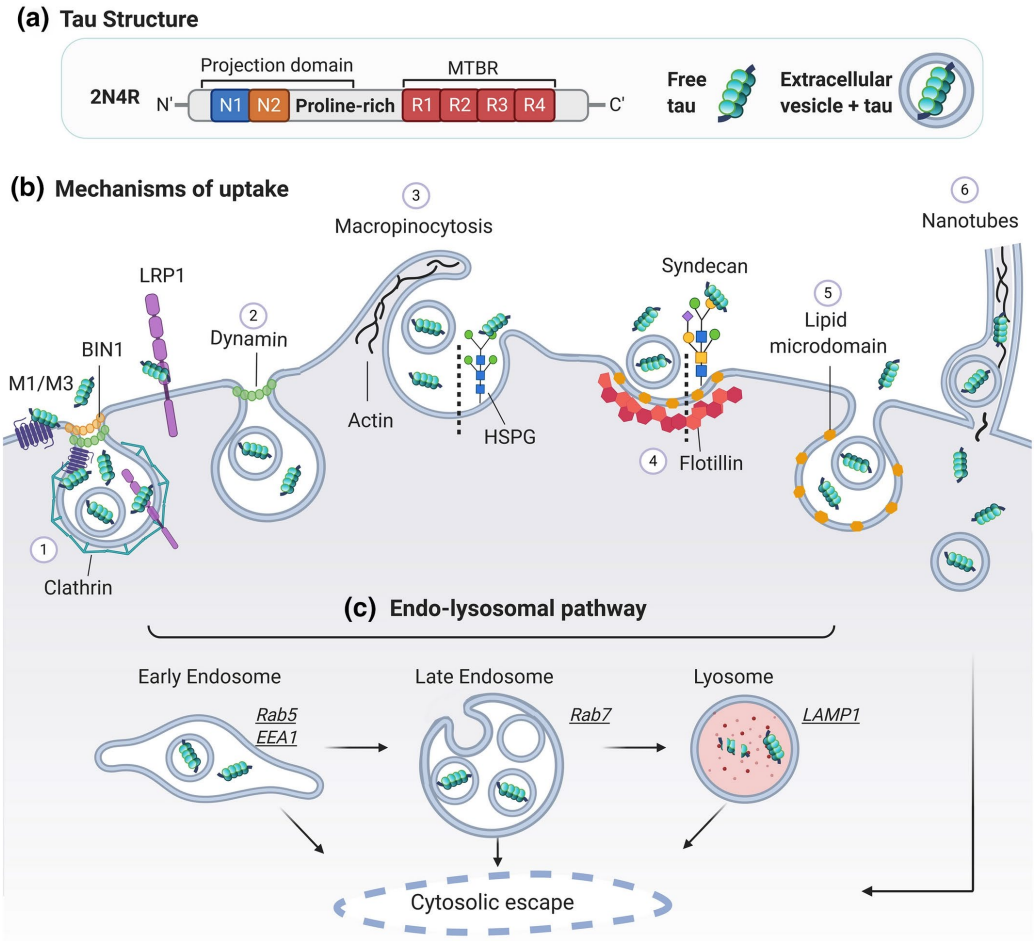

Figure 11. Tau internalization mechanisms [312]. (a) 2N4R tau isoform and its functional domain. In the extracellular environment tau can be present as free tau or associated to extracellular vesicles. (b) Tau uptake mechanisms. (1) Muscarinic acetylcholine receptor subtypes M1 and M3, BIN1 and LRP1 are all associated with tau CME; (2) dynamin was involved both in CME and CIE; (3) HSPG binding facilitates tau uptake via macropinocytosis; (4) (5) Syndecans are members of HSPG family mediating tau uptake in lipid microdomains in a flotillin-dependent or independent way; (6) TNTs are responsible for the transfer of tau between cells. (c) Following the uptake, tau enters early endosomes which mature in late endosomes and then in lysosomes. From these compartments, tau can be released in the cytoplasm.

Following endocytosis, tau escapes the endosomal membranes to act as a seed for further tau molecules. The distinction between endosomal and cytosolic tau populations is complicated by the lack of tools. Recently, a new assay relying on the split luciferase NanoLuc binary technology system (NanoBiT) was developed and it could be helpful to overcome this problem [320]. After being endocytosed, monomeric and fibrillar tau reach Rab5- and EEA1-positive early endosomes [310,311,314], Rab7-positive late endosomes and lysosomes [313,321]. Even though this process seems conserved also in human neurons [322], recent evidence suggest that it may vary according to the tau conformers involved [314].

From the intracellular environment, tau can be secreted through direct translocation across the plasma membrane [323], and this event seems to be influenced by the membrane properties [308]. Moreover, also late endosomes could participate in tau exocytosis, since Rab7a depletion was shown to affect tau secretion [324].

As mentioned before, tau was also found in exosomes, resulting from the fusion of MVBs with the plasma membrane, and in microvesicles, even though the fraction of tau associated with extracellular vesicles is very small [325].

Despite the transfer of tau between cells has been widely demonstrated, its exact mechanisms need to be still clarified and they might represent a useful target to block tau spreading in pathologies.

1.6.6. Tau strains

The ability of tau to spread in a prion-like manner was demonstrated by experiments in which the injection of brain extracts from mutant P301S tau-expressing mice into WT mice induced the deposition of tau filaments and the spreading of the pathology [326]. The observation that, like prions, other amyloid-forming proteins can mediate the same templated conformational change of their physiological counterparts suggested that they might share other features with PrP^{Sc}. In prion diseases, a strain is described as an infectious particle that, when transmitted, exhibits a specific phenotype [60]. For tauopathies, the existence of specific tau conformers was suggested by experiments in which the inoculation of human brain extracts with distinct diseases into recipient mice produced pathologies that resembled those of the initial inoculum [327]. Moreover, Sanders and colleagues generated a cell line that, when seeded with tau fibrils, produced tau strains differing for morphology, aggregate size, seeding capacity, protease digestion patterns, toxicity, and subcellular localization, and that induced unique pathological phenotypes when inoculated in mice [12]. The same group isolated 18 distinct tau strains from recombinant, mouse, or human sources and, after biochemical and biological characterization, they inoculated them into recipient mice, showing peculiar patterns and propagation rates correlating with the *in vitro* parameters [13].

Different tau folds were found for AD, CTE, PiD and CBD [223,288-290] and each peculiar structure is maintained in individuals with the same disease. Recently, Shi and colleagues characterized further 14 tau conformations, some resembling the AD ones and others completely unexpected [188]. In most cases, individuals with the same disease exhibit the same tau strain.

As a result, the authors proposed a structure-based classification of tauopathies which complements clinical diagnosis and neuropathology [188].

Whether tau fibrils are a consequence of the disease or a cause needs to be addressed, but it seems unlikely that so many variations of the same protein could represent a secondary consequence [328]. The authors' findings may also suggest that many different strains can be formed in the healthy brain, but that specific tauopathies favour the propagation of a specific strain in certain cell types, as it was suggested for prions [329]. Alternatively, each fibril type may be specific for each disease according to the specific damage that it can exert on cells.

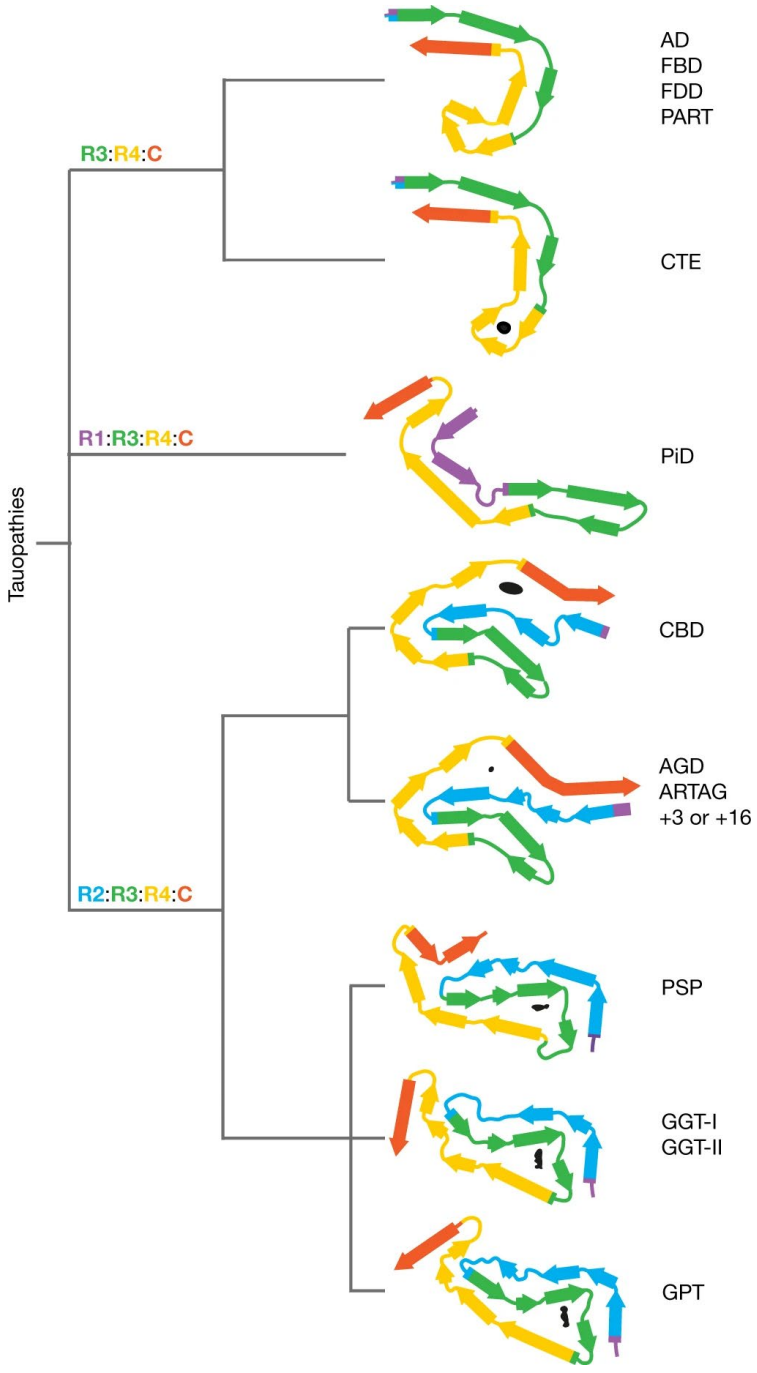

Figure 12. Structure-based classification of tauopathies [188]. Structure of filaments found in tauopathies. FBD, familial British dementia; FDD, familial Danish dementia; ARTAG, aging-related tau astrogliopathy; GPT, GGT-PSP-Tau fold.

1.7. Prion diseases and tau pathology

Neurodegenerative diseases are often seen as separate entities in which only one protein misfolds and accumulates in the brain, leading to neuronal death. However, the concept of "multiproteinopathies" is now arising, according to which many different proteinopathy combinations can be found, especially in the aging brain [6]. The most striking example is found in AD, with the concomitant deposition of Aβ and tau, but many other pathologies showed co-occurrence in a very high rate [330].

Many works reported the presence of tau pathology in inherited prion diseases. In GSS with the *PRNP* P102L mutation, the presence of NFTs of hyperphosphorylated tau was assessed together with PrP plaques [331-334]. In 1997, a paper from Tranchant and colleagues reported the presence of NFTs in a GSS patient affected by the A117V mutation in the prion protein gene. Interestingly, tau deposition could be correlated with the old age of the patient or with the protracted duration of the disease, since the affected individual showed the longest clinical course in his family [335]. A later study suggested that tau accumulation, colocalizing with PrP plaques, might derive from PrP accumulation, and not from Aβ, as poor and diffuse Aβ deposits were detected [336]. A large number of phospho-tau immunoreactive deposits were found also in vCJD patients, clustering around PrP plaques and in the absence of Aβ [337]. The presence of hyperphosphorylated tau was later demonstrated in sCJD patients, also in the absence of amyloid plaques [338].

Although it has been extensively described, the hyperphosphorylation of tau in prion diseases is still unclear and there is no established correlation with the duration or with the clinical course of the disease. Even the connection between these two proteins remains obscure, even though a possible mechanism was described by Pérez and colleagues, who showed that PrP 106-126 peptide, a model construct used to study prion-induced neurodegeneration, increased the activity of glycogen synthase kinase 3 (GSK-3) and the consequent phosphorylation of tau [339]. Moreover, as discussed before, the cellular prion protein acts as a receptor for several amyloid species, promoting their neurotoxic effects and accelerating their spreading.

Interestingly, a similar interplay between prions and other amyloid fibril-forming proteins was described by previous works of our laboratory. α-synuclein amyloid fibrils were seen to

reduce prions burden when administered to neuroblastoma cell lines infected with the RML prion strain [120]. Similarly, recombinantly produced tau K18 amyloid fibrils were found to decrease PrP^{Sc} level, probably because of a direct interaction with PrP^{C}, hindering the conversion event [114].

AIM OF THE RESEARCH

Since different proteins, normally associated to distinct neurodegenerative diseases, were found to co-deposit and to originate a wide spectrum of multiproteinopathies, many works have focused their attention on identifying the mutual relationships between these proteins and their effect on the diseases.

Recently, the cellular form of the prion protein, PrP^{C}, has been identified as one of the putative receptors for many aggregation-prone proteins, such as Aβ, tau and α-synuclein, mediating their toxic effects and accelerating their spreading throughout the brain. Moreover, many forms of prion diseases, characterized by the deposition of the pathogenic form of the prion protein, PrP^{Sc}, develop other protein aggregates, such as tau tangles.

In this regard, in our previous work, we showed an interaction between PrP^{C} and fibrils produced *in vitro* from the truncated construct of tau named K18. Moreover, the administration of tau K18 fibrils in cultured N2a cells resulted in an increased uptake of these fibrils in PrP^{C}-expressing cells compared to the PrP KO ones and in the increased retention of PrP^{C} at the plasma membrane. Surprisingly, the same fibrils were found to reduce the amount of prions when administered to chronically prion infected ScN2a cells, probably because of their binding to PrP^{C}, inhibiting the conversion event.

However, we were unable to exclude whether, besides PrP^{C} binding, tau fibrils could affect prion load by other mechanisms. Therefore, we decided to explore further this effect by:

- Exploiting, together with tau K18, also another construct of tau, named 244-378, that encompasses the sequence shown to represent the core of PHFs and SFs in AD affected brains and that could lead to the formation of fibrils with a different structure. *In vitro* produced tau fibrils from both constructs were used to assess their ability to affect prion load in ScN2a cells.

- Evaluating the possible role of other tau fibrils-mediated mechanisms in reducing PrP^{Sc} load, to establish a link between these two aberrantly folded entities and to shed light on the pathological implications in those diseases in which these proteins were found to co-deposit.

MATERIALS AND METHODS

2.1. Tau 244-378 cloning

Tau 244-378 construct was obtained through the addition of six amino acids to the C-terminus of the human tau K18 sequence in a pET-11a plasmid, using the restriction-free (RF) cloning technique [340]. Briefly, Forward and Reverse primers were designed to partially anneal to the C-terminus of the tau K18 sequence, while the other part is not complementary and represent the sequence ACCCACAAGCTGACCTTC encoding for the amino acids 373-378 (THKLTF). A first polymerase chain reaction (PCR) round was used to obtain and amplify the megaprimers. Being a short sequence, the insert was fully synthesized by the primers themselves, without the need for a template. In the second PCR, pET-11a:HuTauK18 plasmid was added to the reaction to allow the insertion of the desired sequence (Fig. 13).

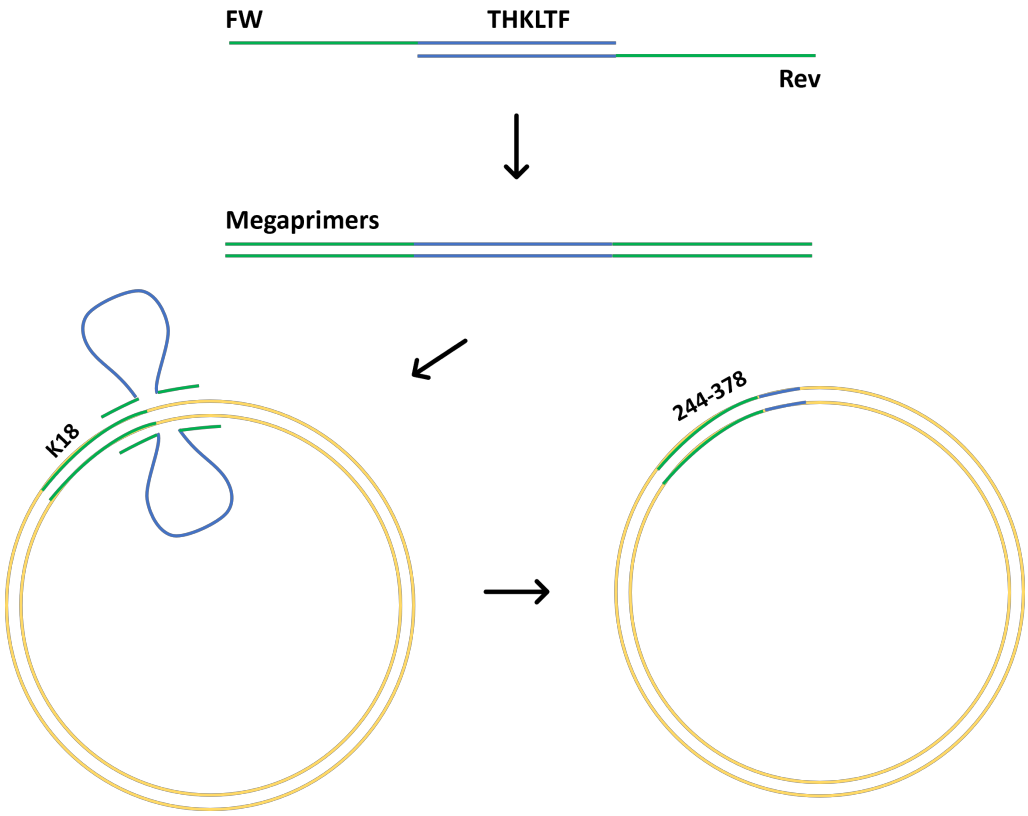

Figure 13. RF-cloning of tau 244-378 construct. Forward (FW) and Reverse (Rev) primers were designed to anneal to the C-terminus of tau K18 sequence in pET-11a plasmid and to contain the sequence encoding for the amino acids THKLTF, that will extend the C-terminus of tau K18. A first PCR round was used to extend and amplify the primers, to produce two megaprimers that were used in a second PCR round to insert the desired sequence.

Finally, 20 units of DpnI (New England Biolabs) were added and the mixture was incubated for 2h at 37° C followed by 20 minutes at 80° C to stop the reaction. DpnI is used to degrade any methylated parental plasmid. Finally, *E. coli* DH5α competent cells were transformed with the obtained reaction mixture and plated in a Luria-Bertani-Agar plate complemented with 100 µg/mL Ampicillin (PanReac Applichem) and incubated at 37° C overnight. The DNA from the resulting colonies was extracted and sequenced to verify the insertion of the desired sequence.

2.2. Tau expression and purification

The expression and purification of Human Tau K18 and Human Tau 244-378 proteins were performed as previously described by Barghorn et al. [341]. pET-11a plasmids containing the sequences encoding for Tau K18 and Tau 244-378 were transformed in *E. coli* BL21 (DE3) (Stratagene). 100 mL of overnight culture were inoculated in 2 L of Luria-Bertani medium complemented with 100 µg/mL ampicillin (PanReac Applichem) and grown at 37° C with 180 rpm shaking until 0.6 $O.D._{600}$. The expression of the proteins was induced with 0.8 mM Isopropil-β-D-1-tiogalattopiranoside (IPTG) (PanReac Applichem) and cells were grown for 6h at 30° C to minimize protein degradation. Cells were harvested by centrifugation and lysed by using PandaPlus Homogenizer (GEA) at 4° C in the presence of protease inhibitors (Complete™ ULTRA Tablets, EDTA-free, glass vials Protease Inhibitor Cocktail, Roche). The homogenates were subjected to a precipitation step boiling the solution for 20 minutes, to precipitate most of the proteins except for tau. The resulting supernatants were loaded onto a cation exchange chromatography column HiTrap SP FF (Cytiva) in Binding Buffer (20 mM MES, 50 mM NaCl, 1 mM EDTA, 0.1 mM MgCl2, 2 mM DTT, 0.1 mM PMSF, pH 6.8) and eluted with a linear gradient from 0 to 60% of Elution Buffer (20 mM MES, 1 M NaCl, 1 mM EDTA, 0.1 mM MgCl2, 2 mM DTT, 0.1 mM PMSF, pH 6.8). Fractions were analysed by Sodium Dodecyl Sulphate - PolyAcrylamide Gel Electrophoresis (SDS-PAGE) and the fractions containing the protein of interest were loaded onto a size-exclusion chromatography (SEC) column (Superdex 200 26/60, Cytiva) in phosphate buffer saline 1X (PBS 1X) pH 7.4. Purified proteins were analysed by SDS-PAGE, dialysed against water, lyophilised and stored at -80° C. All salts were from Sigma-Aldrich.

2.3. Fibrillization of tau proteins

Fibrillization reaction was performed in a 96-well black plate with transparent bottom (BD Falcon), with a 3 mm glass bead in each well (Sigma-Aldrich). All the reagents were filtered with a 0.22 µm filter before use. The 200 µL final volume mixture was composed of tau K18/244-378 0.5 mg/mL, 0.1 mM DTT and 50 µg/mL heparin in PBS 1X pH 7.4. Due to its toxicity to cultured cells, 10 µM Thioflavin T was added only in three wells to monitor the real-time aggregation. The plate was covered with a sealing tape (Fisher Scientific) and it was incubated at 37° C in orbital shaking (50s of 400 rpm shaking and 10s of rest) in FLUOstar Omega Microplate Reader (BMG LABTECH). Fluorescence was monitored every 30 minutes by bottom reading at 444 nm of excitation and 485 nm of emission. The reaction was stopped after 40h, fibrils pelleted by centrifugation at 186.000xg for 1 hour at 4° C, resuspended in 1 mL of 1X PBS pH 7.4 and stored at -80°C. Before use, aliquots were sonicated for 5 minutes in a sonicator Misonix s3000 at 250 W.

2.4. Transmission electron microscopy (TEM) analysis

10 µL of tau K18/244-378 fibril solution was dropped onto 200-mesh Formvar-carbon coated nickel grids (Electron Microscopy Sciences) for 20 min after which samples were stained with 25% Uranyl Acetate Replacement (UAR, Electron Microscopy Sciences) for 10 min. Before the analysis, the staining solution was removed using Whatman filter paper and the grids air-dried for 5 minutes. Samples were visualized using a FEI Tecnai Spirit Transmission Electron Microscope operating at 120 kV and equipped with an Olimpus Megaview G2 camera.

2.5. Cell cultures

Mouse neuroblastoma cells N2a were kindly provided by Prof. Chiara Zurzolo (Unité de traffic membranaire et pathogenèse, Institute Pasteur, Paris, France). ScN2a cells are clones persistently infected with the RML prion strain as described by Prusiner's group [342]. Cells were kept in culture at 37° C and 5% CO_2 in humified atmosphere with minimal essential medium (MEM) + GlutaMAX (Thermo Fisher Scientific) supplemented with 10% fetal bovine serum (Euroclone), 1X non-essential amino acids (Euroclone) and 1X penicillin-streptomycin solution (Euroclone), and they were split every 3-5 days using Trypsin-EDTA 1X solution (Sigma-Aldrich).

2.6. Tau K18 fluorophore-labelled fibrils

Tau K18 fibrils were conjugated to Alexa Fluor™ 488 NHS Ester (Succinimidyl Ester) (Thermo Fischer Scientific) according to the manufacturer's instruction. Tau K18 fibrils were ultracentrifuged at 186.000xg for 1h at 4° C, resuspended in 250 µL (2 mg/mL final concentration) of 0.1 M sodium bicarbonate buffer pH 8.3 and sonicated for 5 minutes. 5 µL of 10 mg/mL reactive dye were added to the fibril mixture and incubated for 1 h at room temperature in stirring. The unbound fluorophore was removed by three subsequent dialyses against sterile PBS pH 7.4 in gamma-irradiated Slide-A-Lyzer dialysis cassettes with a molecular weight cut-off of 3.5 kDa (Thermo Fisher Scientific). Fluorescent fibrils were aliquoted and stored at -20° C.

2.7. Tau fibril treatments

Tau K18 and 244-378 sonicated fibrils, at different concentrations, were directly added to the medium of ScN2a cells cultured in 6 or 10 cm plates. The treatment was performed for variable amount of time according to the experimental setting. In some experiments, not internalized fibrils were removed with trypsin after washing cells with PBS 1X.
For fluorescence experiments, 2 µM of tau K18-Alexa488 fibrils were administered to ScN2a cells cultured in 12-well plates and incubated according to the experimental setting.

2.8. Analysis of internalized tau amyloids

For the evaluation of Alexa-488-tau K18 fibril internalization, cells were incubated for 4h at 37° C or 4° C in the presence of 2 µM of tau K18 fibrils. Then, cells were washed twice with PBS and incubated for 5 min with 1:1 of Trypan Blue in PBS solution before fixation, to quench the fluorescence coming from extracellular tau fibrils [343]. Cells were then rinsed three times in 1X PBS and fixed with 4% Paraformaldehyde (Sigma-Aldrich) for 30 minutes. Permeabilization was performed for 5 minutes in 0.1% Triton X-100 (Sigma-Aldrich) in PBS and coverslips were stained with HCS CellMask™ Blue Stain (Thermo Fischer Scientific) 1:2500, labelling whole-cell cytoplasm. Coverslips were mounted with Fluoromount-G™ (Thermo Fischer Scientific) and stored at 4° C. Images were acquired using a Nikon confocal microscope (Nikon A1plus).

2.9. Metabolic cell activity and cell count

The influence of tau 244-378 amyloid fibrils was evaluated with 3-(4,5-dimethylthiazol-2-yl)-2,5-diphenyltetrazolium bromide (MTT) assay. 10.000/well ScN2a RML cells were plated in a 96-well and, the day after, different concentrations of sonicated tau 244-378 fibrils were directly added to the medium and cells were incubated for 72h. Cells were then incubated for 3h at 37° C with 20 µL of 5 mg/mL of MTT (Sigma-Aldrich) solution in PBS 1X followed by the solubilization with 1:1 DMSO/2-Propanol solution. The absorbance was measured at 570 nm in Enspire™ multimode plate reader (PerkinElmer) with a reference wavelength of 650 nm. Each condition was tested in six replicates and in three independent experiments.

Tau 244-378 fibril effects on proliferation and cell death were assessed by cell counting. 15.000/well ScN2a RML cells were plated in a 12-well and the day after were treated with 2 µM tau 244-378 fibrils. Cells were left in incubation up to 72h after which they were detached with trypsin and counted using Scepter 2.0 Handheld Automated Cell Counter (Millipore) with 60 µM sensors. Three independent experiments were conducted, each one in three technical replicates.

2.10. ScN2a treatments

To test the contribution of cellular degradation pathways, ScN2a RML cells were incubated for 72h with tau K18 fibrils and 10 mM 3-methyladenine (Sigma-Aldrich), 100 mM Bafilomycin A1 (Sigma-Aldrich) or 50 µM Cloroquine were added 16h before lysis. For the inhibition of proteasomal activity, 5 µM of MG132 (Sigma-Aldrich) were added 16h before lysis.

To block tau fibril endocytosis, ScN2a RML cells were pre-incubated for 10 minutes at 37° C or 4° C, after which 2 µM of tau fibrils were directly added to the medium and cells were kept in culture for 4h at 37° C or 4° C. Then, cells were washed twice with 1X PBS to remove the treatment and were kept in culture up to 72h at 37° C.

2.11. Western blotting

After culturing them, ScN2a cells were rinsed in 1X PBS and resuspended in lysis buffer (10mM Tris HCl, 150mM NaCl, 0.5% NP-40, 0.5% Sodium deoxycholate). Lysates were centrifuged for 5 minutes at 5900xg at 4° C. Total protein content was quantified using bicinchoninic acid assay (BCA) (Sigma-Aldrich). 20 µg of proteins were diluted in 2X loading buffer (10% Glycerol, 50 mM Tris-HCl, 2% Sodium dodecyl sulfate, 4M Urea, Bromophenol

blue and fresh-added 200 mM Dithiothreitol) and samples were boiled for 10 minutes at 100° C.

Samples were loaded in 12/15% Tris-Glycine SDS-PAGE gels and transferred onto Immobilon P PVDF membranes (Millipore) for 2 hr at 4° C. Membranes were blocked in 5% non-fat milk in TBS-T and incubated overnight at 4° C with anti-PrP W226 1:1000 [344], anti-tau 7.51 1:500 [345], anti-LC3B 1:1000 (Cell Signaling) antibodies. After three washes in TBS-T, membranes were incubated with goat-anti-mouse IgG horse-radish peroxidase-conjugated antibody (Dako) for 1h at room temperature and they were visualized using Immobilon Classico Western HRP substrate (Millipore). Anti β-actin-HRP antibody 1:10.000 (Sigma-Aldrich) was incubated for 1h at RT and used for normalization. Images were acquired using Uvitec Alliance (Cambridge), and Uviband software was used for densitometric analysis.

2.12. Proteinase K digestion

To detect PrP^{Sc} content, 150 ug of total proteins were digested with 20 µg/mL of proteinase K (Sigma-Aldrich) at 37° C for 1h. The reaction was stopped by adding 2 mM of phenylmethylsulphonyl fluoride (PMSF, Sigma-Aldrich) and samples were ultracentrifuged for 1h at 186.000xg at 4° C. The resulting pellet was resuspended in 1X loading buffer and boiled for 10 minutes.

To assess fibril resistance to PK digestion, 2 µg of K18 or 244-378 fibrils were digested with 0.1, 1, 10, 100 µg/mL of PK for 1h at 37° C. 2 µg of tau K18 fibrils were also digested with 100 µg/mL of PK for 1, 2, 4, 8 and 24h at 37° C.

2.13. Immunofluorescence

For cell organelles colocalization experiments, 30.000 ScN2a RML cells were plated in 12-well plates with a 12 mm coverslip coated for 1h with Poly-L-lysine hydrobromide (Sigma-Aldrich) 100 µg/ml. The day after, cells were treated with 2 µM Alexa-488 tau K18 fibrils and they were incubated for 24h. Cells were then rinsed in 1X PBS twice and fixed with 4% paraformaldehyde (PFA) in PBS for 30 minutes. After permeabilization with 0.1% Triton X-100, coverslips were incubated for 1h with blocking buffer (7% normal goat serum, 1% bovine serum albumin, 0.1% Triton X-100 in 1X PBS) and then for 1h and 30 minutes with primary antibodies (anti-calnexin 1:500 (Abcam), anti-M6PR 1:500 (Abcam), anti-EEA1 1:500 (Abcam), anti-LAMP2 1:100 (Abcam), anti-LC3B 1:200 (Cell Signaling)) in blocking buffer. After three PBS washes, coverslips were incubated with the appropriate secondary Alexa-488/594-

conjugated antibody (Invitrogen) for 1h and nuclei were counter-stained with DAPI 0.5 mg/mL before the mounting with Fluoromount-G™ (ThermoFisher Scientific) and the storage at 4° C. Images were acquired with Nikon confocal (Nikon A1plus) as series of z-stacks, 0.25 µM step, 512x512.

2.14. *De novo* prion infection

De novo prion infection of N2a cells was performed as previously described [346] with some modifications. Briefly, 150.000 N2a cells were plated in 12-well plates and, the day after, they were pre-treated with 2 or 4 µM tau K18/244-378 amyloids for 4h; subsequently, cells were washed twice with PBS 1X to remove the treatment before the addition of the seed. PrP^{Sc} seed was prepared scraping a 10 cm plate of ScN2a RML and sonicating cells in ice 2x5s at 70% amplitude (Sonics VCX 130 PB). Total protein content was quantified using BCA and 100 µg of proteins were added to N2a in a final volume of 500 µL of completed MEM without penicillin-streptomycin. Cells were kept in incubation with the seed for 72h after which cells were detached with trypsin and plated 1:2 in a 6 cm plate. Cells were split two more times every 4 days at 1:5 dilution, and the rest was pelleted and resuspended in 50 µL of lysis buffer and analysed in WB for PrP^{Sc} presence. In all passages, penicillin-streptomycin solution was omitted. Passage 1 was not analysed for PrP^{Sc} to remove the signal deriving from the initial seed.

RESULTS

3.1. Production and *in vitro* fibrillization of tau 244-378

As previously mentioned, the administration of tau K18 amyloid fibrils to prion infected ScN2a cells decreases prion load after 72h of incubation [114]. We decided to explore further this effect by exploiting, together with tau K18 (amino acids 244-372), also another construct made of the amino acids 244-378 of the human tau sequence. The last six amino acids were seen to be important for the formation of the structure of PHFs core [223] and their addition could generate filaments with a different structure compared to the one of K18 filaments. RF-cloning technique was used to extend the C-terminal part of tau K18 sequence (Fig. 14a) in pET-11a plasmid adding the six missing amino acids to obtain the 244-378 construct. The DNA obtained from the transformed colonies was sequenced to check the insertion of the right sequence (Fig. 14b).

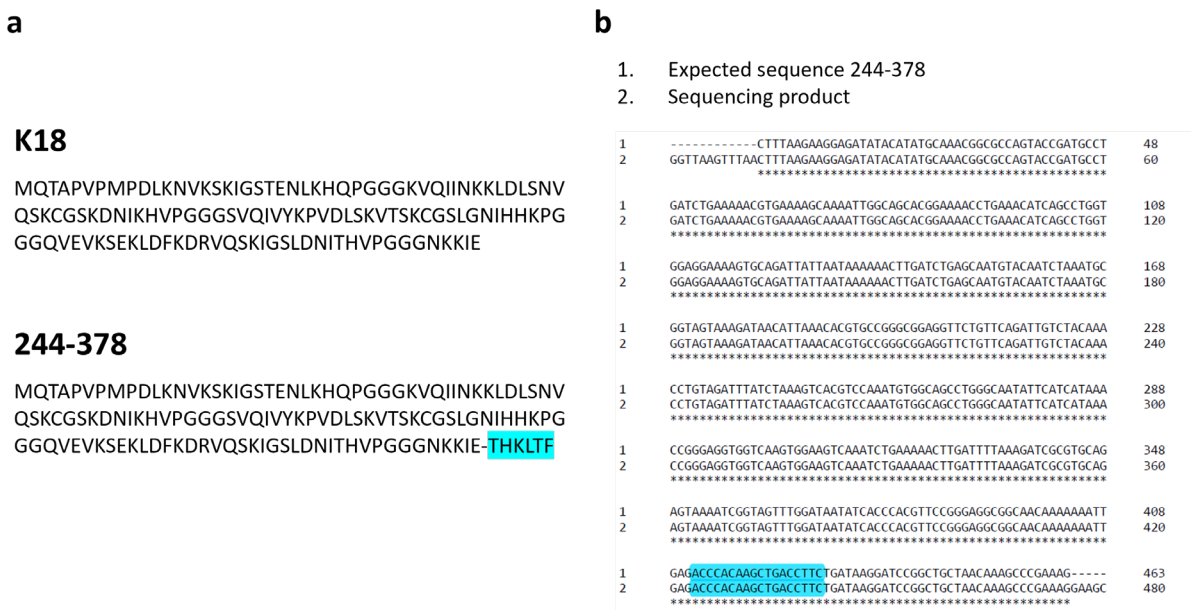

Figure 14. RF-cloning of tau 244-378 construct. (a) Amino acid sequences of tau K18 and tau 244-378. In blue the six amino acids added to tau K18 to produce the 244-378 construct. (b) Alignment of the expected 244-378 nucleotide sequence (1.) and the product obtained from RF-cloning (2.) with in blue the nucleotide sequence encoding for the added six amino acids.

The obtained pET-11a containing the sequence encoding for tau 244-378 was transformed in *E. coli* BL21 (DE3). The expression of the protein was induced with IPTG and the protein purified according to the protocol of Barghorn and colleagues [341]. After two subsequent steps

of chromatography (Fig. 15a), the purity of the protein was assessed by SDS-PAGE. Figure 15b shows a comparison between tau 244-378 and tau K18 and the difference in their molecular weight.

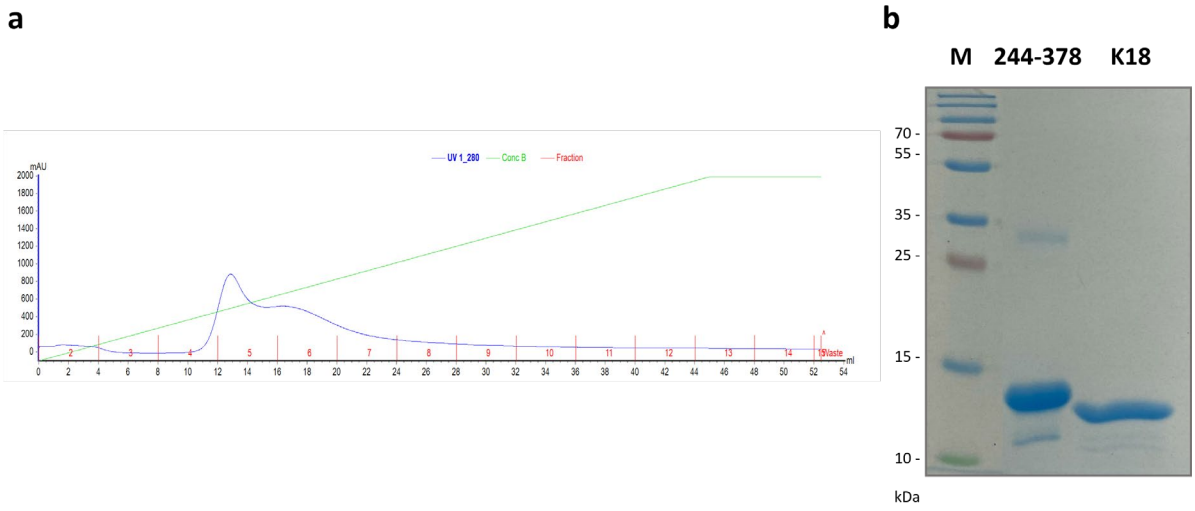

Figure 15. Human tau 244-378 protein purification. (a) Representative chromatogram of tau 244-378 elution. Fractions corresponding to the peaks in the absorbance were further purified through SEC. (b) SDS-PAGE of tau 244-378 (~14,5 kDa) and tau K18 (~13,8 kDa).

Both K18 and 244-378 tau proteins were subjected to an *in vitro* fibrillization protocol to produce amyloid fibrils in the presence of heparin. ThT dye was added to the reaction to monitor the misfolding of the soluble proteins and the assembly of β-sheets-rich amyloid fibrils [347]. For both constructs, the same protocol, showed to be effective in producing tau K18 fibrils, was used [114]. The *in vitro* aggregation process for both proteins followed the nucleation-dependent mechanism, and it was constituted by a short lag phase, followed by a rapid elongation phase. After almost four hours, all the monomers were converted to fibrils and the reaction reached the plateau.

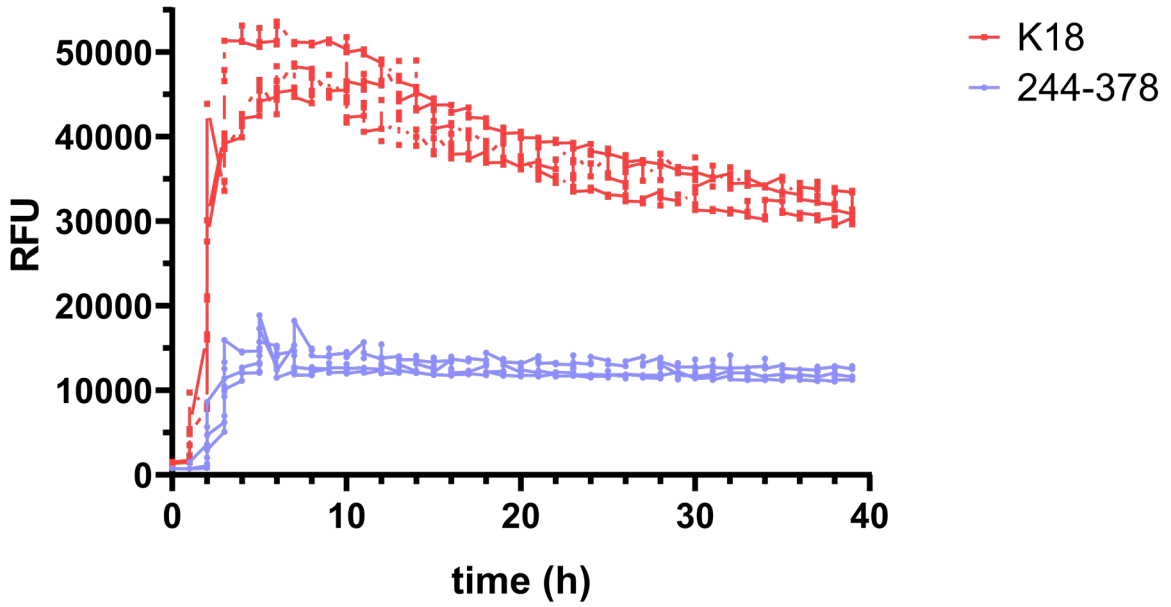

Figure 16. Tau K18 and tau 244-378 *in vitro* fibrillization. Both tau constructs showed a similar aggregation kinetic, with a short lag phase of almost 2h, followed by an exponential phase and a plateau, which was higher in fluorescence values for tau K18. RFU, relative fluorescence unit.

As shown in Fig. 16, both tau K18 and 244-378 presented a similar aggregation kinetic, even though K18 reached a higher fluorescence signal when compared to 244-378. We decided to collect the end-stage products of the fibrillization process and to characterize them by TEM after a small round of sonication to break long fibrils into smaller pieces. TEM analysis showed that both constructs form fibrillary structures *in vitro* (Fig. 17a). To further characterize these new tau fibrils, both *in vitro* fibrillization products were subjected to digestion with increasing concentration of PK followed by WB analysis, because of the known resistance of tau aggregates to protease degradation [348,349]. As shown in figure 17b, both constructs form fibrils characterized by high molecular weights species and by the resistance to denaturation. Moreover, fibrils produced from the tau K18 fragment showed a partial resistance to PK digestion, even at the highest concentration (Fig. 17b, left) and a significant degradation is only observed after 24h of incubation with 100 µg/mL of PK (Fig. 17c). In contrast, tau 244-378 fibrils were way more sensitive to PK (Fig. 17b, right), suggesting that the two tau constructs, differing for six C-terminal amino acids, can assume distinct conformational structures, when subjected to *in vitro* fibrillization.

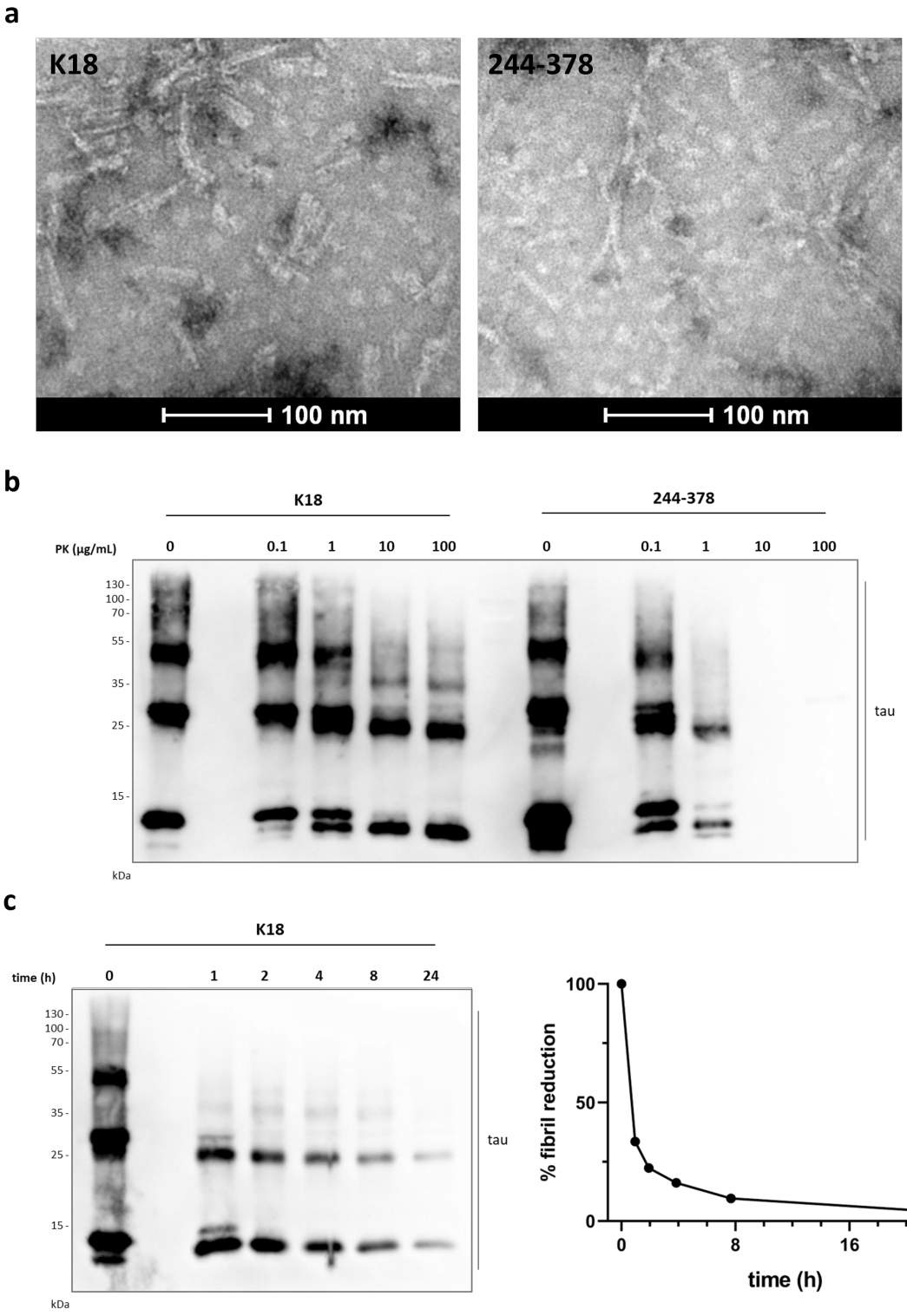

Figure 17. Structural and biochemical characterization of tau K18 and 244-378 fibrils. (a) Transmission electron microscopy images of sonicated K18 (left) and 244-378 (right) tau fibrils. (b) WB analysis of 2 µg of K18 and 244-378 tau fibrils treated with 0, 0.1, 1, 10 and 100 µg/mL of PK for 1h and probed with anti-tau antibody. (c) WB (left) of 2 µg of tau K18 fibrils incubated for 0, 1, 2, 4, 8 and 24h with 100 µg/mL of PK and probed with anti-tau antibody. The graph on the right shows the percentage of fibril reduction in time. $T_{1/2}$ 23.46min.

Before assessing the effect of these fibrils on cultured ScN2a RML cells, we decided to test their effect on cell metabolism by using the MTT assay, which relies on the reduction of the

MTT by succinate dehydrogenase, a mitochondrial enzyme. We tested the effect of different concentrations of tau 244-378 fibrils following 72h of incubation (Fig. 18b), as previously done for tau K18 (Fig. 18a) [114]. When compared to tau K18 fibrils, tau 244-378 fibrils showed a higher significant metabolic effect when administered to ScN2a RML cells, even at the lowest concentration (Fig. 18b). However, as we did not observe any relevant effects on cell viability following cell counting (Fig. 18c), also 244-378 fibrils were used in cell culture experiments.

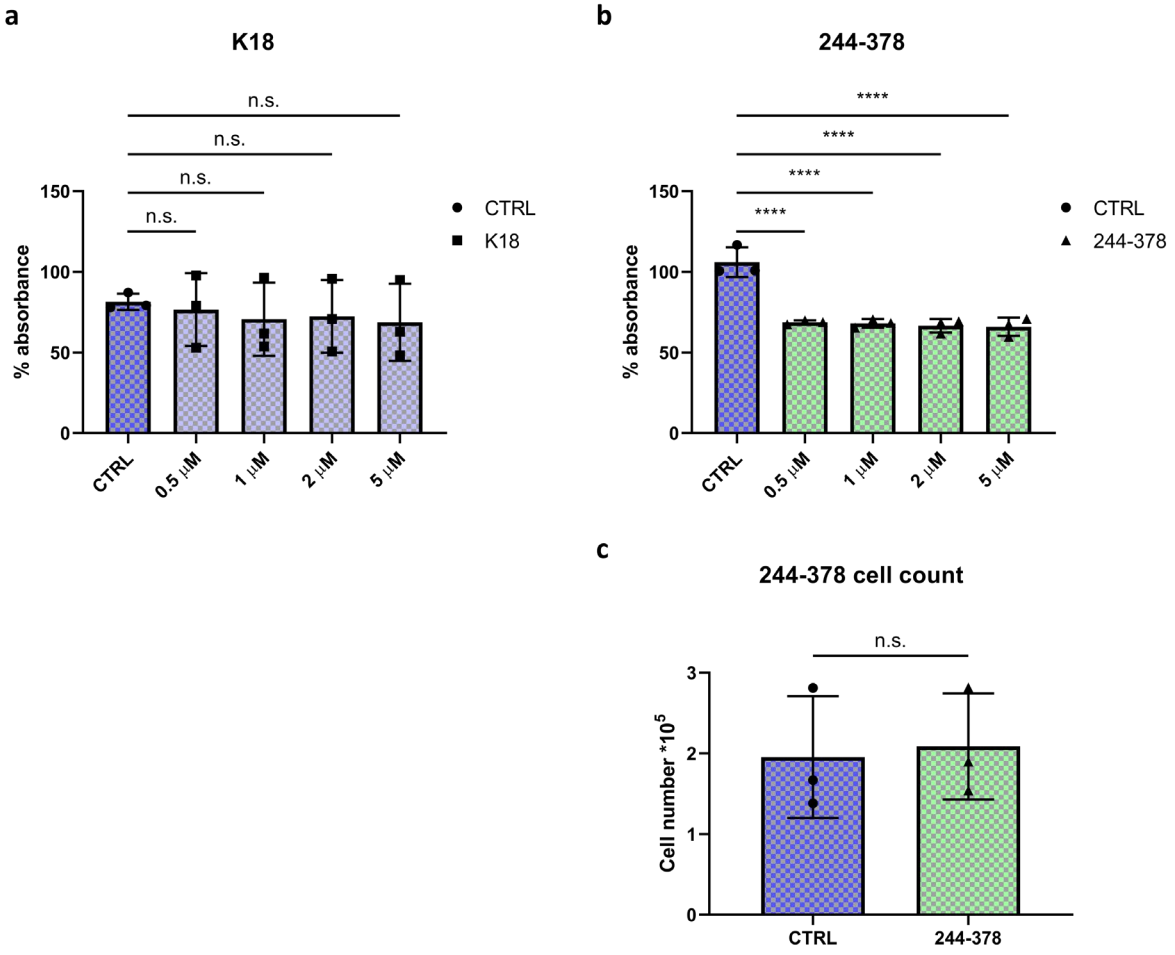

Figure 18. Tau fibril effects in ScN2a RML. (a-b) MTT assay of ScN2a RML cell line treated with different concentrations (0.5 µM, 1 µM, 2 µM, 5 µM) of tau K18 (a) and 244-378 (b) fibrils for 72h. Data in the graphs are reported as mean ± SD, and each dot represents the mean of six technical replicates with each condition tested in three independent experiments. Data were analysed with one-way ANOVA with Dunnett's multiple comparison test: n.s. not significant, ****p≤0.0001. (c) Cell count analysis of ScN2a RML treated with 2 µM of tau 244-378 for 72h. Data in the graph are reported as mean ± SD. Three independent experiments were performed, and each dot represents the mean of three technical replicates. Data were analysed with Wilcoxon matched-pairs signed rank test: n.s. not significant.

3.2. Tau fibril effect on PrP^{Sc}

Previous works have already shown the ability of α-synuclein and tau K18 fibrils to decrease the level of PrP^{Sc} in ScN2a RML cells [114,120]. To further characterize this peculiar effect, we decided to take advantage of both tau constructs, K18 and 244-378, that seem to adopt different structures when assembled *in vitro*. 2 µM of tau K18 fibrils were already shown to efficiently reduce PrP^{Sc} level in ScN2a RML cells, with the main effect obtained after 72h of exposition (Fig. 19a). We decided to test the same experimental setting also for tau 244-378 fibrils. ScN2a RML cells were treated with 2 µM of 244-378 fibrils for 72h and then cells were collected and subjected to PK digestion to evaluate PrP^{Sc} levels. As for tau K18, also 244-378 reduced PrP^{Sc} burden after 72h of incubation (Fig. 19b).

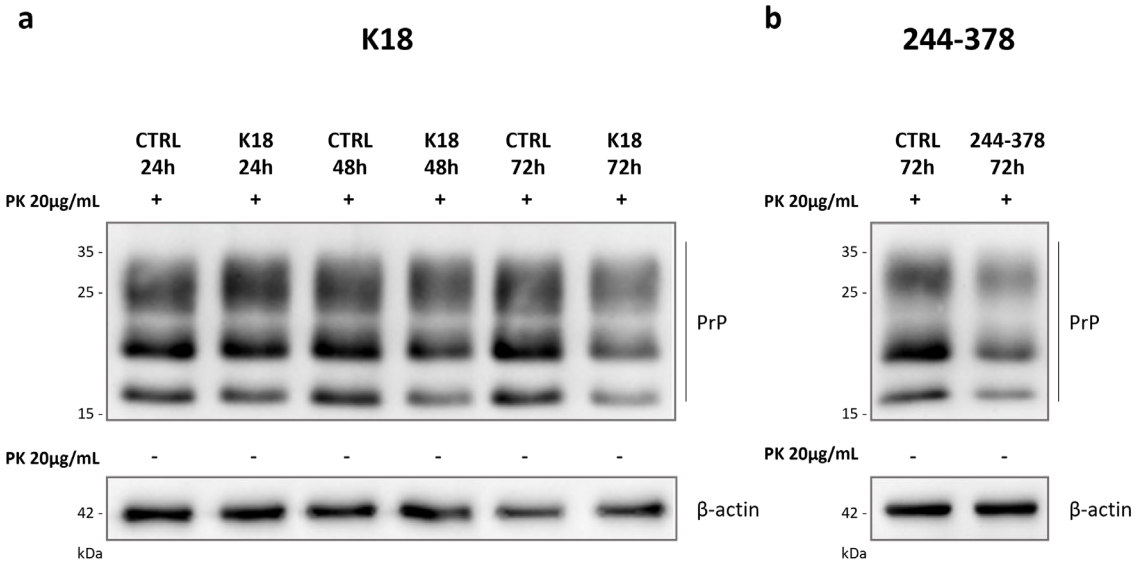

Figure 19. Tau fibrils-mediated reduction of PrP^{Sc}. (a) Representative WB of ScN2a RML cells treated with 2 µM of tau K18 fibrils for 24, 48 and 72h. Samples were treated with 20 µg/mL of PK and the membrane probed with anti-PrP antibody W226 to assay PrP^{Sc} levels. (b) Representative WB of ScN2a RML cells treated for 72h with 2 µM of tau 244-378 fibrils. Samples were treated with PK to evaluate the reduction of PrP^{Sc}. β-actin was used as loading control.

Since PrP^{Sc} reduction is mainly observed after 3 days, we then asked ourselves whether the reduction of PrP^{Sc} needs 72h of continuous incubation with tau fibrils to occur, or whether 3 days are only necessary to observe the effect on PrP^{Sc}, but actually tau fibrils' action starts earlier. To address this question, ScN2a RML cells were incubated with tau K18 fibrils for different periods of time, after which the treatment was removed by PBS washes and cells were kept in culture up to 72h to evaluate the effect on PrP^{Sc} levels. We decided to start with

an incubation with tau K18 fibrils of 24h and 48h, after which the treatment was removed, and cells were kept in culture up to 72h.

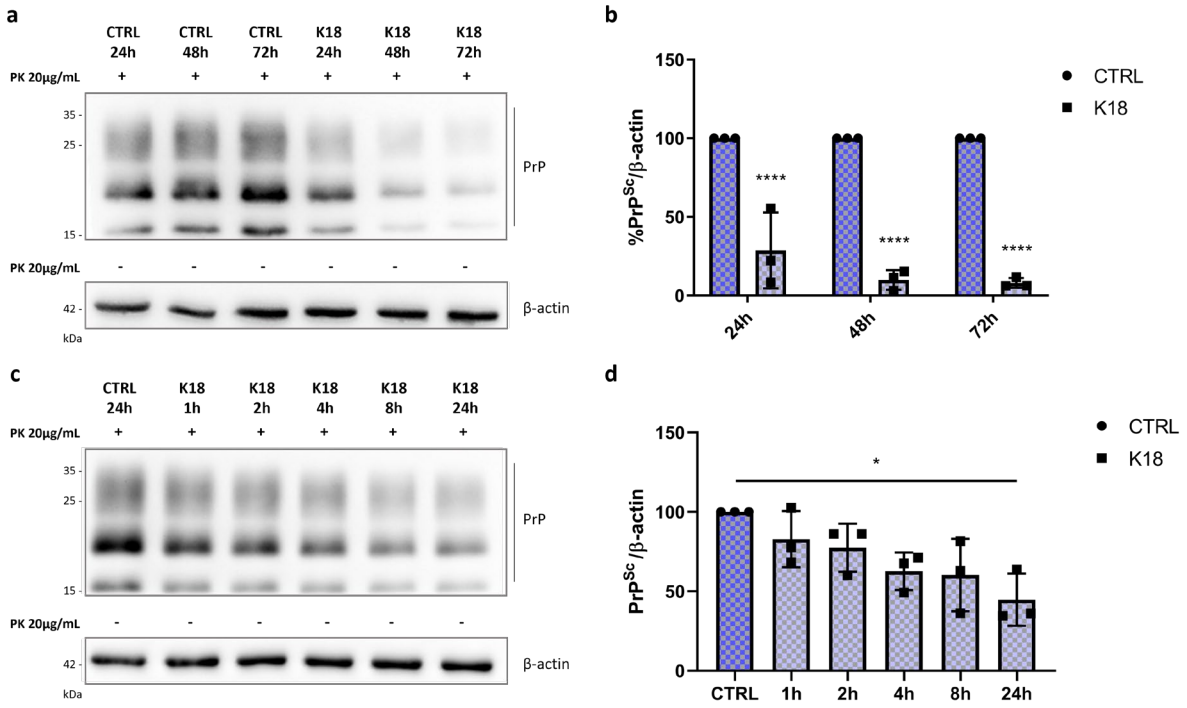

Figure 20. Tau K18 fibril incubation time affects PrP^{Sc} reduction. (a) Representative WB and (b) related quantification of PrP^{Sc} in ScN2a RML cells after the incubation with tau K18 fibrils. ScN2a RML cells were incubated with 2 µM of tau K18 fibrils for 24, 48 or 72h after which the treatment was removed, and cells were kept in culture without the treatment up to 72h to allow the evaluation of PrP^{Sc} reduction. β-actin was used as loading control. (b) Quantification of three independent experiments. Values are shown as percentage of PrP^{Sc} relative to β-actin. Data are reported as mean ± SD. Data were analysed with two-way ANOVA with Sydak's multiple comparisons test: ****p≤0.0001. (c) Representative WB and (d) related quantification of PrP^{Sc} levels. ScN2a RML cells were incubated with 2 µM of tau K18 fibrils for 1, 2, 4, 8 and 24h before the removal of the treatment and the incubation up to 72h to evaluate the reduction of PrP^{Sc}. β-actin was used as loading control. (d) Quantification of three independent experiments. Values are shown as percentage of PrP^{Sc} relative to β-actin. Data are reported as mean ± SD. Data were analysed with Friedman test with Dunn's multiple comparisons test: *p≤0.05.

As shown in figure 20, the incubation for 24h with tau K18 fibrils is sufficient to significantly reduce PrP^{Sc} level after 72h (Fig. 20a, b). Moreover, shorter incubation times, starting from 1h, progressively reduce PrP^{Sc}, suggesting that K18 fibrils start to act in the short period, but the effect on PrP^{Sc} reduction is mainly manifested after 72h. The same experiment was performed also with tau 244-378 fibrils. For this experiment we chose 4h of incubation, since it was the lowest K18 incubation time showing around 50% of PrP^{Sc} reduction. ScN2a RML cells were incubated for 4h with tau 244-378 fibrils, then the treatment was removed by PBS

washes and cells were kept in culture until 72h. Tau K18 treatment was also performed to compare the two constructs (Fig. 21). Both tau fibrils comparably reduced PrP^{Sc} levels following 4h of incubation (Fig. 21a, b). We also decided to check whether tau amyloids were actively internalized by cells as they can act on intracellular degradation mechanisms to promote PrP^{Sc} clearance. Therefore, we evaluated on the same samples the presence of intracellular tau amyloids at 72h. Extracellular tau fibrils were removed by trypsinisation to evaluate the signal coming exclusively from intracellular fibrils [20,313,315,350]. Interestingly, only tau K18 amyloids were present after 3 days following 4h of incubation, while a faint tau signal was detected in cells treated with 244-378 fibrils (Fig. 21c). We hypothesized that cells, unlike K18 fibrils, could not internalize 244-378, or that the internalization occurs within the 4h of incubation, but, being kept in culture for 3 days, the internalized amyloids might be removed. To address these questions, cells were incubated with 244-378 fibrils for short time periods, then they were trypsinised to remove extracellular fibrils and lysed to assess the intracellular presence of tau amyloids. As shown in figure 21d, the cells treated with tau 244-378 fibrils, checked right after 1, 2, 4, 8 and 24h of incubation, showed a higher amount of internalized aggregates, suggesting that both fibril types are internalized, but unlike K18, tau 244-378 are rapidly removed by cells, probably degraded. This may also explain the reduced resistance to PK digestion of tau 244-378 fibrils (Fig. 17b), compared to the K18 ones, and their different effect on cell metabolism (Fig. 18).

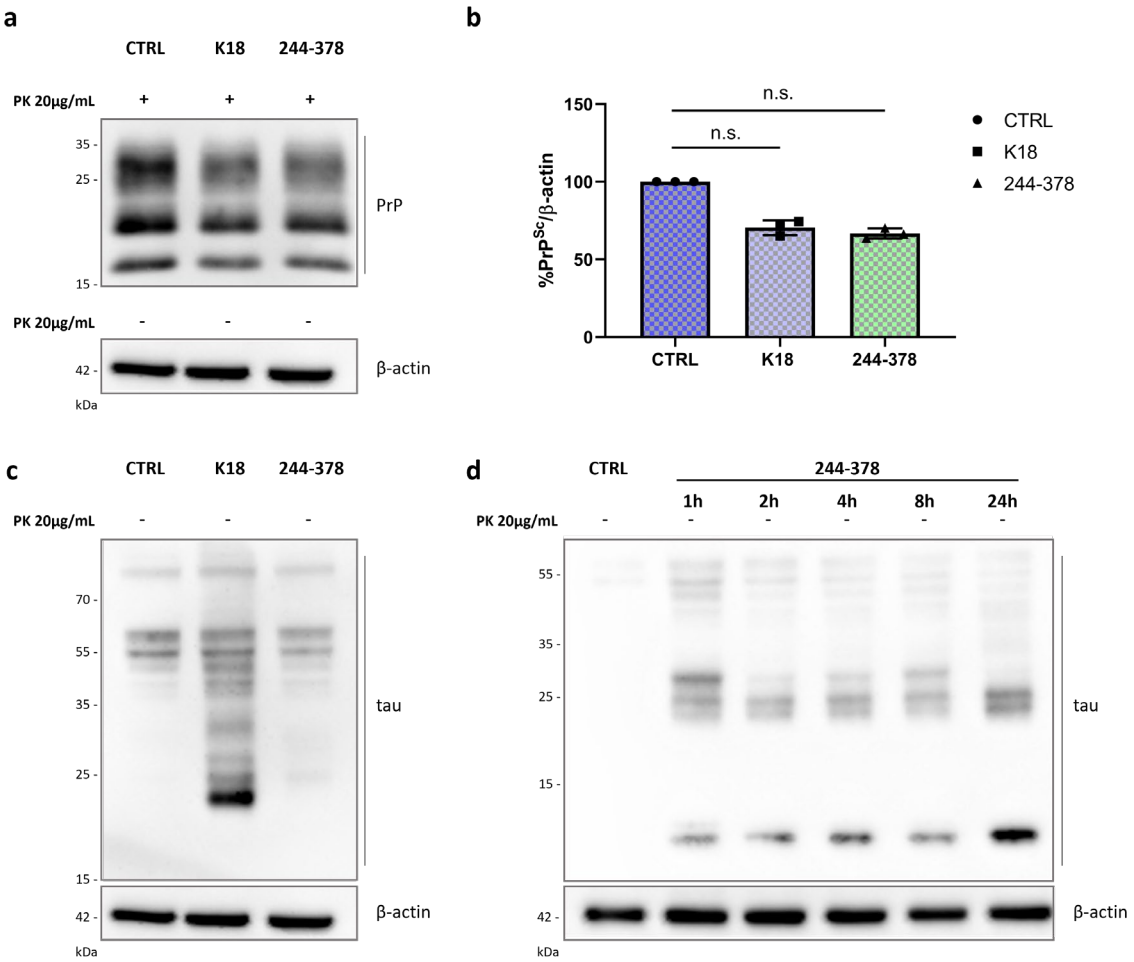

Figure 21. Comparison of tau K18 and 244-378 fibrils on PrP^{Sc} levels. (a) Representative WB and (b) related quantification of ScN2a RML cells after their exposure for 4h to 2 µM of tau K18 and 244-378 fibrils, followed by PBS washes to remove the treatment and culturing up to 72h to assess PrP^{Sc} reduction. PK digestion was performed to reveal PrP^{Sc} content. β-actin was used as loading control. (b) Quantification of three independent experiments. Values are shown as percentage of PrP^{Sc} relative to β-actin and data reported as mean ± SD. Data were analysed with Friedman test with Dunn's multiple comparisons test: n.s. not significant. (c) Samples from experiments in (a) not treated with PK and probed with anti-tau antibody for the presence of intracellular tau K18 and 244-378 fibrils. (d) Internalization of tau 244-378 fibrils. ScN2a RML cells were treated with 2 µM of tau 244-378 fibrils for 1, 2, 4, 8 and 24h and then lysed and tested for the intracellular presence of tau fibrils.

3.3. Tau fibril localization

The administration of both tau amyloid fibrils resulted in a comparable reduction in PrP^{Sc} levels after 3 days and in their internalization, even though with some differences. To deepen this mechanism, we decided to explore the internalization mechanism of these fibrils, as it may be linked to PrP^{Sc} degradation. Tau K18 fibrils were conjugated to Alexa-488 fluorophore, to obtain fluorescent fibrils that are easily detectable without the use of antibodies, that may not bind to amyloid aggregates. After 24h of incubation with tau K18 fluorescent fibrils, cells

were fixed and stained with different antibodies that mark cell organelles. Trypan blue was used before fixation to quench the signal of fibrils that were not internalized, as this dye cannot enter living cells [343]. Cells were stained with EEA1, a protein present in early endosomes, Calnexin for the endoplasmic reticulum, M6PR to stain the Golgi apparatus and LC3B and LAMP2 to stain autophagosomes and lysosomes respectively. Images of a single cell were taken as multiple sections along the z-axis to take into account the whole cell volume, and they are shown in 2-D with orthogonal planes to assess the colocalization both in XZ and YZ axes. As shown in figure 22, no colocalization was observed after 24h between tau K18 fibrils and EEA1 or Calnexin, suggesting that fibrils may not enter through these pathways or that we did not choose the right incubation time to observe a colocalization. However, K18 fibrils showed a significant colocalization signal with Golgi apparatus (M6PR) and with the autophagolysosomal pathway. This may suggest a possible role of tau fibrils in stimulating the activity of the cell degradation pathways, that could in turn degrade PrP^{Sc} and explain its reduction observed after 3 days, following tau fibril exposure.

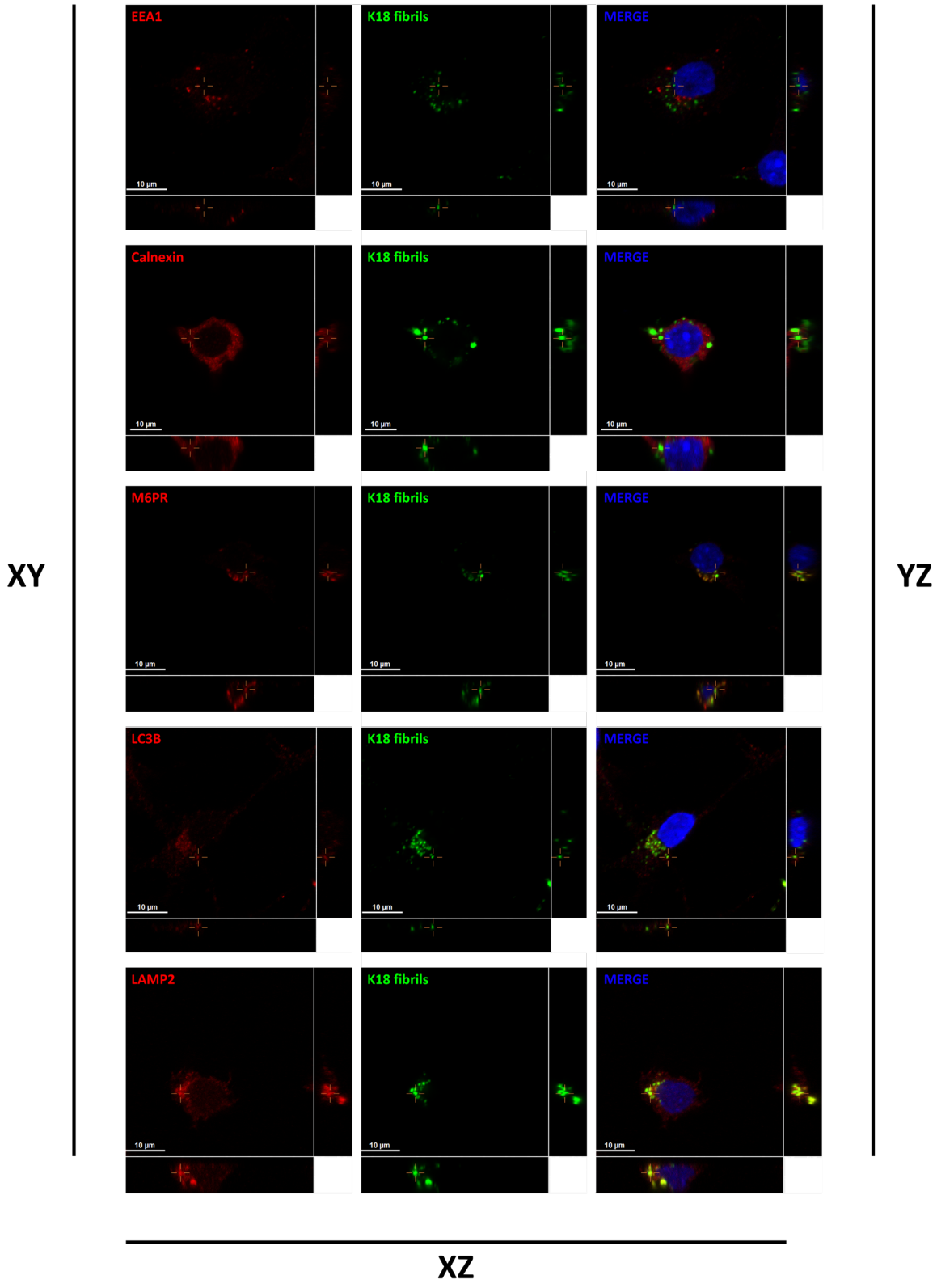

Figure 22. Tau K18 fibril subcellular localization. ScN2a RML cells were treated for 24h with tau K18-Alexa488 fibrils and then fixed and stained for EEA1 (early endosomes), Calnexin (endoplasmic reticulum), M6PR (Golgi apparatus), LC3B (autophagosomes) and LAMP2 (lysosomes). DAPI was used to stain nuclei. Images show one of the central sections of the entire z-stack. All three orthogonal planes (XY, XZ and YZ) are represented.

To investigate the potential role of lysosomal and proteasomal pathways in mediating the clearance induced by tau K18 fibrils, we decided to take advantage of different inhibitors known to block the autophagolysosomal pathway at different steps. 3-methyladenine (3-MA) is known to block macroautophagy by inhibiting the class III phosphoinositide 3-kinase (PI3K) [351,352], thus impairing the formation of the preautophagosomal structure. Bafilomycin A_1 is widely used as Vacuolar H^+ ATPase inhibitor, which controls lysosomal pH, resulting in the prevention of endosomal and lysosomal acidification and in the disruption of autophagic flux [353]. Similarly, chloroquine changes the lysosomal pH, inhibiting the degradation of autophagosomal cargoes into lysosomes [354]. We also tested the effect of a proteasomal inhibitor, MG132, which blocks the activity of the 26S proteasome complex [355].

ScN2a RML cells were incubated with tau K18 fibrils for 72h, and, before lysis, they were treated with the above-mentioned inhibitors, with time and concentration depending on the specific inhibitor. PK-treated samples were used for PrP^{Sc} analysis while, in the case of autophagic inhibitors, LC3B levels were analysed in the PK-untreated ones, to confirm the efficacy of the specific compound. LC3B protein levels are often used to monitor autophagic flux, since LC3B-I is converted into LC3B-II during autophagosome formation which, in turn, is degraded into lysosomes at the end of the autophagic pathway [356]. As shown in figure 23a, 3-MA administration efficiently blocked the conversion of LC3B-I into LC3B-II, demonstrating the efficacy of the treatment. In contrast, the administration of bafilomycin A_1 and chloroquine led to LC3B-II accumulation, in agreement with their role on blocking the lysosomal degradation (Fig 23b, c). Despite the efficient inhibition of the autophagic flux at different steps, none of these inhibitors was able to revert, or to even reduce, the PrP^{Sc} clearance mediated by tau K18 amyloids. Interestingly, K18 fibril administration, together with bafilomycin A_1 and chloroquine, produced an additive effect on PrP^{Sc} clearance. Moreover, not even the proteasomal inhibition with MG132 affected the PrP^{Sc} reduction mediated by tau K18 fibrils (Fig. 23d). We concluded that the intracellular degradation pathways do not represent the way through which tau amyloid fibrils reduce prion levels in our cellular model, or that the conditions used in our study were not suitable to observe an inhibitory effect.

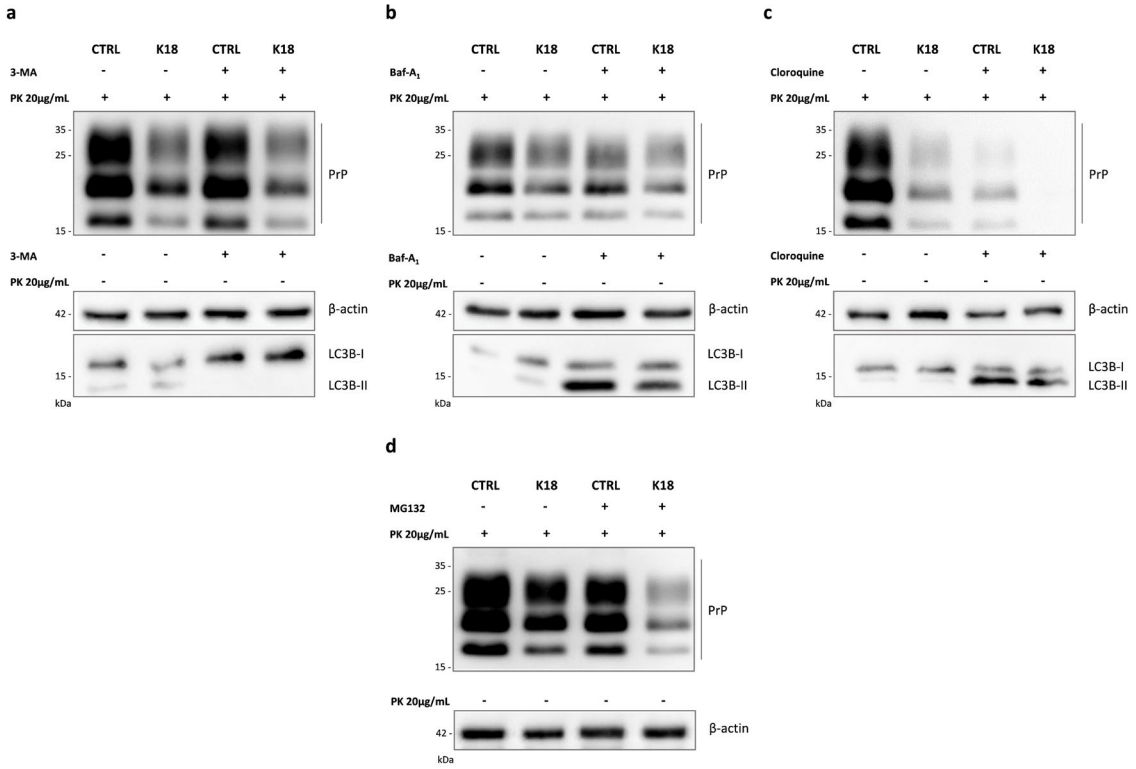

Figure 23. Role of degradation pathways in tau fibrils mediated PrP^{Sc} clearance. Representative WB of ScN2a RML cells incubated for 72h with tau K18 fibrils and treated with (a) 3-methyladenine (3-MA), (b) bafilomycin A_1 (Baf A_1), (c) chloroquine and (d) MG132. PK digestion was performed to evaluate PrP^{Sc} levels. β-actin was used as loading control and the amount of LC3B-I and LC3B-II was evaluated to confirm the efficacy of the inhibitors.

3.4. Tau fibrils do not reduce PrP^{Sc} levels by entering cells

Our experiments demonstrated that tau fibrils efficiently reduce prion levels in ScN2a RML cells, and that they are uptaken by cells, localizing in different subcellular compartments. However, if internalization is involved, there should be another mechanism by which tau fibrils promote the reduction of PrP^{Sc}, as we have already ruled out the contribution of cellular degradation pathways. To test whether the internalization of tau amyloids and the reduction in PrP^{Sc} level are connected, we decided to block tau amyloid uptake and to evaluate the effect on PrP^{Sc} clearance. As discussed before, many mechanisms and receptors are involved in the uptake of tau aggregates by cells. To avoid any misinterpretation due to the blocking of a specific pathway or another, we decided to block all energy-dependent endocytosis mechanisms by incubating cells at 4° C. At this restrictive temperature, fibrils are still able to adhere to the plasma membrane but should not be able to be internalized [315]. To validate the experimental design and the efficacy in blocking fibril endocytosis, ScN2a RML

cells were incubated for 4h at 37° C and 4° C in the presence of 2 µM Alexa-488-labelled tau K18 fibrils. Trypan blue was used to quench the fluorescence coming from the extracellular environment and to allow the evaluation of the internalized fibrils. HCS CellMask™ was used to label the entire cell.

As shown in figure 24, the incubation at 4° C almost completely prevented the internalization of fluorescent tau K18 fibrils.

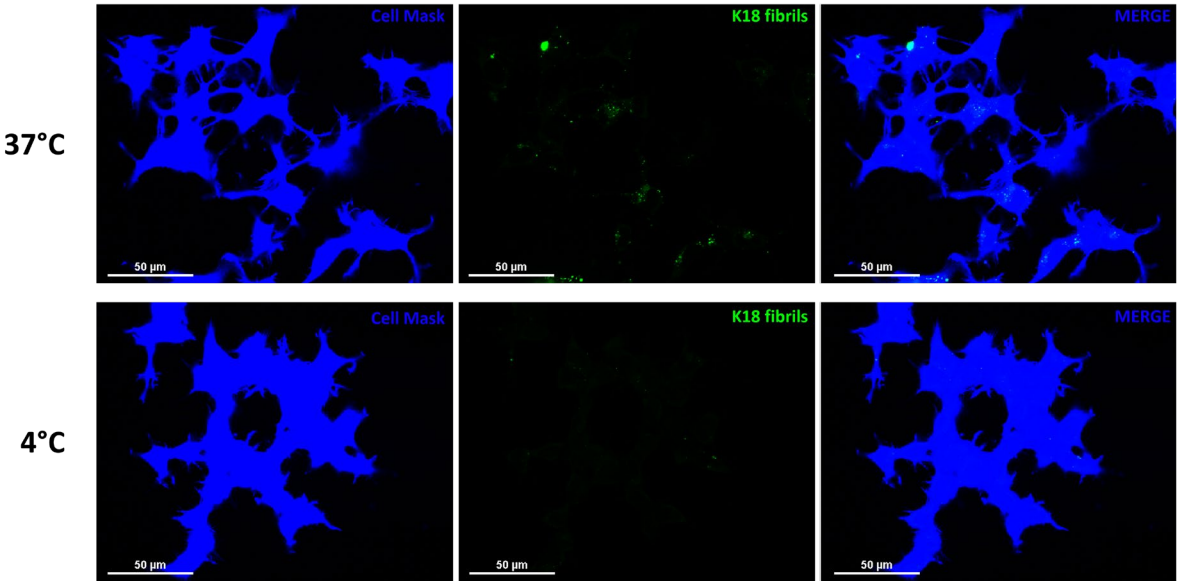

Figure 24. Tau K18 internalization is inhibited at 4° C. ScN2a RML cells were incubated for 4h with tau K18-Alexa488 fibrils at 37° C (upper panels) and 4° C (bottom panels). Trypan blue was used to quench the fluorescence deriving from extracellular fibrils. Blue CellMask™ was used to stain the entire cell.

We decided to test the effect on PrP^{Sc} following the inhibition of tau K18 fibril uptake. ScN2a RML cells were treated with 2µM tau K18 fibrils both at 37° C and 4° C, then the treatment was removed by PBS washing and cells were kept in incubation at 37° C up to 72h to evaluate PrP^{Sc} clearance mediated by tau fibrils. Before lysis, extracellular fibrils were removed by trypsin.

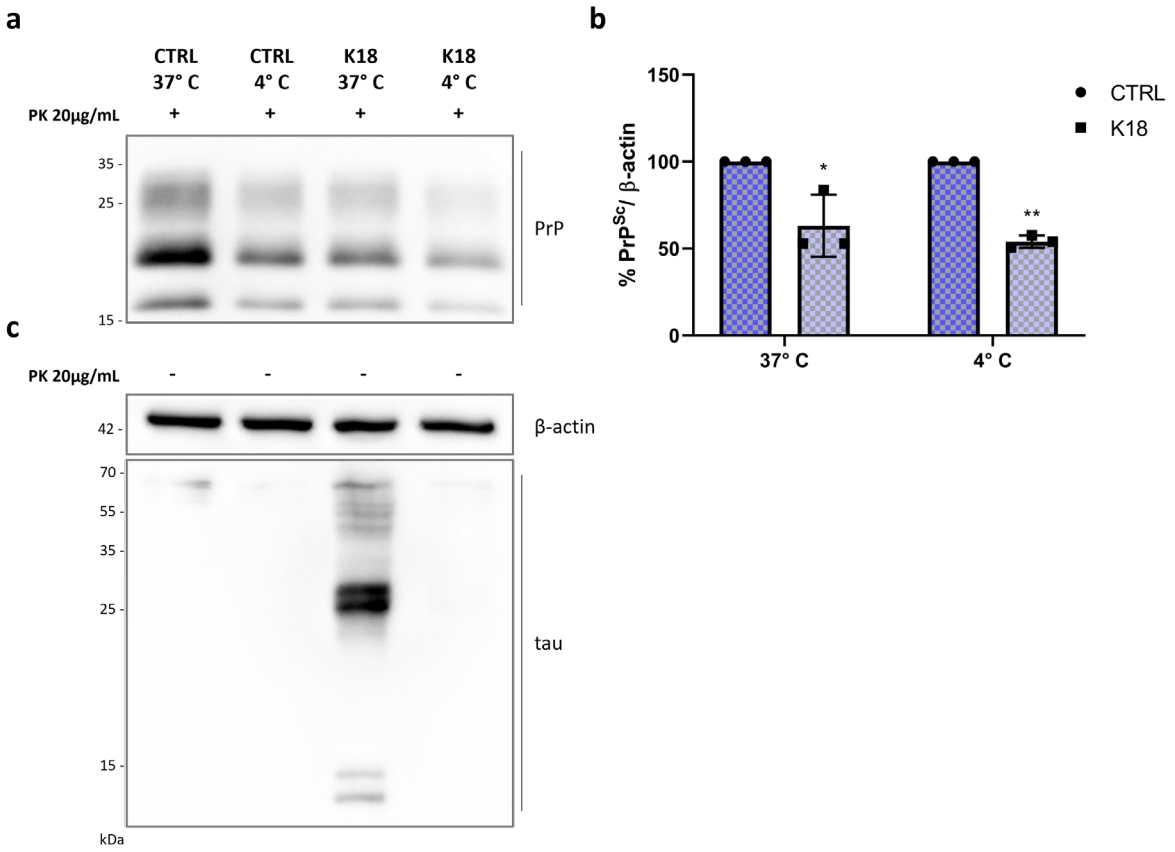

Figure 25. Effect of the inhibition of tau K18 fibril uptake on PrP^{Sc}. (a) Representative WB and (b) related quantification of ScN2a RML cells incubated for 4h with 2 µM of tau K18 fibrils at 37° C and 4° C. Then, the treatment was removed by PBS washing and cells were kept in culture up to 72h to evaluate the reduction in PrP^{Sc} after PK digestion of samples. β-actin was used as loading control. (b) Graph shows the quantification of three independent experiments. Values are shown as percentage of PrP^{Sc} relative to β-actin and data are reported as mean ± SD. Data were analysed with two-way ANOVA with Sidak's multiple comparisons test: *p≤0.05, **p≤0.01. (c) Evaluation of internalized tau K18 fibrils at 37° C and 4° C. Trypsin was used to remove extracellular fibrils.

Figure 25 shows the WB of the PrP^{Sc} levels after the treatment and the corresponding quantification. To confirm the effective blocking of tau fibril uptake, the same samples were assayed for tau presence. As shown in the bottom panel, no signal corresponding to tau K18 fibrils was observed when cells were incubated with fibrils at 4° C, demonstrating the efficient inhibition of the uptake at this restrictive temperature. However, no major differences were observed in PrP^{Sc} clearance, with a similar decrease in K18-treated cells, both at 37° C and 4° C. This result suggests that, despite being internalized, tau K18 fibrils do not mediate PrP^{Sc} reduction by entering the cells.

The same experiment was repeated with tau 244-378 fibrils, to assess whether fibrils showing different biochemical and biological behaviours may act on PrP^{Sc} reduction with similar mechanisms.

As shown before, tau 244-378 fibrils are less resistant to protease degradation compared to K18 fibrils (Fig. 17b) and, despite being quickly internalized, they are efficiently removed after 3 days of incubation (Fig.21c, d). To overcome this problem, the blocking of tau 244-378 fibril internalization at 4° C was performed also by incubating cells for 4h and by immediately lysing them, to avoid fibril removal and to validate the experimental design. Figure 26a (right) shows how, as for tau K18 fibrils, 244-378 fibril internalization is efficiently reduced by incubating cells at 4° C. Moreover, the complete absence of tau signal, when, after the treatment, cells are left in the incubator until 72h, demonstrates again that after the initial uptake 244-378 fibrils are efficiently removed by cells (Fig. 26a, left). However, having demonstrated the inhibition of the initial uptake at 4° C, we decided to evaluate PrP^{Sc} reduction by incubating cells with fibrils for 4h at 37° C and 4° C and by leaving them in culture up to 72h, after treatment removal. As shown in figure 26b, after 3 days, the 244-378-mediated reduction in PrP^{Sc} levels between cells incubated at 37° C and 4° C was comparable. These results demonstrate that, despite being internalized and exhibiting different biochemical and biological properties, both K18 and 244-378 fibrils reduce prion levels in a way that is independent from their uptake.

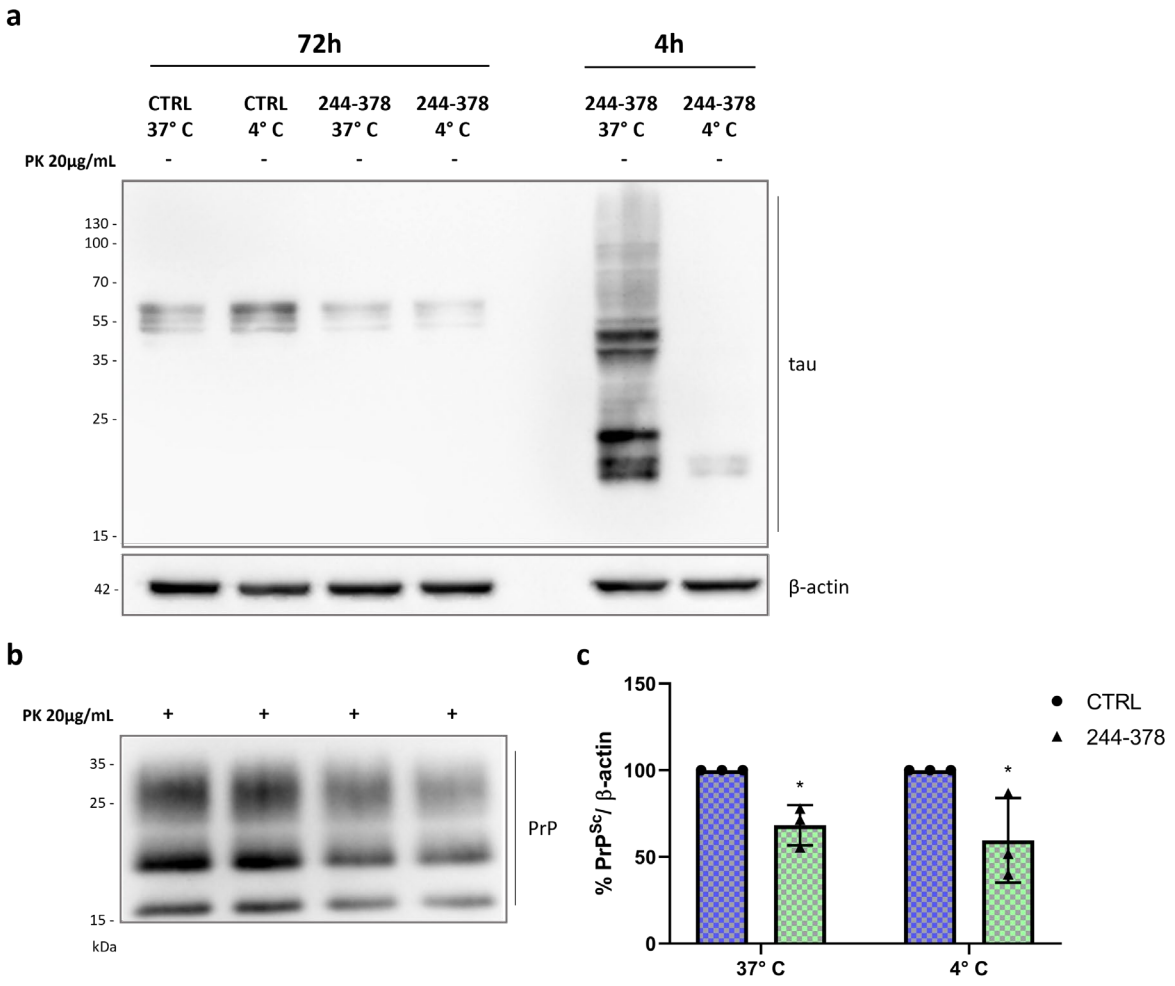

Figure 26. Inhibition of tau 244-378 fibril uptake and effect on PrP^{Sc}. (a) Representative WB of ScN2a RML cells incubated with 2 µM of tau 244-378 fibrils for 4h at 37° C or 4° C and then incubated up to 72h (left lanes) or immediately lysed (right lanes). Trypsin was used to remove extracellular fibrils. Membranes were probed with anti-tau antibody. (b) Representative WB and (c) related quantification of ScN2a RML cells incubated for 4h with tau 244-378 fibrils at 37° C and 4° C and kept in culture up to 72h after the removal of the treatment to determine PrP^{Sc} reduction. β-actin was used as loading control. (c) Graph shows the quantification of three independent experiments. Values are shown as percentage of PrP^{Sc} relative to β-actin and data are reported as mean ± SD. Data were analysed with two-way ANOVA with Sidak's multiple comparisons test: *p≤0.05.

3.5. Tau fibrils hinder prion *de novo* infection

Our previous work demonstrated how tau K18 fibrils can bind to the cellular form of the prion protein PrP^{C} and how their administration is able to promote the stabilization of PrP^{C} at the plasma membrane. Having excluded a role of the uptake and of the degradation pathways in mediating the clearance of PrP^{Sc}, we conclude that tau fibrils may act as an antibody directed to PrP^{C}, stabilizing it at the plasma membrane and preventing its conversion to PrP^{Sc} [357,358].

However, despite showing poor localization in this compartment [359], we cannot rule out that, besides PrP^C binding, tau fibrils bind also to PrP^{Sc}, hindering the conversion event.

In any case, according to this hypothesis, tau fibrils binding to both PrP^C and PrP^{Sc} should not only be able to reduce PrP^{Sc} levels in chronically prion-infected cells, but also to hinder the conversion of PrP^C in not infected cells.

To test this, we decided to take advantage of a *de novo* prion infection protocol [346], which allows the conversion of PrP^C in naïve cells using an inoculum obtained from prion-infected cells.

To assess the contribution of tau fibrils in preventing the infection, not infected N2a cells were pre-treated for 4h with 2 or 4 µM of tau K18 fibrils, then they were washed with PBS to remove the treatment and finally they were exposed for 72h to ScN2a RML cells homogenate. In this way, the PrP^{Sc} present in the inoculum should convert the PrP^C of the not infected N2a cells. After the initial infection step, cells were passaged for three times to allow the removal of the initial inoculum and the onset of the *de novo* prions. The first passage was not analysed to avoid the interference of the initial inoculum in the analysis.

As shown in figure 27, the efficacy of the *de novo* cell infection is demonstrated by the increase of PrP^{Sc} content from p2 to p3, suggesting that cells are actively replicating prions.

Tau K18 fibril pre-treatment, either at 2 µM or 4 µM, was efficiently able to reduce prion accumulation in both passages, confirming the impairment of the *de novo* infection process.

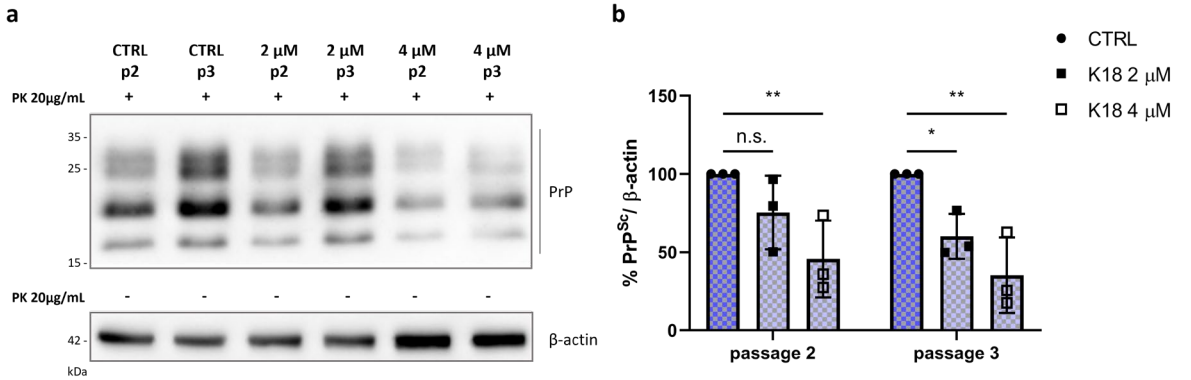

Figure 27. Tau K18 fibril effect on *de novo* infection. (a) Representative WB and (b) related quantification of N2a cells pre-treated with 2 or 4 µM of tau K18 fibrils and then infected with ScN2a RML homogenate. Cells were passaged for three times to allow prion replication. β-actin was used as loading control. (b) Graph shows the quantification of three independent experiments. Values are shown as percentage of PrP^{Sc} relative to β-actin and data are reported as mean ± SD. Data were analysed with two-way ANOVA with Sidak's multiple comparisons test: n.s. not significant, *p≤0.05, **p≤0.01.

The same experiment was repeated with 244-378 fibrils, to confirm the ability also of this fibril type to hinder prion infection establishment. As for tau K18, not infected N2a cells were pre-treated with 2 or 4 µM of tau 244-378 fibrils for 4h followed by the exposure to PrP^{Sc} seed. As expected, both tau fibril concentrations were able to reduce prion accumulation following the *de novo* infection (Fig. 28).

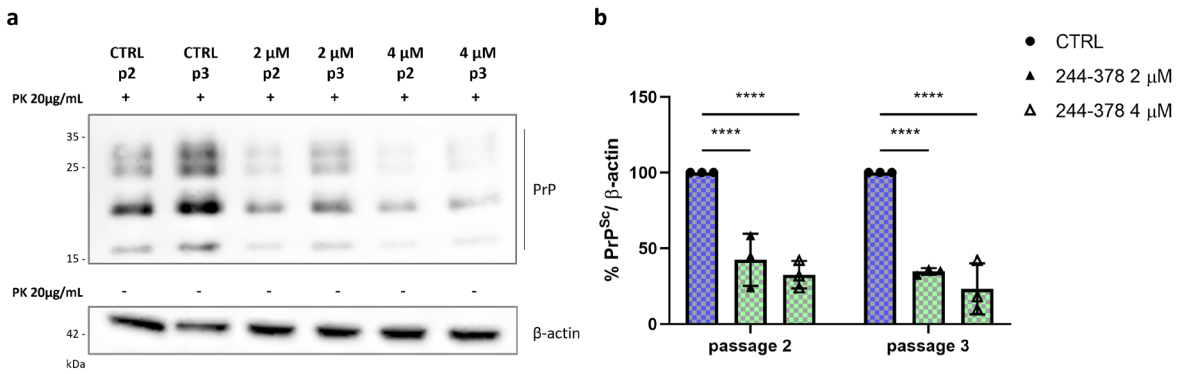

Figure 28. Tau 244-378 fibril effect on *de novo* infection. (a) Representative WB and (b) related quantification of N2a cells pre-treated with 2 or 4 µM of tau 244-378 fibrils and then infected with ScN2a RML homogenate. Cells were passaged for three times to allow prion replication. β-actin was used as loading control. (b) Graph shows the quantification of three independent experiments. Values are shown as percentage of PrP^{Sc} relative to β-actin and data are reported as mean ± SD. Data were analysed with two-way ANOVA with Sidak's multiple comparisons test: ****p≤0.0001.

DISCUSSION AND CONCLUSIONS

The idea that neurodegenerative diseases were characterized by distinct traits and unique features has been set aside, since different protein aggregates, usually considered distinctive of different pathologies, were seen to co-deposit. In fact, although Aβ, tau, α-synuclein, prions and TDP-43 are usually found aggregated in distinct pathologies, their deposition is often found in non-diseased individuals and they can co-exist in the same brain [360]. An example is represented by the observation of LBs, typically found in synucleinopathies, in Alzheimer's disease cases [361]. In addition, LBs were found abundant in tauopathies such as PiD, AGD and CBD, normally characterized by tau aggregates only. This suggests that the aggregation of tau may predispose neurons to develop secondary LBs [362,363]. Furthermore, in PD and DLB patients, tau oligomer accumulation has been seen to accompany the one of α-synuclein, also forming hybrid oligomers made of the two proteins [364]. The *in vitro* interaction of these two proteins has been observed through the MBDs of tau and the C-terminus of α-synuclein [365], with the latter stimulating the phosphorylation of tau and indirectly affecting the microtubule stability. Moreover, some of these proteins can induce the aggregation of other proteins in a process known as "cross-seeding". This process was suggested for tau and Aβ and it may explain their simultaneous accumulation in AD [366]. Much clearer is the case of α-synuclein and tau, where α-synuclein was shown to promote the fibrillization of tau and their coincubation induces the fibrillization of both proteins [367]. Similarly, *in vitro* cross-seeding between Aβ and α-synuclein has been observed [368].

The same also applies to prion diseases, with described cases of co-deposition of PrP^{Sc} with α-synuclein and Aβ [338,369], and with phosphorylated tau aggregates found in many different prion diseases, as discussed before. In this regard, it is now widely recognized that the cellular form of the prion protein, PrP^{c}, binds many different β-sheet-enriched amyloid proteins. Recently, in fact, Corbett and colleagues showed the ability of PrP^{C} to bind soluble aggregates of tau, α-synuclein and Aβ, and how the ablation of PrP^{C} was able to reduce the toxic effects that these aggregates normally exert [100]. Similarly, our lab demonstrated an interplay between PrP^{C} and α-synuclein amyloid fibrils, with an increased uptake and spreading of α-synuclein aggregates in the presence of PrP^{C}, both *in vitro* and *in vivo* [120]. Moreover, the N-terminus of PrP^{C} was found to interact with tau K18 amyloid fibrils, facilitating their uptake in N2a cell line [114]. Interestingly, both α-synuclein and tau fibrils were able to reduce the

amount of PrP^{Sc} when administered to prion-infected N2a cell, possibly by hindering the conversion event of PrP^{C}.

To further explore this effect, we decided to take advantage of the previously used tau K18 construct, made of the 4 MBDs and used as a model for 4R tauopathy aggregates, and of a new tau construct, which extends the tau K18 one and that contains the sequence shown to be important for the core of PHFs in AD [223]. This construct could result in the formation of fibrils with a different structure compared to the one of K18. Recently, the use of *in vitro*-prepared amyloid fibrils has been questioned [223,370], expecially for tau, where the use of heparin was already shown to alter the structure of the obtained fibrils [292]. However, the ability of PrP^{C} to bind not only PrP^{Sc}, but also other amyloid proteins, suggests that this interaction may depend on a property shared by all these aggregates, such as the β-sheet content.

Therefore, we decided to test whether, as for tau K18, also the new tau 244-378 fibrils produce an effect on PrP^{Sc} content.

As shown by Fitzpatrick et al., in PHFs and SFs extracted from AD brain, the hexapeptide 306-311 packs with the opposing residues 373-378, contributing to the formation of the filament core. The addition of the six missing amino acids to tau K18, which ends at residue 372, may reconstitute the packing interface, conferring a different structure to the filaments. Therefore, we decided to extend the K18 sequence up to the amino acid 378 and to subject both constructs to the same *in vitro* fibrilizzation protocol. RF-cloning technique was used to extend the K18 construct, then both proteins were produced in parallel using the same protocol described by Barghorn et al., proved to be effective for tau K18. To test the ability of 244-378 construct to form fibrils, monomers were subjected to cycles of shaking and rest in the presence of heparin, and the ability to form β-sheet structures was monitored using ThT dye. Both tau constructs showed the same aggregation kinetic, even though the fluorescence signal emitted was higher for tau K18. TEM analysis of the end-stage products revealed that, as for tau K18, also 244-378 forms fibrils *in vitro*. We decided to further characterize 244-378 fibrils by subjecting them to protease degradation, as the resistance to proteolysis represents one of the features of amyloid proteins and it correlates with the structural organization and the amount of β-sheets [371]. We were surprised to find that 244-378 fibrils, unlike K18 ones, were way more sensitive to PK digestion, suggesting different conformational structures and different β-sheet content, that may explain also the lower ThT fluorescence emission when fibrillized *in vitro*. This result may also suggest that 244-378, containing the *in vivo* PHFs and SFs AD sequence, may reflect a more phisiological

conformational structure, since it was already demonstrated that *in vivo* filaments are less resistant to protease degradation compared to the *in vitro* produced ones [349,372].

Before cellular studies, we decided to test the metabolic effect of 244-378 fibrils in our cellular model. In contrast to tau K18 fibrils, tau 244-378 fibrils exhibited a marked effect in the reduction of the metabolic activity in ScN2a RML cells, again confirming the different nature of these two amyloid preparations. However, no effects on cell proliferation and viability were observed at 2 µM concentration.

As already shown for tau K18, also 244-378 produced a decrease in PrP^{Sc} levels when administered for 72h directly to the medium of prion-infected ScN2a RML cells.

The direct binding between tau fibrils and PrP^{C}, showed in our previous paper, and the increased accumulation of PrP^{C} at the plasma membrane following tau K18 administration led us to conclude that tau K18 fibrils probably act sequestering PrP^{C} to the plasma membrane and preventing its conversion to PrP^{Sc}. However, being also internalized, we were unable to exclude that tau fibril uptake may contribute to the observed reduction of PrP^{Sc}. Moreover, even though prion reduction was most likely the result of the binding of tau fibrils to PrP^{C}, we were unable to rule out a possible involvement also of PrP^{Sc}; in fact, tau fibrils might also sequester PrP^{Sc} molecules, thus hindering their interaction with PrP^{C} and the conversion process.

To further explore this mechanism, we firstly demonstrated that the reduction of prions needs 72h to occur, and incubation times as short as 1 hour are enough to cause a substantial decrease of prion levels after 3 days, suggesting that a continous exposure to tau fibrils is not needed. Moreover, as expected, both tau fibrils are spontaneously internalized and cause a comparable reduction effect on PrP^{Sc}, despite the fact that the 244-378 ones are almost completely removed after 72h, probably degraded. Their active digestion by cells would be in agreement with the lower resistance of 244-378 fibrils to protease degradation, and it may also explain the reduced metabolic activity observed in the MTT assay.

We also observed that, following the internalization, tau K18 fibrils localize in Golgi apparatus and in the autophagolysosomal pathway, suggesting a possible stimulation of the cellular degradation pathways and a consequent decrease also in PrP^{Sc} levels. However, the treatment with inhibitors, aimed at blocking the autophagic and proteasomal degradation, had no effect, thus ruling out an involvement of these pathways in the tau fibril-mediated PrP^{Sc} clearance.

Despite the lack of involvement of degradation pathways, to assess whether the internalization of tau fibrils was connected to the PrP^{Sc} reduction observed, we decided to

test prion reduction in the absence of tau fibril uptake. We took advantage of low temperatures, as it was already proved that at 4° C the endocytosis of tau aggregates is reduced [114,313,315,373]. Both tau K18 and 244-378 fibril uptake was impaired when cells were incubated at 4° C, resulting in an almost complete inhibition of the signal coming from the intracellular amyloids. However, we were surprised to observe that the presence or the absence of tau fibrils within the cells did not affect their ability to reduce PrP^{Sc}, as prion reduction was fully comparable between cells incubated at 37° C or 4° C. These findings strongly support the idea that tau fibrils-mediated PrP^{Sc} clearance is driven by a direct binding between PrP^{C}/PrP^{Sc} and tau fibrils at the plasma membrane, subtracting one of the two partners necessary for prion conversion. Moreover, exploiting their action on the plasma membrane, it is more likely that PrP^{C} is the binding partner of tau fibrils, since PrP^{C} is mostly localized in this cellular compartment, while PrP^{Sc} is mainly present at the intracellular level [149,374], with poor localization at the plasma membrane [359].

After having demonstrated that tau fibrils reduce PrP^{Sc} level in chronically prion-infected cells, we wondered whether this effect is limited to the established prion infection or whether tau amyloids can also affect the first stages of prion infection. To address this question we decided to take advantage of a *de novo* prion infection protocol, by exposing the uninfected N2a cells to an homogenate of ScN2a cells. In this way, the PrP^{Sc} present in the inoculum of ScN2a is able to convert the PrP^{C} of the uninfected N2a cells, starting the infection cycle. To test the possible role of tau in this process, we pre-treated the uninfected N2a with tau K18 and 244-378 fibrils before the exposure to the ScN2a inoculum. Following our hypothesis, the administration of tau fibrils before the addition of prion inoculum should have hampered prion infection. Our results indicated that both tau K18 and 244-378 fibrils, administered before the exposure of cells to prion homogenate, reduced significantly the accumulation of PrP^{Sc} following the *de novo* infection. Moreover, since tau fibrils were removed before the addition of PrP^{Sc} inoculum, this experiment further supports the binding of tau fibrils with PrP^{C}, through which they exert their effect on PrP^{Sc}. The mechanisms of prion infection cycle are still poorly understood since, in the established prion infection, the conversion into PrP^{Sc} was suggested to occur mostly in intracellular compartments [149,150], whereas, during the earlier phases, it seems to involve more the plasma membrane [148]. Based on our data, in the first phases of the infection process, tau binding to PrP^{C} could either prevent his physical interaction with PrP^{Sc}, inhibiting the conversion, or block PrP^{C} at the plasma membrane, inhibiting its recycling through the endocytic compartments. Moreover,

in the chronically infected cells, the increased retention of PrP^{C} at the plasma membrane, mediated by tau fibrils, could be responsible for PrP^{Sc} clearance due to an impaired recycling. In conclusion, our findings confirmed the role of tau fibrils in mediating the reduction of prions in our cellular model. Moreover, this effect seems to reside on the ability of tau fibrils to bind to the PrP^{C} present on the plasma membrane, thus stabilizing the protein and hindering its conversion to PrP^{Sc}. Here we show also that PrP^{C} may act as a receptor for different tau fibril types, that, despite showing different conformational properties, are able to comparably reduce prions in our chronically prion-infected model. In addition, tau amyloid fibrils impair the initial phase of prion conversion, hindering PrP^{C}/PrP^{Sc} interaction and/or stabilizing PrP^{C} at the plasma membrane. These results may suggest a dual interplay between the prion protein and other amyloidogenic proteins. While, as previously shown for tau and α-synuclein, the presence of PrP^{C} at the plasma membrane facilitates the uptake of pathological aggregates that may result in a faster spreading of the pathology, here we show that, in the case of prion diseases, tau circulating species may protect PrP^{C} from PrP^{Sc} interaction, thus slowing prion conversion and the progression of the disease. This may also explain why, in some prion disease patients, the presence of tau aggregates may correlate with a longer disease incubation. In this regard, the interaction between different amyloidogenic proteins may result in different outcomes depending on the specific disease, and the study of these relationships can be crucial for the development of targeted therapies.

REFERENCES

1. United Nations Department of Economic and Social Affairs PD. World Population Ageing 2020 Highlights: Living arrangements of older persons (ST/ESA/SER.A/451). 2020;
2. Livingston G, Huntley J, Sommerlad A, et al. Dementia prevention, intervention, and care: 2020 report of the Lancet Commission. *Lancet*. Aug 8 2020;396(10248):413-446. doi:10.1016/S0140-6736(20)30367-6
3. international Asd. World Alzheimer Report 2015. 2015;
4. Prusiner SB. Prions. *Proc Natl Acad Sci U S A*. Nov 10 1998;95(23):13363-83. doi:10.1073/pnas.95.23.13363
5. Frost B, Diamond MI. Prion-like mechanisms in neurodegenerative diseases. *Nat Rev Neurosci*. Mar 2010;11(3):155-9. doi:10.1038/nrn2786
6. Kovacs GG. Concepts and classification of neurodegenerative diseases. *Handb Clin Neurol*. 2017;145:301-307. doi:10.1016/B978-0-12-802395-2.00021-3
7. Telling GC, Parchi P, DeArmond SJ, et al. Evidence for the conformation of the pathologic isoform of the prion protein enciphering and propagating prion diversity. *Science*. Dec 20 1996;274(5295):2079-82. doi:10.1126/science.274.5295.2079
8. Legname G, Nguyen HO, Peretz D, Cohen FE, DeArmond SJ, Prusiner SB. Continuum of prion protein structures enciphers a multitude of prion isolate-specified phenotypes. *Proc Natl Acad Sci U S A*. Dec 12 2006;103(50):19105-10. doi:10.1073/pnas.0608970103
9. Petkova AT, Leapman RD, Guo Z, Yau WM, Mattson MP, Tycko R. Self-propagating, molecular-level polymorphism in Alzheimer's beta-amyloid fibrils. *Science*. Jan 14 2005;307(5707):262-5. doi:10.1126/science.1105850
10. Watts JC, Condello C, Stohr J, et al. Serial propagation of distinct strains of Abeta prions from Alzheimer's disease patients. *Proc Natl Acad Sci U S A*. Jul 15 2014;111(28):10323-8. doi:10.1073/pnas.1408900111
11. Qiang W, Yau WM, Lu JX, Collinge J, Tycko R. Structural variation in amyloid-beta fibrils from Alzheimer's disease clinical subtypes. *Nature*. Jan 12 2017;541(7636):217-221. doi:10.1038/nature20814
12. Sanders DW, Kaufman SK, DeVos SL, et al. Distinct tau prion strains propagate in cells and mice and define different tauopathies. *Neuron*. Jun 18 2014;82(6):1271-88. doi:10.1016/j.neuron.2014.04.047
13. Kaufman SK, Sanders DW, Thomas TL, et al. Tau Prion Strains Dictate Patterns of Cell Pathology, Progression Rate, and Regional Vulnerability In Vivo. *Neuron*. Nov 23 2016;92(4):796-812. doi:10.1016/j.neuron.2016.09.055
14. Narasimhan S, Guo JL, Changolkar L, et al. Pathological Tau Strains from Human Brains Recapitulate the Diversity of Tauopathies in Nontransgenic Mouse Brain. *J Neurosci*. Nov 22 2017;37(47):11406-11423. doi:10.1523/JNEUROSCI.1230-17.2017
15. Guo JL, Covell DJ, Daniels JP, et al. Distinct alpha-synuclein strains differentially promote tau inclusions in neurons. *Cell*. Jul 3 2013;154(1):103-17. doi:10.1016/j.cell.2013.05.057
16. Bousset L, Pieri L, Ruiz-Arlandis G, et al. Structural and functional characterization of two alpha-synuclein strains. *Nat Commun*. 2013;4:2575. doi:10.1038/ncomms3575
17. Peelaerts W, Bousset L, Van der Perren A, et al. alpha-Synuclein strains cause distinct synucleinopathies after local and systemic administration. *Nature*. Jun 18 2015;522(7556):340-4. doi:10.1038/nature14547
18. Prusiner SB, Woerman AL, Mordes DA, et al. Evidence for alpha-synuclein prions causing multiple system atrophy in humans with parkinsonism. *Proc Natl Acad Sci U S A*. Sep 22 2015;112(38):E5308-17. doi:10.1073/pnas.1514475112
19. Kane MD, Lipinski WJ, Callahan MJ, et al. Evidence for seeding of beta -amyloid by intracerebral infusion of Alzheimer brain extracts in beta -amyloid precursor protein-transgenic mice. *J Neurosci*. May 15 2000;20(10):3606-11.

20. Frost B, Jacks RL, Diamond MI. Propagation of tau misfolding from the outside to the inside of a cell. *J Biol Chem*. May 8 2009;284(19):12845-52. doi:10.1074/jbc.M808759200
21. Kordower JH, Chu Y, Hauser RA, Freeman TB, Olanow CW. Lewy body-like pathology in long-term embryonic nigral transplants in Parkinson's disease. *Nat Med*. May 2008;14(5):504-6. doi:10.1038/nm1747
22. Li JY, Englund E, Holton JL, et al. Lewy bodies in grafted neurons in subjects with Parkinson's disease suggest host-to-graft disease propagation. *Nat Med*. May 2008;14(5):501-3. doi:10.1038/nm1746
23. Geschwind MD. Prion Diseases. *Continuum (Minneap Minn)*. Dec 2015;21(6 Neuroinfectious Disease):1612-38. doi:10.1212/CON.0000000000000251
24. Prusiner SB, ebrary Inc. *Prion biology and diseases*. Cold Spring Harbor Laboratory Press,; 1999:xiii, 794 p. ill. (some col.) 24 cm. http://site.ebrary.com/lib/princeton/Doc?id=10006734852
25. Greenfield JG, Graham DI, Lantos PL. *Greenfield's Neuropathology*. 6th ed. Arnold ; Oxford University Press; 1997:2 volumes.
26. Creutzfeldt HG. Über eine eigenartige herdförmige erkrankung des zentralnervensystems (Vorläufige mitteilung). *Zeitschrift für die gesamte Neurologie und Psychiatrie*. 1920/12/01 1920;57(1):1-18. doi:10.1007/BF02866081
27. Jakob A. Ubereigenartige Erkrankungen des Zentralnervensystems mit bemerkenswerten anatomischern Befunde (Spastische Pseudosklerose-Encephalomyelopathie mit disseminierten Degenerationsherden). *Dtsch Zeitschr f Nervenheilk*. 1921 1921;70:132-146.
28. Jakob A. Uber eine der multiplen Sklerose klinis nahestehende Erkankung des Zentralnervensystems (spastiche Pseudosklerose) mit bemerkenswertem anastomische Befunde. *Med Klin*. 1921 1921;17:372-376.
29. Gajdusek DC, Zigas V. Degenerative disease of the central nervous system in New Guinea; the endemic occurrence of kuru in the native population. *N Engl J Med*. Nov 14 1957;257(20):974-8. doi:10.1056/NEJM195711142572005
30. Zigas V, Gajdusek DC. Kuru: clinical study of a new syndrome resembling paralysis agitans in natives of the Eastern Highlands of Australian New Guinea. *Med J Aust*. Nov 23 1957;44(21):745-54. doi:10.5694/j.1326-5377.1957.tb60287.x
31. Gajdusek DC, Gibbs CJ. Attempts to Demonstrate a Transmissible Agent in Kuru, Amyotrophic Lateral Sclerosis, and Other Sub-Acute and Chronic Nervous System Degenerations of Man. *Nature*. Oct 17 1964;204:257-9. doi:10.1038/204257a0
32. Gajdusek DC, Gibbs CJ, Alpers M. Experimental transmission of a Kuru-like syndrome to chimpanzees. *Nature*. Feb 19 1966;209(5025):794-6. doi:10.1038/209794a0
33. Gajdusek DC, Gibbs CJ, Jr., Alpers M. Transmission and passage of experimenal "kuru" to chimpanzees. *Science*. Jan 13 1967;155(3759):212-4.
34. Prusiner SB. Novel proteinaceous infectious particles cause scrapie. *Science*. Apr 9 1982;216(4542):136-44. doi:10.1126/science.6801762
35. Prusiner SB, Bolton DC, Groth DF, Bowman KA, Cochran SP, McKinley MP. Further purification and characterization of scrapie prions. *Biochemistry*. Dec 21 1982;21(26):6942-50. doi:10.1021/bi00269a050
36. Bolton DC, McKinley MP, Prusiner SB. Identification of a protein that purifies with the scrapie prion. *Science*. Dec 24 1982;218(4579):1309-11. doi:10.1126/science.6815801
37. Gambetti P, Dong Z, Yuan J, et al. A novel human disease with abnormal prion protein sensitive to protease. *Ann Neurol*. Jun 2008;63(6):697-708. doi:10.1002/ana.21420
38. Puoti G, Bizzi A, Forloni G, Safar JG, Tagliavini F, Gambetti P. Sporadic human prion diseases: molecular insights and diagnosis. *Lancet Neurol*. Jul 2012;11(7):618-28. doi:10.1016/S1474-4422(12)70063-7
39. Rabinovici GD, Wang PN, Levin J, et al. First symptom in sporadic Creutzfeldt-Jakob disease. *Neurology*. Jan 24 2006;66(2):286-7. doi:10.1212/01.wnl.0000196440.00297.67
40. Brown K, Mastrianni JA. The prion diseases. *J Geriatr Psychiatry Neurol*. Dec 2010;23(4):277-98. doi:10.1177/0891988710383576
41. Johnson RT. Prion diseases. *Lancet Neurol*. Oct 2005;4(10):635-42. doi:10.1016/S1474-4422(05)70192-7

42. Palmer MS, Dryden AJ, Hughes JT, Collinge J. Homozygous prion protein genotype predisposes to sporadic Creutzfeldt-Jakob disease. *Nature*. Jul 25 1991;352(6333):340-2. doi:10.1038/352340a0
43. Lloyd S, Mead S, Collinge J. Genetics of prion disease. *Top Curr Chem*. 2011;305:1-22. doi:10.1007/128_2011_157
44. Rogaeva E, Zadikoff C, Ponesse J, et al. Childhood onset in familial prion disease with a novel mutation in the PRNP gene. *Arch Neurol*. Jul 2006;63(7):1016-21. doi:10.1001/archneur.63.7.1016
45. Johnson RT, Gibbs CJ, Jr. Creutzfeldt-Jakob disease and related transmissible spongiform encephalopathies. *N Engl J Med*. Dec 31 1998;339(27):1994-2004. doi:10.1056/NEJM199812313392707
46. Monari L, Chen SG, Brown P, et al. Fatal familial insomnia and familial Creutzfeldt-Jakob disease: different prion proteins determined by a DNA polymorphism. *Proc Natl Acad Sci U S A*. Mar 29 1994;91(7):2839-42. doi:10.1073/pnas.91.7.2839
47. Heath CA, Cooper SA, Murray K, et al. Diagnosing variant Creutzfeldt-Jakob disease: a retrospective analysis of the first 150 cases in the UK. *J Neurol Neurosurg Psychiatry*. Jun 2011;82(6):646-51. doi:10.1136/jnnp.2010.232264
48. Knight R. The risk of transmitting prion disease by blood or plasma products. *Transfus Apher Sci*. Dec 2010;43(3):387-391. doi:10.1016/j.transci.2010.09.003
49. Brown P, Preece M, Brandel JP, et al. Iatrogenic Creutzfeldt-Jakob disease at the millennium. *Neurology*. Oct 24 2000;55(8):1075-81. doi:10.1212/wnl.55.8.1075
50. Jaunmuktane Z, Mead S, Ellis M, et al. Evidence for human transmission of amyloid-beta pathology and cerebral amyloid angiopathy. *Nature*. Sep 10 2015;525(7568):247-50. doi:10.1038/nature15369
51. Tousseyn T, Bajsarowicz K, Sanchez H, et al. Prion Disease Induces Alzheimer Disease-Like Neuropathologic Changes. *J Neuropathol Exp Neurol*. Sep 2015;74(9):873-88. doi:10.1097/NEN.0000000000000228
52. Zerr I, Schulz-Schaeffer WJ, Giese A, et al. Current clinical diagnosis in Creutzfeldt-Jakob disease: identification of uncommon variants. *Ann Neurol*. Sep 2000;48(3):323-9.
53. Glatzel M, Stoeck K, Seeger H, Luhrs T, Aguzzi A. Human prion diseases: molecular and clinical aspects. *Arch Neurol*. Apr 2005;62(4):545-52. doi:10.1001/archneur.62.4.545
54. Skillback T, Rosen C, Asztely F, Mattsson N, Blennow K, Zetterberg H. Diagnostic performance of cerebrospinal fluid total tau and phosphorylated tau in Creutzfeldt-Jakob disease: results from the Swedish Mortality Registry. *JAMA Neurol*. Apr 2014;71(4):476-83. doi:10.1001/jamaneurol.2013.6455
55. Jankovska N, Rusina R, Bruzova M, Parobkova E, Olejar T, Matej R. Human Prion Disorders: Review of the Current Literature and a Twenty-Year Experience of the National Surveillance Center in the Czech Republic. *Diagnostics (Basel)*. Oct 1 2021;11(10)doi:10.3390/diagnostics11101821
56. Hamlin C, Puoti G, Berri S, et al. A comparison of tau and 14-3-3 protein in the diagnosis of Creutzfeldt-Jakob disease. *Neurology*. Aug 7 2012;79(6):547-52. doi:10.1212/WNL.0b013e318263565f
57. Atarashi R, Satoh K, Sano K, et al. Ultrasensitive human prion detection in cerebrospinal fluid by real-time quaking-induced conversion. *Nat Med*. Feb 2011;17(2):175-8. doi:10.1038/nm.2294
58. Alperovitch A, Zerr I, Pocchiari M, et al. Codon 129 prion protein genotype and sporadic Creutzfeldt-Jakob disease. *Lancet*. May 15 1999;353(9165):1673-4. doi:10.1016/s0140-6736(99)01342-2
59. Mok T, Jaunmuktane Z, Joiner S, et al. Variant Creutzfeldt-Jakob Disease in a Patient with Heterozygosity at PRNP Codon 129. *N Engl J Med*. Jan 19 2017;376(3):292-294. doi:10.1056/NEJMc1610003
60. Aguzzi A, Heikenwalder M, Polymenidou M. Insights into prion strains and neurotoxicity. *Nat Rev Mol Cell Biol*. Jul 2007;8(7):552-61. doi:10.1038/nrm2204
61. Bessen RA, Marsh RF. Distinct PrP properties suggest the molecular basis of strain variation in transmissible mink encephalopathy. *J Virol*. Dec 1994;68(12):7859-68. doi:10.1128/JVI.68.12.7859-7868.1994
62. Safar J, Wille H, Itri V, et al. Eight prion strains have PrP(Sc) molecules with different conformations. *Nat Med*. Oct 1998;4(10):1157-65. doi:10.1038/2654

63. Collinge J. Molecular neurology of prion disease. *J Neurol Neurosurg Psychiatry*. Jul 2005;76(7):906-19. doi:10.1136/jnnp.2004.048660
64. Brandner S, Jaunmuktane Z. Prion disease: experimental models and reality. *Acta Neuropathol*. Feb 2017;133(2):197-222. doi:10.1007/s00401-017-1670-5
65. Collinge J, Sidle KC, Meads J, Ironside J, Hill AF. Molecular analysis of prion strain variation and the aetiology of 'new variant' CJD. *Nature*. Oct 24 1996;383(6602):685-90. doi:10.1038/383685a0
66. Colby DW, Prusiner SB. Prions. *Cold Spring Harb Perspect Biol*. Jan 1 2011;3(1):a006833. doi:10.1101/cshperspect.a006833
67. Stahl N, Borchelt DR, Hsiao K, Prusiner SB. Scrapie prion protein contains a phosphatidylinositol glycolipid. *Cell*. Oct 23 1987;51(2):229-40. doi:10.1016/0092-8674(87)90150-4
68. Maiti NR, Surewicz WK. The role of disulfide bridge in the folding and stability of the recombinant human prion protein. *J Biol Chem*. Jan 26 2001;276(4):2427-31. doi:10.1074/jbc.M007862200
69. Lawson VA, Collins SJ, Masters CL, Hill AF. Prion protein glycosylation. *J Neurochem*. May 2005;93(4):793-801. doi:10.1111/j.1471-4159.2005.03104.x
70. Legname G. Elucidating the function of the prion protein. *PLoS Pathog*. Aug 2017;13(8):e1006458. doi:10.1371/journal.ppat.1006458
71. Ying YS, Anderson RG, Rothberg KG. Each caveola contains multiple glycosyl-phosphatidylinositol-anchored membrane proteins. *Cold Spring Harb Symp Quant Biol*. 1992;57:593-604. doi:10.1101/sqb.1992.057.01.065
72. Walter ED, Stevens DJ, Visconte MP, Millhauser GL. The prion protein is a combined zinc and copper binding protein: Zn2+ alters the distribution of Cu2+ coordination modes. *J Am Chem Soc*. Dec 19 2007;129(50):15440-1. doi:10.1021/ja077146j
73. Zahn R, Liu A, Luhrs T, et al. NMR solution structure of the human prion protein. *Proc Natl Acad Sci U S A*. Jan 4 2000;97(1):145-50. doi:10.1073/pnas.97.1.145
74. Abskharon RN, Giachin G, Wohlkonig A, et al. Probing the N-terminal beta-sheet conversion in the crystal structure of the human prion protein bound to a nanobody. *J Am Chem Soc*. Jan 22 2014;136(3):937-44. doi:10.1021/ja407527p
75. Linsenmeier L, Altmeppen HC, Wetzel S, Mohammadi B, Saftig P, Glatzel M. Diverse functions of the prion protein - Does proteolytic processing hold the key? *Biochim Biophys Acta Mol Cell Res*. Nov 2017;1864(11 Pt B):2128-2137. doi:10.1016/j.bbamcr.2017.06.022
76. Guillot-Sestier MV, Sunyach C, Druon C, Scarzello S, Checler F. The alpha-secretase-derived N-terminal product of cellular prion, N1, displays neuroprotective function in vitro and in vivo. *J Biol Chem*. Dec 18 2009;284(51):35973-86. doi:10.1074/jbc.M109.051086
77. Westergard L, Turnbaugh JA, Harris DA. A naturally occurring C-terminal fragment of the prion protein (PrP) delays disease and acts as a dominant-negative inhibitor of PrPSc formation. *J Biol Chem*. Dec 23 2011;286(51):44234-44242. doi:10.1074/jbc.M111.286195
78. Jimenez-Huete A, Lievens PM, Vidal R, et al. Endogenous proteolytic cleavage of normal and disease-associated isoforms of the human prion protein in neural and non-neural tissues. *Am J Pathol*. Nov 1998;153(5):1561-72. doi:10.1016/S0002-9440(10)65744-6
79. Caughey B, Raymond GJ, Ernst D, Race RE. N-terminal truncation of the scrapie-associated form of PrP by lysosomal protease(s): implications regarding the site of conversion of PrP to the protease-resistant state. *J Virol*. Dec 1991;65(12):6597-603. doi:10.1128/JVI.65.12.6597-6603.1991
80. Altmeppen HC, Puig B, Dohler F, et al. Proteolytic processing of the prion protein in health and disease. *Am J Neurodegener Dis*. 2012;1(1):15-31.
81. Benvegnu S, Poggiolini I, Legname G. Neurodevelopmental expression and localization of the cellular prion protein in the central nervous system of the mouse. *J Comp Neurol*. Jun 1 2010;518(11):1879-91. doi:10.1002/cne.22357
82. Bendheim PE, Brown HR, Rudelli RD, et al. Nearly ubiquitous tissue distribution of the scrapie agent precursor protein. *Neurology*. Jan 1992;42(1):149-56. doi:10.1212/wnl.42.1.149
83. Bueler H, Fischer M, Lang Y, et al. Normal development and behaviour of mice lacking the neuronal cell-surface PrP protein. *Nature*. Apr 16 1992;356(6370):577-82. doi:10.1038/356577a0
84. Bueler H, Aguzzi A, Sailer A, et al. Mice devoid of PrP are resistant to scrapie. *Cell*. Jul 2 1993;73(7):1339-47. doi:10.1016/0092-8674(93)90360-3

85. Tobler I, Gaus SE, Deboer T, et al. Altered circadian activity rhythms and sleep in mice devoid of prion protein. *Nature*. Apr 18 1996;380(6575):639-42. doi:10.1038/380639a0
86. Steele AD, Emsley JG, Ozdinler PH, Lindquist S, Macklis JD. Prion protein (PrPc) positively regulates neural precursor proliferation during developmental and adult mammalian neurogenesis. *Proc Natl Acad Sci U S A*. Feb 28 2006;103(9):3416-21. doi:10.1073/pnas.0511290103
87. Caiati MD, Safiulina VF, Fattorini G, Sivakumaran S, Legname G, Cherubini E. PrPC controls via protein kinase A the direction of synaptic plasticity in the immature hippocampus. *J Neurosci*. Feb 13 2013;33(7):2973-83. doi:10.1523/JNEUROSCI.4149-12.2013
88. Bremer J, Baumann F, Tiberi C, et al. Axonal prion protein is required for peripheral myelin maintenance. *Nat Neurosci*. Mar 2010;13(3):310-8. doi:10.1038/nn.2483
89. Linden R, Martins VR, Prado MA, Cammarota M, Izquierdo I, Brentani RR. Physiology of the prion protein. *Physiol Rev*. Apr 2008;88(2):673-728. doi:10.1152/physrev.00007.2007
90. Manni G, Lewis V, Senesi M, et al. The cellular prion protein beyond prion diseases. *Swiss Med Wkly*. Apr 20 2020;150:w20222. doi:10.4414/smw.2020.20222
91. Brandner S, Isenmann S, Raeber A, et al. Normal host prion protein necessary for scrapie-induced neurotoxicity. *Nature*. Jan 25 1996;379(6563):339-43. doi:10.1038/379339a0
92. Mallucci G, Dickinson A, Linehan J, Klohn PC, Brandner S, Collinge J. Depleting neuronal PrP in prion infection prevents disease and reverses spongiosis. *Science*. Oct 31 2003;302(5646):871-4. doi:10.1126/science.1090187
93. Resenberger UK, Harmeier A, Woerner AC, et al. The cellular prion protein mediates neurotoxic signalling of beta-sheet-rich conformers independent of prion replication. *EMBO J*. May 18 2011;30(10):2057-70. doi:10.1038/emboj.2011.86
94. Benilova I, Karran E, De Strooper B. The toxic Abeta oligomer and Alzheimer's disease: an emperor in need of clothes. *Nat Neurosci*. Jan 29 2012;15(3):349-57. doi:10.1038/nn.3028
95. Condello C, Lemmin T, Stohr J, et al. Structural heterogeneity and intersubject variability of Abeta in familial and sporadic Alzheimer's disease. *Proc Natl Acad Sci U S A*. Jan 23 2018;115(4):E782-E791. doi:10.1073/pnas.1714966115
96. Li S, Selkoe DJ. A mechanistic hypothesis for the impairment of synaptic plasticity by soluble Abeta oligomers from Alzheimer's brain. *J Neurochem*. Sep 2020;154(6):583-597. doi:10.1111/jnc.15007
97. Cohen M, Appleby B, Safar JG. Distinct prion-like strains of amyloid beta implicated in phenotypic diversity of Alzheimer's disease. *Prion*. 2016;10(1):9-17. doi:10.1080/19336896.2015.1123371
98. Lauren J, Gimbel DA, Nygaard HB, Gilbert JW, Strittmatter SM. Cellular prion protein mediates impairment of synaptic plasticity by amyloid-beta oligomers. *Nature*. Feb 26 2009;457(7233):1128-32. doi:10.1038/nature07761
99. Freir DB, Nicoll AJ, Klyubin I, et al. Interaction between prion protein and toxic amyloid beta assemblies can be therapeutically targeted at multiple sites. *Nat Commun*. Jun 7 2011;2:336. doi:10.1038/ncomms1341
100. Corbett GT, Wang Z, Hong W, et al. PrP is a central player in toxicity mediated by soluble aggregates of neurodegeneration-causing proteins. *Acta Neuropathol*. Mar 2020;139(3):503-526. doi:10.1007/s00401-019-02114-9
101. Chen S, Yadav SP, Surewicz WK. Interaction between human prion protein and amyloid-beta (Abeta) oligomers: role OF N-terminal residues. *J Biol Chem*. Aug 20 2010;285(34):26377-83. doi:10.1074/jbc.M110.145516
102. Nicoll AJ, Panico S, Freir DB, et al. Amyloid-beta nanotubes are associated with prion protein-dependent synaptotoxicity. *Nat Commun*. 2013;4:2416. doi:10.1038/ncomms3416
103. Um JW, Nygaard HB, Heiss JK, et al. Alzheimer amyloid-beta oligomer bound to postsynaptic prion protein activates Fyn to impair neurons. *Nat Neurosci*. Sep 2012;15(9):1227-35. doi:10.1038/nn.3178
104. Balducci C, Beeg M, Stravalaci M, et al. Synthetic amyloid-beta oligomers impair long-term memory independently of cellular prion protein. *Proc Natl Acad Sci U S A*. Feb 2 2010;107(5):2295-300. doi:10.1073/pnas.0911829107
105. Cisse M, Sanchez PE, Kim DH, Ho K, Yu GQ, Mucke L. Ablation of cellular prion protein does not ameliorate abnormal neural network activity or cognitive dysfunction in the J20 line of human

amyloid precursor protein transgenic mice. *J Neurosci*. Jul 20 2011;31(29):10427-31. doi:10.1523/JNEUROSCI.1459-11.2011
106. Kessels HW, Nguyen LN, Nabavi S, Malinow R. The prion protein as a receptor for amyloid-beta. *Nature*. Aug 12 2010;466(7308):E3-4; discussion E4-5. doi:10.1038/nature09217
107. Wang Y, Mandelkow E. Tau in physiology and pathology. *Nat Rev Neurosci*. Jan 2016;17(1):5-21. doi:10.1038/nrn.2015.1
108. Santacruz K, Lewis J, Spires T, et al. Tau suppression in a neurodegenerative mouse model improves memory function. *Science*. Jul 15 2005;309(5733):476-81. doi:10.1126/science.1113694
109. Van der Jeugd A, Hochgrafe K, Ahmed T, et al. Cognitive defects are reversible in inducible mice expressing pro-aggregant full-length human Tau. *Acta Neuropathol*. Jun 2012;123(6):787-805. doi:10.1007/s00401-012-0987-3
110. Wang XF, Dong CF, Zhang J, et al. Human tau protein forms complex with PrP and some GSS- and fCJD-related PrP mutants possess stronger binding activities with tau in vitro. *Mol Cell Biochem*. Mar 2008;310(1-2):49-55. doi:10.1007/s11010-007-9664-6
111. Hu NW, Corbett GT, Moore S, et al. Extracellular Forms of Abeta and Tau from iPSC Models of Alzheimer's Disease Disrupt Synaptic Plasticity. *Cell Rep*. May 15 2018;23(7):1932-1938. doi:10.1016/j.celrep.2018.04.040
112. Ondrejcak T, Klyubin I, Corbett GT, et al. Cellular Prion Protein Mediates the Disruption of Hippocampal Synaptic Plasticity by Soluble Tau In Vivo. *J Neurosci*. Dec 12 2018;38(50):10595-10606. doi:10.1523/JNEUROSCI.1700-18.2018
113. Ondrejcak T, Hu NW, Qi Y, et al. Soluble tau aggregates inhibit synaptic long-term depression and amyloid beta-facilitated LTD in vivo. *Neurobiol Dis*. Jul 2019;127:582-590. doi:10.1016/j.nbd.2019.03.022
114. De Cecco E, Celauro L, Vanni S, et al. The uptake of tau amyloid fibrils is facilitated by the cellular prion protein and hampers prion propagation in cultured cells. *J Neurochem*. Dec 2020;155(5):577-591. doi:10.1111/jnc.15040
115. Bernal-Conde LD, Ramos-Acevedo R, Reyes-Hernandez MA, et al. Alpha-Synuclein Physiology and Pathology: A Perspective on Cellular Structures and Organelles. *Front Neurosci*. 2019;13:1399. doi:10.3389/fnins.2019.01399
116. Lashuel HA, Overk CR, Oueslati A, Masliah E. The many faces of alpha-synuclein: from structure and toxicity to therapeutic target. *Nat Rev Neurosci*. Jan 2013;14(1):38-48. doi:10.1038/nrn3406
117. Ip CW, Klaus LC, Karikari AA, et al. AAV1/2-induced overexpression of A53T-alpha-synuclein in the substantia nigra results in degeneration of the nigrostriatal system with Lewy-like pathology and motor impairment: a new mouse model for Parkinson's disease. *Acta Neuropathol Commun*. Feb 1 2017;5(1):11. doi:10.1186/s40478-017-0416-x
118. Wakabayashi K, Tanji K, Mori F, Takahashi H. The Lewy body in Parkinson's disease: molecules implicated in the formation and degradation of alpha-synuclein aggregates. *Neuropathology*. Oct 2007;27(5):494-506. doi:10.1111/j.1440-1789.2007.00803.x
119. Urrea L, Segura-Feliu M, Masuda-Suzukake M, et al. Involvement of Cellular Prion Protein in alpha-Synuclein Transport in Neurons. *Mol Neurobiol*. Mar 2018;55(3):1847-1860. doi:10.1007/s12035-017-0451-4
120. Aulic S, Masperone L, Narkiewicz J, et al. alpha-Synuclein Amyloids Hijack Prion Protein to Gain Cell Entry, Facilitate Cell-to-Cell Spreading and Block Prion Replication. *Sci Rep*. Aug 30 2017;7(1):10050. doi:10.1038/s41598-017-10236-x
121. Ferreira DG, Temido-Ferreira M, Vicente Miranda H, et al. alpha-synuclein interacts with PrP(C) to induce cognitive impairment through mGluR5 and NMDAR2B. *Nat Neurosci*. Nov 2017;20(11):1569-1579. doi:10.1038/nn.4648
122. La Vitola P, Beeg M, Balducci C, et al. Cellular prion protein neither binds to alpha-synuclein oligomers nor mediates their detrimental effects. *Brain*. Feb 1 2019;142(2):249-254. doi:10.1093/brain/awy318
123. Campana V, Sarnataro D, Zurzolo C. The highways and byways of prion protein trafficking. *Trends Cell Biol*. Feb 2005;15(2):102-11. doi:10.1016/j.tcb.2004.12.002
124. Shyng SL, Huber MT, Harris DA. A prion protein cycles between the cell surface and an endocytic compartment in cultured neuroblastoma cells. *J Biol Chem*. Jul 25 1993;268(21):15922-8.

125. Agostini F, Dotti CG, Perez-Canamas A, Ledesma MD, Benetti F, Legname G. Prion protein accumulation in lipid rafts of mouse aging brain. *PLoS One*. 2013;8(9):e74244. doi:10.1371/journal.pone.0074244
126. Sarnataro D, Campana V, Paladino S, Stornaiuolo M, Nitsch L, Zurzolo C. PrP(C) association with lipid rafts in the early secretory pathway stabilizes its cellular conformation. *Mol Biol Cell*. Sep 2004;15(9):4031-42. doi:10.1091/mbc.e03-05-0271
127. Simons K, Ikonen E. Functional rafts in cell membranes. *Nature*. Jun 5 1997;387(6633):569-72. doi:10.1038/42408
128. Sunyach C, Jen A, Deng J, et al. The mechanism of internalization of glycosylphosphatidylinositol-anchored prion protein. *EMBO J*. Jul 15 2003;22(14):3591-601. doi:10.1093/emboj/cdg344
129. Shyng SL, Heuser JE, Harris DA. A glycolipid-anchored prion protein is endocytosed via clathrin-coated pits. *J Cell Biol*. Jun 1994;125(6):1239-50. doi:10.1083/jcb.125.6.1239
130. Gauczynski S, Peyrin JM, Haik S, et al. The 37-kDa/67-kDa laminin receptor acts as the cell-surface receptor for the cellular prion protein. *EMBO J*. Nov 1 2001;20(21):5863-75. doi:10.1093/emboj/20.21.5863
131. Taylor DR, Hooper NM. The low-density lipoprotein receptor-related protein 1 (LRP1) mediates the endocytosis of the cellular prion protein. *Biochem J*. Feb 15 2007;402(1):17-23. doi:10.1042/BJ20061736
132. Kang YS, Zhao X, Lovaas J, Eisenberg E, Greene LE. Clathrin-independent internalization of normal cellular prion protein in neuroblastoma cells is associated with the Arf6 pathway. *J Cell Sci*. Nov 15 2009;122(Pt 22):4062-9. doi:10.1242/jcs.046292
133. Magalhaes AC, Silva JA, Lee KS, et al. Endocytic intermediates involved with the intracellular trafficking of a fluorescent cellular prion protein. *J Biol Chem*. Sep 6 2002;277(36):33311-8. doi:10.1074/jbc.M203661200
134. Parton RG, McMahon KA, Wu Y. Caveolae: Formation, dynamics, and function. *Curr Opin Cell Biol*. Aug 2020;65:8-16. doi:10.1016/j.ceb.2020.02.001
135. Peters PJ, Mironov A, Jr., Peretz D, et al. Trafficking of prion proteins through a caveolae-mediated endosomal pathway. *J Cell Biol*. Aug 18 2003;162(4):703-17. doi:10.1083/jcb.200304140
136. Shi Q, Jing YY, Wang SB, et al. PrP octarepeats region determined the interaction with caveolin-1 and phosphorylation of caveolin-1 and Fyn. *Med Microbiol Immunol*. Jun 2013;202(3):215-27. doi:10.1007/s00430-012-0284-8
137. Ren K, Gao C, Zhang J, et al. Flotillin-1 mediates PrPc endocytosis in the cultured cells during Cu(2)(+) stimulation through molecular interaction. *Mol Neurobiol*. Dec 2013;48(3):631-46. doi:10.1007/s12035-013-8452-4
138. Fevrier B, Vilette D, Archer F, et al. Cells release prions in association with exosomes. *Proc Natl Acad Sci U S A*. Jun 29 2004;101(26):9683-8. doi:10.1073/pnas.0308413101
139. Li X, Bao H, Wang Z, et al. Biogenesis and Function of Multivesicular Bodies in Plant Immunity. *Front Plant Sci*. 2018;9:979. doi:10.3389/fpls.2018.00979
140. Dias MV, Teixeira BL, Rodrigues BR, et al. PRNP/prion protein regulates the secretion of exosomes modulating CAV1/caveolin-1-suppressed autophagy. *Autophagy*. Nov 2016;12(11):2113-2128. doi:10.1080/15548627.2016.1226735
141. Zhu S, Victoria GS, Marzo L, Ghosh R, Zurzolo C. Prion aggregates transfer through tunneling nanotubes in endocytic vesicles. *Prion*. 2015;9(2):125-35. doi:10.1080/19336896.2015.1025189
142. Gousset K, Schiff E, Langevin C, et al. Prions hijack tunnelling nanotubes for intercellular spread. *Nat Cell Biol*. Mar 2009;11(3):328-36. doi:10.1038/ncb1841
143. Porto-Carreiro I, Fevrier B, Paquet S, Vilette D, Raposo G. Prions and exosomes: from PrPc trafficking to PrPsc propagation. *Blood Cells Mol Dis*. Sep-Oct 2005;35(2):143-8. doi:10.1016/j.bcmd.2005.06.013
144. Ballmer BA, Moos R, Liberali P, Pelkmans L, Hornemann S, Aguzzi A. Modifiers of prion protein biogenesis and recycling identified by a highly parallel endocytosis kinetics assay. *J Biol Chem*. May 19 2017;292(20):8356-8368. doi:10.1074/jbc.M116.773283
145. Walker LC, Jucker M. Neurodegenerative diseases: expanding the prion concept. *Annu Rev Neurosci*. Jul 8 2015;38:87-103. doi:10.1146/annurev-neuro-071714-033828

146. Pan KM, Baldwin M, Nguyen J, et al. Conversion of alpha-helices into beta-sheets features in the formation of the scrapie prion proteins. *Proc Natl Acad Sci U S A*. Dec 1 1993;90(23):10962-6. doi:10.1073/pnas.90.23.10962
147. Vorberg I, Raines A, Priola SA. Acute formation of protease-resistant prion protein does not always lead to persistent scrapie infection in vitro. *J Biol Chem*. Jul 9 2004;279(28):29218-25. doi:10.1074/jbc.M402576200
148. Goold R, Rabbanian S, Sutton L, et al. Rapid cell-surface prion protein conversion revealed using a novel cell system. *Nat Commun*. 2011;2:281. doi:10.1038/ncomms1282
149. Taraboulos A, Serban D, Prusiner SB. Scrapie prion proteins accumulate in the cytoplasm of persistently infected cultured cells. *J Cell Biol*. Jun 1990;110(6):2117-32. doi:10.1083/jcb.110.6.2117
150. Marijanovic Z, Caputo A, Campana V, Zurzolo C. Identification of an intracellular site of prion conversion. *PLoS Pathog*. May 2009;5(5):e1000426. doi:10.1371/journal.ppat.1000426
151. Goold R, McKinnon C, Rabbanian S, Collinge J, Schiavo G, Tabrizi SJ. Alternative fates of newly formed PrPSc upon prion conversion on the plasma membrane. *J Cell Sci*. Aug 15 2013;126(Pt 16):3552-62. doi:10.1242/jcs.120477
152. Yim YI, Park BC, Yadavalli R, Zhao X, Eisenberg E, Greene LE. The multivesicular body is the major internal site of prion conversion. *J Cell Sci*. Apr 1 2015;128(7):1434-43. doi:10.1242/jcs.165472
153. Fehlinger A, Wolf H, Hossinger A, et al. Prion strains depend on different endocytic routes for productive infection. *Sci Rep*. Jul 31 2017;7(1):6923. doi:10.1038/s41598-017-07260-2
154. Gauczynski S, Nikles D, El-Gogo S, et al. The 37-kDa/67-kDa laminin receptor acts as a receptor for infectious prions and is inhibited by polysulfated glycanes. *J Infect Dis*. Sep 1 2006;194(5):702-9. doi:10.1086/505914
155. Morel E, Andrieu T, Casagrande F, et al. Bovine prion is endocytosed by human enterocytes via the 37 kDa/67 kDa laminin receptor. *Am J Pathol*. Oct 2005;167(4):1033-42. doi:10.1016/S0002-9440(10)61192-3
156. Jen A, Parkyn CJ, Mootoosamy RC, et al. Neuronal low-density lipoprotein receptor-related protein 1 binds and endocytoses prion fibrils via receptor cluster 4. *J Cell Sci*. Jan 15 2010;123(Pt 2):246-55. doi:10.1242/jcs.058099
157. Simon Davis DA, Parish CR. Heparan sulfate: a ubiquitous glycosaminoglycan with multiple roles in immunity. *Front Immunol*. Dec 18 2013;4:470. doi:10.3389/fimmu.2013.00470
158. Horonchik L, Tzaban S, Ben-Zaken O, et al. Heparan sulfate is a cellular receptor for purified infectious prions. *J Biol Chem*. Apr 29 2005;280(17):17062-7. doi:10.1074/jbc.M500122200
159. Hijazi N, Kariv-Inbal Z, Gasset M, Gabizon R. PrPSc incorporation to cells requires endogenous glycosaminoglycan expression. *J Biol Chem*. Apr 29 2005;280(17):17057-61. doi:10.1074/jbc.M411314200
160. Bett C, Lawrence J, Kurt TD, et al. Enhanced neuroinvasion by smaller, soluble prions. *Acta Neuropathol Commun*. Apr 21 2017;5(1):32. doi:10.1186/s40478-017-0430-z
161. Paquet S, Daude N, Courageot MP, Chapuis J, Laude H, Vilette D. PrPc does not mediate internalization of PrPSc but is required at an early stage for de novo prion infection of Rov cells. *J Virol*. Oct 2007;81(19):10786-91. doi:10.1128/JVI.01137-07
162. Wadia JS, Schaller M, Williamson RA, Dowdy SF. Pathologic prion protein infects cells by lipid-raft dependent macropinocytosis. *PLoS One*. 2008;3(10):e3314. doi:10.1371/journal.pone.0003314
163. Magalhaes AC, Baron GS, Lee KS, et al. Uptake and neuritic transport of scrapie prion protein coincident with infection of neuronal cells. *J Neurosci*. May 25 2005;25(21):5207-16. doi:10.1523/JNEUROSCI.0653-05.2005
164. Kanu N, Imokawa Y, Drechsel DN, et al. Transfer of scrapie prion infectivity by cell contact in culture. *Curr Biol*. Apr 2 2002;12(7):523-30. doi:10.1016/s0960-9822(02)00722-4
165. Paquet S, Langevin C, Chapuis J, Jackson GS, Laude H, Vilette D. Efficient dissemination of prions through preferential transmission to nearby cells. *J Gen Virol*. Feb 2007;88(Pt 2):706-713. doi:10.1099/vir.0.82336-0
166. Victoria GS, Arkhipenko A, Zhu S, Syan S, Zurzolo C. Astrocyte-to-neuron intercellular prion transfer is mediated by cell-cell contact. *Sci Rep*. Feb 9 2016;6:20762. doi:10.1038/srep20762
167. Coleman BM, Hanssen E, Lawson VA, Hill AF. Prion-infected cells regulate the release of exosomes with distinct ultrastructural features. *FASEB J*. Oct 2012;26(10):4160-73. doi:10.1096/fj.11-202077

168. Guo BB, Bellingham SA, Hill AF. Stimulating the Release of Exosomes Increases the Intercellular Transfer of Prions. *J Biol Chem*. Mar 4 2016;291(10):5128-37. doi:10.1074/jbc.M115.684258
169. Vella LJ, Sharples RA, Lawson VA, Masters CL, Cappai R, Hill AF. Packaging of prions into exosomes is associated with a novel pathway of PrP processing. *J Pathol*. Apr 2007;211(5):582-590. doi:10.1002/path.2145
170. Arellano-Anaya ZE, Huor A, Leblanc P, et al. Prion strains are differentially released through the exosomal pathway. *Cell Mol Life Sci*. Mar 2015;72(6):1185-96. doi:10.1007/s00018-014-1735-8
171. Mattei V, Barenco MG, Tasciotti V, et al. Paracrine diffusion of PrP(C) and propagation of prion infectivity by plasma membrane-derived microvesicles. *PLoS One*. 2009;4(4):e5057. doi:10.1371/journal.pone.0005057
172. Vilette D, Laulagnier K, Huor A, et al. Efficient inhibition of infectious prions multiplication and release by targeting the exosomal pathway. *Cell Mol Life Sci*. Nov 2015;72(22):4409-27. doi:10.1007/s00018-015-1945-8
173. Trajkovic K, Hsu C, Chiantia S, et al. Ceramide triggers budding of exosome vesicles into multivesicular endosomes. *Science*. Feb 29 2008;319(5867):1244-7. doi:10.1126/science.1153124
174. Guo BB, Bellingham SA, Hill AF. The neutral sphingomyelinase pathway regulates packaging of the prion protein into exosomes. *J Biol Chem*. Feb 6 2015;290(6):3455-67. doi:10.1074/jbc.M114.605253
175. Sexton C, Snyder H, Beher D, et al. Current directions in tau research: Highlights from Tau 2020. *Alzheimers Dement*. May 2022;18(5):988-1007. doi:10.1002/alz.12452
176. Kovacs GG. Tauopathies. *Handb Clin Neurol*. 2017;145:355-368. doi:10.1016/B978-0-12-802395-2.00025-0
177. Imbimbo BP, Ippati S, Watling M, Balducci C. A critical appraisal of tau-targeting therapies for primary and secondary tauopathies. *Alzheimers Dement*. May 2022;18(5):1008-1037. doi:10.1002/alz.12453
178. Weingarten MD, Lockwood AH, Hwo SY, Kirschner MW. A protein factor essential for microtubule assembly. *Proc Natl Acad Sci U S A*. May 1975;72(5):1858-62. doi:10.1073/pnas.72.5.1858
179. Goedert M, Spillantini MG, Jakes R, Rutherford D, Crowther RA. Multiple isoforms of human microtubule-associated protein tau: sequences and localization in neurofibrillary tangles of Alzheimer's disease. *Neuron*. Oct 1989;3(4):519-26. doi:10.1016/0896-6273(89)90210-9
180. Strang KH, Golde TE, Giasson BI. MAPT mutations, tauopathy, and mechanisms of neurodegeneration. *Lab Invest*. Jul 2019;99(7):912-928. doi:10.1038/s41374-019-0197-x
181. Dickson DW, Kouri N, Murray ME, Josephs KA. Neuropathology of frontotemporal lobar degeneration-tau (FTLD-tau). *J Mol Neurosci*. Nov 2011;45(3):384-9. doi:10.1007/s12031-011-9589-0
182. Ghetti B, Oblak AL, Boeve BF, Johnson KA, Dickerson BC, Goedert M. Invited review: Frontotemporal dementia caused by microtubule-associated protein tau gene (MAPT) mutations: a chameleon for neuropathology and neuroimaging. *Neuropathol Appl Neurobiol*. Feb 2015;41(1):24-46. doi:10.1111/nan.12213
183. van Swieten JC, Bronner IF, Azmani A, et al. The DeltaK280 mutation in MAP tau favors exon 10 skipping in vivo. *J Neuropathol Exp Neurol*. Jan 2007;66(1):17-25. doi:10.1097/nen.0b013e31802c39a4
184. Caillet-Boudin ML, Buee L, Sergeant N, Lefebvre B. Regulation of human MAPT gene expression. *Mol Neurodegener*. Jul 14 2015;10:28. doi:10.1186/s13024-015-0025-8
185. Kouri N, Ross OA, Dombroski B, et al. Genome-wide association study of corticobasal degeneration identifies risk variants shared with progressive supranuclear palsy. *Nat Commun*. Jun 16 2015;6:7247. doi:10.1038/ncomms8247
186. Myers AJ, Pittman AM, Zhao AS, et al. The MAPT H1c risk haplotype is associated with increased expression of tau and especially of 4 repeat containing transcripts. *Neurobiol Dis*. Mar 2007;25(3):561-70. doi:10.1016/j.nbd.2006.10.018
187. Gong CX, Iqbal K. Hyperphosphorylation of microtubule-associated protein tau: a promising therapeutic target for Alzheimer disease. *Curr Med Chem*. 2008;15(23):2321-8. doi:10.2174/092986708785909111

188. Shi Y, Zhang W, Yang Y, et al. Structure-based classification of tauopathies. *Nature*. Oct 2021;598(7880):359-363. doi:10.1038/s41586-021-03911-7
189. Pick A. Uber die Beziehungen der senilen Hirnatrophie zur Aphasie. *Prag Med Wochenschr*. 1892 1892;17:165-167.
190. Probst A, Tolnay M, Langui D, Goedert M, Spillantini MG. Pick's disease: hyperphosphorylated tau protein segregates to the somatoaxonal compartment. *Acta Neuropathol*. Dec 1996;92(6):588-96. doi:10.1007/s004010050565
191. Ferrer I, Lopez-Gonzalez I, Carmona M, et al. Glial and neuronal tau pathology in tauopathies: characterization of disease-specific phenotypes and tau pathology progression. *J Neuropathol Exp Neurol*. Jan 2014;73(1):81-97. doi:10.1097/NEN.0000000000000030
192. Steele JC, Richardson JC, Olszewski J. Progressive Supranuclear Palsy. A Heterogeneous Degeneration Involving the Brain Stem, Basal Ganglia and Cerebellum with Vertical Gaze and Pseudobulbar Palsy, Nuchal Dystonia and Dementia. *Arch Neurol*. Apr 1964;10:333-59. doi:10.1001/archneur.1964.00460160003001
193. Yamada T, McGeer PL, McGeer EG. Appearance of paired nucleated, Tau-positive glia in patients with progressive supranuclear palsy brain tissue. *Neurosci Lett*. Jan 20 1992;135(1):99-102. doi:10.1016/0304-3940(92)90145-w
194. Nishimura T, Ikeda K, Akiyama H, et al. Immunohistochemical investigation of tau-positive structures in the cerebral cortex of patients with progressive supranuclear palsy. *Neurosci Lett*. Dec 8 1995;201(2):123-6. doi:10.1016/0304-3940(95)12151-x
195. Valentino RR, Koga S, Walton RL, et al. MAPT subhaplotypes in corticobasal degeneration: assessing associations with disease risk, severity of tau pathology, and clinical features. *Acta Neuropathol Commun*. Dec 7 2020;8(1):218. doi:10.1186/s40478-020-01097-z
196. Svenningsson P. Corticobasal degeneration: advances in clinicopathology and biomarkers. *Curr Opin Neurol*. Aug 2019;32(4):597-603. doi:10.1097/WCO.0000000000000707
197. Dugger BN, Dickson DW. Pathology of Neurodegenerative Diseases. *Cold Spring Harb Perspect Biol*. Jul 5 2017;9(7)doi:10.1101/cshperspect.a028035
198. Kovacs GG, Majtenyi K, Spina S, et al. White matter tauopathy with globular glial inclusions: a distinct sporadic frontotemporal lobar degeneration. *J Neuropathol Exp Neurol*. Oct 2008;67(10):963-75. doi:10.1097/NEN.0b013e318187a80f
199. Bigio EH, Lipton AM, Yen SH, et al. Frontal lobe dementia with novel tauopathy: sporadic multiple system tauopathy with dementia. *J Neuropathol Exp Neurol*. Apr 2001;60(4):328-41. doi:10.1093/jnen/60.4.328
200. Ahmed Z, Doherty KM, Silveira-Moriyama L, et al. Globular glial tauopathies (GGT) presenting with motor neuron disease or frontotemporal dementia: an emerging group of 4-repeat tauopathies. *Acta Neuropathol*. Oct 2011;122(4):415-28. doi:10.1007/s00401-011-0857-4
201. Zhang Y, Wu KM, Yang L, Dong Q, Yu JT. Tauopathies: new perspectives and challenges. *Mol Neurodegener*. Apr 7 2022;17(1):28. doi:10.1186/s13024-022-00533-z
202. Ikeda K, Akiyama H, Kondo H, Haga C. A study of dementia with argyrophilic grains. Possible cytoskeletal abnormality in dendrospinal portion of neurons and oligodendroglia. *Acta Neuropathol*. 1995;89(5):409-14. doi:10.1007/BF00307644
203. Gotz J, Halliday G, Nisbet RM. Molecular Pathogenesis of the Tauopathies. *Annu Rev Pathol*. Jan 24 2019;14:239-261. doi:10.1146/annurev-pathmechdis-012418-012936
204. Humphrey WO, Martindale R, Pendlebury WW, DeWitt JC. Primary age-related tauopathy (PART) in the general autopsy setting: Not just a disease of the elderly. *Brain Pathol*. Mar 2021;31(2):381-384. doi:10.1111/bpa.12919
205. Jellinger KA, Attems J. Neurofibrillary tangle-predominant dementia: comparison with classical Alzheimer disease. *Acta Neuropathol*. Feb 2007;113(2):107-17. doi:10.1007/s00401-006-0156-7
206. Jellinger KA. Primary age-related tauopathy (PART) and Alzheimer's disease (AD). *Alzheimers Dement*. May 2019;15(5):720. doi:10.1016/j.jalz.2019.01.005
207. Dumurgier J, Sabia S. [Epidemiology of Alzheimer's disease: latest trends]. *Rev Prat*. Feb 2020;70(2):149-151. Nouvelles tendances epidemiologiques de la maladie d'Alzheimer.
208. Knopman DS, Amieva H, Petersen RC, et al. Alzheimer disease. *Nat Rev Dis Primers*. May 13 2021;7(1):33. doi:10.1038/s41572-021-00269-y

209. Dubois B, Hampel H, Feldman HH, et al. Preclinical Alzheimer's disease: Definition, natural history, and diagnostic criteria. *Alzheimers Dement*. Mar 2016;12(3):292-323. doi:10.1016/j.jalz.2016.02.002
210. Pimenova AA, Goate AM. Novel presenilin 1 and 2 double knock-out cell line for in vitro validation of PSEN1 and PSEN2 mutations. *Neurobiol Dis*. May 2020;138:104785. doi:10.1016/j.nbd.2020.104785
211. Haass C, Kaether C, Thinakaran G, Sisodia S. Trafficking and proteolytic processing of APP. *Cold Spring Harb Perspect Med*. May 2012;2(5):a006270. doi:10.1101/cshperspect.a006270
212. van der Lee SJ, Wolters FJ, Ikram MK, et al. The effect of APOE and other common genetic variants on the onset of Alzheimer's disease and dementia: a community-based cohort study. *Lancet Neurol*. May 2018;17(5):434-444. doi:10.1016/S1474-4422(18)30053-X
213. Huynh TV, Davis AA, Ulrich JD, Holtzman DM. Apolipoprotein E and Alzheimer's disease: the influence of apolipoprotein E on amyloid-beta and other amyloidogenic proteins. *J Lipid Res*. May 2017;58(5):824-836. doi:10.1194/jlr.R075481
214. Zhao N, Liu CC, Van Ingelgom AJ, et al. APOE epsilon2 is associated with increased tau pathology in primary tauopathy. *Nat Commun*. Oct 22 2018;9(1):4388. doi:10.1038/s41467-018-06783-0
215. Shi Y, Manis M, Long J, et al. Microglia drive APOE-dependent neurodegeneration in a tauopathy mouse model. *J Exp Med*. Nov 4 2019;216(11):2546-2561. doi:10.1084/jem.20190980
216. Thinakaran G, Koo EH. Amyloid precursor protein trafficking, processing, and function. *J Biol Chem*. Oct 31 2008;283(44):29615-9. doi:10.1074/jbc.R800019200
217. Weggen S, Beher D. Molecular consequences of amyloid precursor protein and presenilin mutations causing autosomal-dominant Alzheimer's disease. *Alzheimers Res Ther*. Mar 30 2012;4(2):9. doi:10.1186/alzrt107
218. Gu L, Guo Z. Alzheimer's Abeta42 and Abeta40 peptides form interlaced amyloid fibrils. *J Neurochem*. Aug 2013;126(3):305-11. doi:10.1111/jnc.12202
219. Goedert M, Spillantini MG, Cairns NJ, Crowther RA. Tau proteins of Alzheimer paired helical filaments: abnormal phosphorylation of all six brain isoforms. *Neuron*. Jan 1992;8(1):159-68. doi:10.1016/0896-6273(92)90117-v
220. Bancher C, Brunner C, Lassmann H, et al. Accumulation of abnormally phosphorylated tau precedes the formation of neurofibrillary tangles in Alzheimer's disease. *Brain Res*. Jan 16 1989;477(1-2):90-9. doi:10.1016/0006-8993(89)91396-6
221. Iqbal K, Alonso Adel C, Chen S, et al. Tau pathology in Alzheimer disease and other tauopathies. *Biochim Biophys Acta*. Jan 3 2005;1739(2-3):198-210. doi:10.1016/j.bbadis.2004.09.008
222. Crowther RA. Straight and paired helical filaments in Alzheimer disease have a common structural unit. *Proc Natl Acad Sci U S A*. Mar 15 1991;88(6):2288-92. doi:10.1073/pnas.88.6.2288
223. Fitzpatrick AWP, Falcon B, He S, et al. Cryo-EM structures of tau filaments from Alzheimer's disease. *Nature*. Jul 13 2017;547(7662):185-190. doi:10.1038/nature23002
224. Hardy J, Selkoe DJ. The amyloid hypothesis of Alzheimer's disease: progress and problems on the road to therapeutics. *Science*. Jul 19 2002;297(5580):353-6. doi:10.1126/science.1072994
225. van der Kant R, Goldstein LSB, Ossenkoppele R. Amyloid-beta-independent regulators of tau pathology in Alzheimer disease. *Nat Rev Neurosci*. Jan 2020;21(1):21-35. doi:10.1038/s41583-019-0240-3
226. Small SA, Duff K. Linking Abeta and tau in late-onset Alzheimer's disease: a dual pathway hypothesis. *Neuron*. Nov 26 2008;60(4):534-42. doi:10.1016/j.neuron.2008.11.007
227. Busche MA, Hyman BT. Synergy between amyloid-beta and tau in Alzheimer's disease. *Nat Neurosci*. Oct 2020;23(10):1183-1193. doi:10.1038/s41593-020-0687-6
228. Iqbal K, Liu F, Gong CX, Grundke-Iqbal I. Tau in Alzheimer disease and related tauopathies. *Curr Alzheimer Res*. Dec 2010;7(8):656-64. doi:10.2174/156720510793611592
229. Grundke-Iqbal I, Iqbal K, Quinlan M, Tung YC, Zaidi MS, Wisniewski HM. Microtubule-associated protein tau. A component of Alzheimer paired helical filaments. *J Biol Chem*. May 5 1986;261(13):6084-9.
230. Grundke-Iqbal I, Iqbal K, Tung YC, Quinlan M, Wisniewski HM, Binder LI. Abnormal phosphorylation of the microtubule-associated protein tau (tau) in Alzheimer cytoskeletal pathology. *Proc Natl Acad Sci U S A*. Jul 1986;83(13):4913-7. doi:10.1073/pnas.83.13.4913

231. Neve RL, Harris P, Kosik KS, Kurnit DM, Donlon TA. Identification of cDNA clones for the human microtubule-associated protein tau and chromosomal localization of the genes for tau and microtubule-associated protein 2. *Brain Res*. Dec 1986;387(3):271-80. doi:10.1016/0169-328x(86)90033-1
232. Guo T, Noble W, Hanger DP. Roles of tau protein in health and disease. *Acta Neuropathol*. May 2017;133(5):665-704. doi:10.1007/s00401-017-1707-9
233. Majounie E, Cross W, Newsway V, et al. Variation in tau isoform expression in different brain regions and disease states. *Neurobiol Aging*. Jul 2013;34(7):1922 e7-1922 e12. doi:10.1016/j.neurobiolaging.2013.01.017
234. Jeganathan S, von Bergen M, Brutlach H, Steinhoff HJ, Mandelkow E. Global hairpin folding of tau in solution. *Biochemistry*. Feb 21 2006;45(7):2283-93. doi:10.1021/bi0521543
235. Mandelkow EM, Mandelkow E. Biochemistry and cell biology of tau protein in neurofibrillary degeneration. *Cold Spring Harb Perspect Med*. Jul 2012;2(7):a006247. doi:10.1101/cshperspect.a006247
236. Mukrasch MD, Bibow S, Korukottu J, et al. Structural polymorphism of 441-residue tau at single residue resolution. *PLoS Biol*. Feb 17 2009;7(2):e34. doi:10.1371/journal.pbio.1000034
237. Chen J, Kanai Y, Cowan NJ, Hirokawa N. Projection domains of MAP2 and tau determine spacings between microtubules in dendrites and axons. *Nature*. Dec 17 1992;360(6405):674-7. doi:10.1038/360674a0
238. Matsumoto SE, Motoi Y, Ishiguro K, et al. The twenty-four KDa C-terminal tau fragment increases with aging in tauopathy mice: implications of prion-like properties. *Hum Mol Genet*. Nov 15 2015;24(22):6403-16. doi:10.1093/hmg/ddv351
239. Liu C, Gotz J. Profiling murine tau with 0N, 1N and 2N isoform-specific antibodies in brain and peripheral organs reveals distinct subcellular localization, with the 1N isoform being enriched in the nucleus. *PLoS One*. 2013;8(12):e84849. doi:10.1371/journal.pone.0084849
240. Mukrasch MD, von Bergen M, Biernat J, et al. The "jaws" of the tau-microtubule interaction. *J Biol Chem*. Apr 20 2007;282(16):12230-9. doi:10.1074/jbc.M607159200
241. Connell JW, Gibb GM, Betts JC, et al. Effects of FTDP-17 mutations on the in vitro phosphorylation of tau by glycogen synthase kinase 3beta identified by mass spectrometry demonstrate certain mutations exert long-range conformational changes. *FEBS Lett*. Mar 23 2001;493(1):40-4. doi:10.1016/s0014-5793(01)02267-0
242. Hirokawa N, Funakoshi T, Sato-Harada R, Kanai Y. Selective stabilization of tau in axons and microtubule-associated protein 2C in cell bodies and dendrites contributes to polarized localization of cytoskeletal proteins in mature neurons. *J Cell Biol*. Feb 1996;132(4):667-79. doi:10.1083/jcb.132.4.667
243. Hong XP, Peng CX, Wei W, et al. Essential role of tau phosphorylation in adult hippocampal neurogenesis. *Hippocampus*. Dec 2010;20(12):1339-49. doi:10.1002/hipo.20712
244. Kimura T, Whitcomb DJ, Jo J, et al. Microtubule-associated protein tau is essential for long-term depression in the hippocampus. *Philos Trans R Soc Lond B Biol Sci*. Jan 5 2014;369(1633):20130144. doi:10.1098/rstb.2013.0144
245. Kadavath H, Hofele RV, Biernat J, et al. Tau stabilizes microtubules by binding at the interface between tubulin heterodimers. *Proc Natl Acad Sci U S A*. Jun 16 2015;112(24):7501-6. doi:10.1073/pnas.1504081112
246. Stamer K, Vogel R, Thies E, Mandelkow E, Mandelkow EM. Tau blocks traffic of organelles, neurofilaments, and APP vesicles in neurons and enhances oxidative stress. *J Cell Biol*. Mar 18 2002;156(6):1051-63. doi:10.1083/jcb.200108057
247. Dixit R, Ross JL, Goldman YE, Holzbaur EL. Differential regulation of dynein and kinesin motor proteins by tau. *Science*. Feb 22 2008;319(5866):1086-9. doi:10.1126/science.1152993
248. Caceres A, Kosik KS. Inhibition of neurite polarity by tau antisense oligonucleotides in primary cerebellar neurons. *Nature*. Feb 1 1990;343(6257):461-3. doi:10.1038/343461a0
249. Frandemiche ML, De Seranno S, Rush T, et al. Activity-dependent tau protein translocation to excitatory synapse is disrupted by exposure to amyloid-beta oligomers. *J Neurosci*. Apr 23 2014;34(17):6084-97. doi:10.1523/JNEUROSCI.4261-13.2014

250. Loomis PA, Howard TH, Castleberry RP, Binder LI. Identification of nuclear tau isoforms in human neuroblastoma cells. *Proc Natl Acad Sci U S A*. Nov 1990;87(21):8422-6. doi:10.1073/pnas.87.21.8422
251. Sjoberg MK, Shestakova E, Mansuroglu Z, Maccioni RB, Bonnefoy E. Tau protein binds to pericentromeric DNA: a putative role for nuclear tau in nucleolar organization. *J Cell Sci*. May 15 2006;119(Pt 10):2025-34. doi:10.1242/jcs.02907
252. Violet M, Delattre L, Tardivel M, et al. A major role for Tau in neuronal DNA and RNA protection in vivo under physiological and hyperthermic conditions. *Front Cell Neurosci*. 2014;8:84. doi:10.3389/fncel.2014.00084
253. Harada A, Oguchi K, Okabe S, et al. Altered microtubule organization in small-calibre axons of mice lacking tau protein. *Nature*. Jun 9 1994;369(6480):488-91. doi:10.1038/369488a0
254. Fuster-Matanzo A, de Barreda EG, Dawson HN, Vitek MP, Avila J, Hernandez F. Function of tau protein in adult newborn neurons. *FEBS Lett*. Sep 17 2009;583(18):3063-8. doi:10.1016/j.febslet.2009.08.017
255. Lei P, Ayton S, Finkelstein DI, et al. Tau deficiency induces parkinsonism with dementia by impairing APP-mediated iron export. *Nat Med*. Jan 29 2012;18(2):291-5. doi:10.1038/nm.2613
256. Whiteman IT, Gervasio OL, Cullen KM, et al. Activated actin-depolymerizing factor/cofilin sequesters phosphorylated microtubule-associated protein during the assembly of alzheimer-like neuritic cytoskeletal striations. *J Neurosci*. Oct 14 2009;29(41):12994-3005. doi:10.1523/JNEUROSCI.3531-09.2009
257. Pickering-Brown SM, Baker M, Nonaka T, et al. Frontotemporal dementia with Pick-type histology associated with Q336R mutation in the tau gene. *Brain*. Jun 2004;127(Pt 6):1415-26. doi:10.1093/brain/awh147
258. Tacik P, DeTure M, Hinkle KM, et al. A Novel Tau Mutation in Exon 12, p.Q336H, Causes Hereditary Pick Disease. *J Neuropathol Exp Neurol*. Nov 2015;74(11):1042-52. doi:10.1097/NEN.0000000000000248
259. Magnani E, Fan J, Gasparini L, et al. Interaction of tau protein with the dynactin complex. *EMBO J*. Oct 31 2007;26(21):4546-54. doi:10.1038/sj.emboj.7601878
260. Kfoury N, Holmes BB, Jiang H, Holtzman DM, Diamond MI. Trans-cellular propagation of Tau aggregation by fibrillar species. *J Biol Chem*. Jun 1 2012;287(23):19440-51. doi:10.1074/jbc.M112.346072
261. Boluda S, Iba M, Zhang B, Raible KM, Lee VM, Trojanowski JQ. Differential induction and spread of tau pathology in young PS19 tau transgenic mice following intracerebral injections of pathological tau from Alzheimer's disease or corticobasal degeneration brains. *Acta Neuropathol*. Feb 2015;129(2):221-37. doi:10.1007/s00401-014-1373-0
262. Ahmed Z, Cooper J, Murray TK, et al. A novel in vivo model of tau propagation with rapid and progressive neurofibrillary tangle pathology: the pattern of spread is determined by connectivity, not proximity. *Acta Neuropathol*. May 2014;127(5):667-83. doi:10.1007/s00401-014-1254-6
263. Peeraer E, Bottelbergs A, Van Kolen K, et al. Intracerebral injection of preformed synthetic tau fibrils initiates widespread tauopathy and neuronal loss in the brains of tau transgenic mice. *Neurobiol Dis*. Jan 2015;73:83-95. doi:10.1016/j.nbd.2014.08.032
264. Lu M, Kosik KS. Competition for microtubule-binding with dual expression of tau missense and splice isoforms. *Mol Biol Cell*. Jan 2001;12(1):171-84. doi:10.1091/mbc.12.1.171
265. D'Souza I, Poorkaj P, Hong M, et al. Missense and silent tau gene mutations cause frontotemporal dementia with parkinsonism-chromosome 17 type, by affecting multiple alternative RNA splicing regulatory elements. *Proc Natl Acad Sci U S A*. May 11 1999;96(10):5598-603. doi:10.1073/pnas.96.10.5598
266. Drechsel DN, Hyman AA, Cobb MH, Kirschner MW. Modulation of the dynamic instability of tubulin assembly by the microtubule-associated protein tau. *Mol Biol Cell*. Oct 1992;3(10):1141-54. doi:10.1091/mbc.3.10.1141
267. Drewes G, Trinczek B, Illenberger S, et al. Microtubule-associated protein/microtubule affinity-regulating kinase (p110mark). A novel protein kinase that regulates tau-microtubule interactions and dynamic instability by phosphorylation at the Alzheimer-specific site serine 262. *J Biol Chem*. Mar 31 1995;270(13):7679-88. doi:10.1074/jbc.270.13.7679

268. Sengupta A, Kabat J, Novak M, Wu Q, Grundke-Iqbal I, Iqbal K. Phosphorylation of tau at both Thr 231 and Ser 262 is required for maximal inhibition of its binding to microtubules. *Arch Biochem Biophys*. Sep 15 1998;357(2):299-309. doi:10.1006/abbi.1998.0813
269. Kopke E, Tung YC, Shaikh S, Alonso AC, Iqbal K, Grundke-Iqbal I. Microtubule-associated protein tau. Abnormal phosphorylation of a non-paired helical filament pool in Alzheimer disease. *J Biol Chem*. Nov 15 1993;268(32):24374-84.
270. Alonso Adel C, Mederlyova A, Novak M, Grundke-Iqbal I, Iqbal K. Promotion of hyperphosphorylation by frontotemporal dementia tau mutations. *J Biol Chem*. Aug 13 2004;279(33):34873-81. doi:10.1074/jbc.M405131200
271. Thies E, Mandelkow EM. Missorting of tau in neurons causes degeneration of synapses that can be rescued by the kinase MARK2/Par-1. *J Neurosci*. Mar 14 2007;27(11):2896-907. doi:10.1523/JNEUROSCI.4674-06.2007
272. Eidenmuller J, Fath T, Maas T, Pool M, Sontag E, Brandt R. Phosphorylation-mimicking glutamate clusters in the proline-rich region are sufficient to simulate the functional deficiencies of hyperphosphorylated tau protein. *Biochem J*. Aug 1 2001;357(Pt 3):759-67. doi:10.1042/0264-6021:3570759
273. Dickey CA, Kamal A, Lundgren K, et al. The high-affinity HSP90-CHIP complex recognizes and selectively degrades phosphorylated tau client proteins. *J Clin Invest*. Mar 2007;117(3):648-58. doi:10.1172/JCI29715
274. Moreno H, Morfini G, Buitrago L, et al. Tau pathology-mediated presynaptic dysfunction. *Neuroscience*. Jun 14 2016;325:30-8. doi:10.1016/j.neuroscience.2016.03.044
275. Ittner LM, Ke YD, Gotz J. Phosphorylated Tau interacts with c-Jun N-terminal kinase-interacting protein 1 (JIP1) in Alzheimer disease. *J Biol Chem*. Jul 31 2009;284(31):20909-16. doi:10.1074/jbc.M109.014472
276. Hanger DP, Anderton BH, Noble W. Tau phosphorylation: the therapeutic challenge for neurodegenerative disease. *Trends Mol Med*. Mar 2009;15(3):112-9. doi:10.1016/j.molmed.2009.01.003
277. Limorenko G, Lashuel HA. Revisiting the grammar of Tau aggregation and pathology formation: how new insights from brain pathology are shaping how we study and target Tauopathies. *Chem Soc Rev*. Jan 24 2022;51(2):513-565. doi:10.1039/d1cs00127b
278. Goedert M, Jakes R, Spillantini MG, Hasegawa M, Smith MJ, Crowther RA. Assembly of microtubule-associated protein tau into Alzheimer-like filaments induced by sulphated glycosaminoglycans. *Nature*. Oct 10 1996;383(6600):550-3. doi:10.1038/383550a0
279. Eschmann NA, Do TD, LaPointe NE, et al. Tau Aggregation Propensity Engrained in Its Solution State. *J Phys Chem B*. Nov 12 2015;119(45):14421-32. doi:10.1021/acs.jpcb.5b08092
280. Ait-Bouziad N, Chiki A, Limorenko G, Xiao S, Eliezer D, Lashuel HA. Phosphorylation of the overlooked tyrosine 310 regulates the structure, aggregation, and microtubule- and lipid-binding properties of Tau. *J Biol Chem*. Jun 5 2020;295(23):7905-7922. doi:10.1074/jbc.RA119.012517
281. von Bergen M, Friedhoff P, Biernat J, Heberle J, Mandelkow EM, Mandelkow E. Assembly of tau protein into Alzheimer paired helical filaments depends on a local sequence motif ((306)VQIVYK(311)) forming beta structure. *Proc Natl Acad Sci U S A*. May 9 2000;97(10):5129-34. doi:10.1073/pnas.97.10.5129
282. von Bergen M, Barghorn S, Li L, et al. Mutations of tau protein in frontotemporal dementia promote aggregation of paired helical filaments by enhancing local beta-structure. *J Biol Chem*. Dec 21 2001;276(51):48165-74. doi:10.1074/jbc.M105196200
283. Wischik CM, Novak M, Thogersen HC, et al. Isolation of a fragment of tau derived from the core of the paired helical filament of Alzheimer disease. *Proc Natl Acad Sci U S A*. Jun 1988;85(12):4506-10. doi:10.1073/pnas.85.12.4506
284. Wang YP, Biernat J, Pickhardt M, Mandelkow E, Mandelkow EM. Stepwise proteolysis liberates tau fragments that nucleate the Alzheimer-like aggregation of full-length tau in a neuronal cell model. *Proc Natl Acad Sci U S A*. Jun 12 2007;104(24):10252-7. doi:10.1073/pnas.0703676104
285. Gustke N, Trinczek B, Biernat J, Mandelkow EM, Mandelkow E. Domains of tau protein and interactions with microtubules. *Biochemistry*. Aug 16 1994;33(32):9511-22. doi:10.1021/bi00198a017

286. Friedhoff P, Schneider A, Mandelkow EM, Mandelkow E. Rapid assembly of Alzheimer-like paired helical filaments from microtubule-associated protein tau monitored by fluorescence in solution. *Biochemistry*. Jul 14 1998;37(28):10223-30. doi:10.1021/bi980537d
287. Barghorn S, Mandelkow E. Toward a unified scheme for the aggregation of tau into Alzheimer paired helical filaments. *Biochemistry*. Dec 17 2002;41(50):14885-96. doi:10.1021/bi026469j
288. Falcon B, Zhang W, Murzin AG, et al. Structures of filaments from Pick's disease reveal a novel tau protein fold. *Nature*. Sep 2018;561(7721):137-140. doi:10.1038/s41586-018-0454-y
289. Falcon B, Zivanov J, Zhang W, et al. Novel tau filament fold in chronic traumatic encephalopathy encloses hydrophobic molecules. *Nature*. Apr 2019;568(7752):420-423. doi:10.1038/s41586-019-1026-5
290. Zhang W, Tarutani A, Newell KL, et al. Novel tau filament fold in corticobasal degeneration. *Nature*. Apr 2020;580(7802):283-287. doi:10.1038/s41586-020-2043-0
291. Goedert M. Cryo-EM structures of tau filaments from human brain. *Essays Biochem*. Dec 22 2021;65(7):949-959. doi:10.1042/EBC20210025
292. Zhang W, Falcon B, Murzin AG, et al. Heparin-induced tau filaments are polymorphic and differ from those in Alzheimer's and Pick's diseases. *Elife*. Feb 5 2019;8doi:10.7554/eLife.43584
293. Friedhoff P, von Bergen M, Mandelkow EM, Davies P, Mandelkow E. A nucleated assembly mechanism of Alzheimer paired helical filaments. *Proc Natl Acad Sci U S A*. Dec 22 1998;95(26):15712-7. doi:10.1073/pnas.95.26.15712
294. Kuret J, Chirita CN, Congdon EE, et al. Pathways of tau fibrillization. *Biochim Biophys Acta*. Jan 3 2005;1739(2-3):167-78. doi:10.1016/j.bbadis.2004.06.016
295. Nizynski B, Dzwolak W, Nieznanski K. Amyloidogenesis of Tau protein. *Protein Sci*. Nov 2017;26(11):2126-2150. doi:10.1002/pro.3275
296. Maeda S, Sahara N, Saito Y, et al. Granular tau oligomers as intermediates of tau filaments. *Biochemistry*. Mar 27 2007;46(12):3856-61. doi:10.1021/bi061359o
297. Kayed R, Sokolov Y, Edmonds B, et al. Permeabilization of lipid bilayers is a common conformation-dependent activity of soluble amyloid oligomers in protein misfolding diseases. *J Biol Chem*. Nov 5 2004;279(45):46363-6. doi:10.1074/jbc.C400260200
298. Fang YS, Tsai KJ, Chang YJ, et al. Full-length TDP-43 forms toxic amyloid oligomers that are present in frontotemporal lobar dementia-TDP patients. *Nat Commun*. Sep 12 2014;5:4824. doi:10.1038/ncomms5824
299. Lasagna-Reeves CA, Castillo-Carranza DL, Sengupta U, Clos AL, Jackson GR, Kayed R. Tau oligomers impair memory and induce synaptic and mitochondrial dysfunction in wild-type mice. *Mol Neurodegener*. Jun 6 2011;6:39. doi:10.1186/1750-1326-6-39
300. Lasagna-Reeves CA, Castillo-Carranza DL, Sengupta U, et al. Alzheimer brain-derived tau oligomers propagate pathology from endogenous tau. *Sci Rep*. 2012;2:700. doi:10.1038/srep00700
301. Alonso Adel C, Li B, Grundke-Iqbal I, Iqbal K. Polymerization of hyperphosphorylated tau into filaments eliminates its inhibitory activity. *Proc Natl Acad Sci U S A*. Jun 6 2006;103(23):8864-9. doi:10.1073/pnas.0603214103
302. Chai X, Dage JL, Citron M. Constitutive secretion of tau protein by an unconventional mechanism. *Neurobiol Dis*. Dec 2012;48(3):356-66. doi:10.1016/j.nbd.2012.05.021
303. Karch CM, Jeng AT, Goate AM. Extracellular Tau levels are influenced by variability in Tau that is associated with tauopathies. *J Biol Chem*. Dec 14 2012;287(51):42751-62. doi:10.1074/jbc.M112.380642
304. Wang Y, Balaji V, Kaniyappan S, et al. The release and trans-synaptic transmission of Tau via exosomes. *Mol Neurodegener*. Jan 13 2017;12(1):5. doi:10.1186/s13024-016-0143-y
305. Dujardin S, Begard S, Caillierez R, et al. Ectosomes: a new mechanism for non-exosomal secretion of tau protein. *PLoS One*. 2014;9(6):e100760. doi:10.1371/journal.pone.0100760
306. Plouffe V, Mohamed NV, Rivest-McGraw J, Bertrand J, Lauzon M, Leclerc N. Hyperphosphorylation and cleavage at D421 enhance tau secretion. *PLoS One*. 2012;7(5):e36873. doi:10.1371/journal.pone.0036873
307. Wegmann S, Nicholls S, Takeda S, Fan Z, Hyman BT. Formation, release, and internalization of stable tau oligomers in cells. *J Neurochem*. Dec 2016;139(6):1163-1174. doi:10.1111/jnc.13866
308. Merezhko M, Brunello CA, Yan X, et al. Secretion of Tau via an Unconventional Non-vesicular Mechanism. *Cell Rep*. Nov 20 2018;25(8):2027-2035 e4. doi:10.1016/j.celrep.2018.10.078

309. Guerreiro PS, Gerhardt E, Lopes da Fonseca T, Bahr M, Outeiro TF, Eckermann K. LRRK2 Promotes Tau Accumulation, Aggregation and Release. *Mol Neurobiol*. Jul 2016;53(5):3124-3135. doi:10.1007/s12035-015-9209-z
310. Falcon B, Noad J, McMahon H, Randow F, Goedert M. Galectin-8-mediated selective autophagy protects against seeded tau aggregation. *J Biol Chem*. Feb 16 2018;293(7):2438-2451. doi:10.1074/jbc.M117.809293
311. Calafate S, Flavin W, Verstreken P, Moechars D. Loss of Bin1 Promotes the Propagation of Tau Pathology. *Cell Rep*. Oct 18 2016;17(4):931-940. doi:10.1016/j.celrep.2016.09.063
312. De La-Rocque S, Moretto E, Butnaru I, Schiavo G. Knockin' on heaven's door: Molecular mechanisms of neuronal tau uptake. *J Neurochem*. Mar 2021;156(5):563-588. doi:10.1111/jnc.15144
313. Wu JW, Herman M, Liu L, et al. Small misfolded Tau species are internalized via bulk endocytosis and anterogradely and retrogradely transported in neurons. *J Biol Chem*. Jan 18 2013;288(3):1856-70. doi:10.1074/jbc.M112.394528
314. Puangmalai N, Bhatt N, Montalbano M, et al. Internalization mechanisms of brain-derived tau oligomers from patients with Alzheimer's disease, progressive supranuclear palsy and dementia with Lewy bodies. *Cell Death Dis*. May 4 2020;11(5):314. doi:10.1038/s41419-020-2503-3
315. Holmes BB, DeVos SL, Kfoury N, et al. Heparan sulfate proteoglycans mediate internalization and propagation of specific proteopathic seeds. *Proc Natl Acad Sci U S A*. Aug 13 2013;110(33):E3138-47. doi:10.1073/pnas.1301440110
316. Rauch JN, Luna G, Guzman E, et al. LRP1 is a master regulator of tau uptake and spread. *Nature*. Apr 2020;580(7803):381-385. doi:10.1038/s41586-020-2156-5
317. Hudak A, Kusz E, Domonkos I, et al. Contribution of syndecans to cellular uptake and fibrillation of alpha-synuclein and tau. *Sci Rep*. Nov 12 2019;9(1):16543. doi:10.1038/s41598-019-53038-z
318. Shin WS, Di J, Cao Q, et al. Amyloid beta-protein oligomers promote the uptake of tau fibril seeds potentiating intracellular tau aggregation. *Alzheimers Res Ther*. Oct 18 2019;11(1):86. doi:10.1186/s13195-019-0541-9
319. Tardivel M, Begard S, Bousset L, et al. Tunneling nanotube (TNT)-mediated neuron-to neuron transfer of pathological Tau protein assemblies. *Acta Neuropathol Commun*. Nov 4 2016;4(1):117. doi:10.1186/s40478-016-0386-4
320. Tuck BJ, Miller LVC, Katsinelos T, et al. Cholesterol determines the cytosolic entry and seeded aggregation of tau. *Cell Rep*. May 3 2022;39(5):110776. doi:10.1016/j.celrep.2022.110776
321. Chen JJ, Nathaniel DL, Raghavan P, et al. Compromised function of the ESCRT pathway promotes endolysosomal escape of tau seeds and propagation of tau aggregation. *J Biol Chem*. Dec 13 2019;294(50):18952-18966. doi:10.1074/jbc.RA119.009432
322. Evans LD, Wassmer T, Fraser G, et al. Extracellular Monomeric and Aggregated Tau Efficiently Enter Human Neurons through Overlapping but Distinct Pathways. *Cell Rep*. Mar 27 2018;22(13):3612-3624. doi:10.1016/j.celrep.2018.03.021
323. Katsinelos T, Zeitler M, Dimou E, et al. Unconventional Secretion Mediates the Trans-cellular Spreading of Tau. *Cell Rep*. May 15 2018;23(7):2039-2055. doi:10.1016/j.celrep.2018.04.056
324. Rodriguez L, Mohamed NV, Desjardins A, Lippe R, Fon EA, Leclerc N. Rab7A regulates tau secretion. *J Neurochem*. May 2017;141(4):592-605. doi:10.1111/jnc.13994
325. Kanmert D, Cantlon A, Muratore CR, et al. C-Terminally Truncated Forms of Tau, But Not Full-Length Tau or Its C-Terminal Fragments, Are Released from Neurons Independently of Cell Death. *J Neurosci*. Jul 29 2015;35(30):10851-65. doi:10.1523/JNEUROSCI.0387-15.2015
326. Clavaguera F, Bolmont T, Crowther RA, et al. Transmission and spreading of tauopathy in transgenic mouse brain. *Nat Cell Biol*. Jul 2009;11(7):909-13. doi:10.1038/ncb1901
327. Clavaguera F, Akatsu H, Fraser G, et al. Brain homogenates from human tauopathies induce tau inclusions in mouse brain. *Proc Natl Acad Sci U S A*. Jun 4 2013;110(23):9535-40. doi:10.1073/pnas.1301175110
328. Stahlberg H, Riek R. Structural strains of misfolded tau protein define different diseases. *Nature*. Oct 2021;598(7880):264-265. doi:10.1038/d41586-021-02611-6
329. Li J, Browning S, Mahal SP, Oelschlegel AM, Weissmann C. Darwinian evolution of prions in cell culture. *Science*. Feb 12 2010;327(5967):869-72. doi:10.1126/science.1183218

330. Kovacs GG, Alafuzoff I, Al-Sarraj S, et al. Mixed brain pathologies in dementia: the BrainNet Europe consortium experience. *Dement Geriatr Cogn Disord*. 2008;26(4):343-50. doi:10.1159/000161560
331. Ghetti B, Tagliavini F, Masters CL, et al. Gerstmann-Straussler-Scheinker disease. II. Neurofibrillary tangles and plaques with PrP-amyloid coexist in an affected family. *Neurology*. Nov 1989;39(11):1453-61. doi:10.1212/wnl.39.11.1453
332. Tagliavini F, Prelli F, Ghiso J, et al. Amyloid protein of Gerstmann-Straussler-Scheinker disease (Indiana kindred) is an 11 kd fragment of prion protein with an N-terminal glycine at codon 58. *EMBO J*. Mar 1991;10(3):513-9. doi:10.1002/j.1460-2075.1991.tb07977.x
333. Amano N, Yagishita S, Yokoi S, et al. Gerstmann-Straussler syndrome--a variant type: amyloid plaques and Alzheimer's neurofibrillary tangles in cerebral cortex. *Acta Neuropathol*. 1992;84(1):15-23. doi:10.1007/BF00427210
334. Ghetti B, Tagliavini F, Giaccone G, et al. Familial Gerstmann-Straussler-Scheinker disease with neurofibrillary tangles. *Mol Neurobiol*. Feb 1994;8(1):41-8. doi:10.1007/BF02778006
335. Tranchant C, Sergeant N, Wattez A, Mohr M, Warter JM, Delacourte A. Neurofibrillary tangles in Gerstmann-Straussler-Scheinker syndrome with the A117V prion gene mutation. *J Neurol Neurosurg Psychiatry*. Aug 1997;63(2):240-6. doi:10.1136/jnnp.63.2.240
336. Ishizawa K, Komori T, Shimazu T, et al. Hyperphosphorylated tau deposition parallels prion protein burden in a case of Gerstmann-Straussler-Scheinker syndrome P102L mutation complicated with dementia. *Acta Neuropathol*. Oct 2002;104(4):342-50. doi:10.1007/s00401-002-0547-3
337. Giaccone G, Mangieri M, Capobianco R, et al. Tauopathy in human and experimental variant Creutzfeldt-Jakob disease. *Neurobiol Aging*. Dec 2008;29(12):1864-73. doi:10.1016/j.neurobiolaging.2007.04.026
338. Reiniger L, Lukic A, Linehan J, et al. Tau, prions and Abeta: the triad of neurodegeneration. *Acta Neuropathol*. Jan 2011;121(1):5-20. doi:10.1007/s00401-010-0691-0
339. Perez M, Rojo AI, Wandosell F, Diaz-Nido J, Avila J. Prion peptide induces neuronal cell death through a pathway involving glycogen synthase kinase 3. *Biochem J*. May 15 2003;372(Pt 1):129-36. doi:10.1042/BJ20021596
340. van den Ent F, Lowe J. RF cloning: a restriction-free method for inserting target genes into plasmids. *J Biochem Biophys Methods*. Apr 30 2006;67(1):67-74. doi:10.1016/j.jbbm.2005.12.008
341. Barghorn S, Biernat J, Mandelkow E. Purification of recombinant tau protein and preparation of Alzheimer-paired helical filaments in vitro. *Methods Mol Biol*. 2005;299:35-51. doi:10.1385/1-59259-874-9:035
342. Butler DA, Scott MR, Bockman JM, et al. Scrapie-infected murine neuroblastoma cells produce protease-resistant prion proteins. *J Virol*. May 1988;62(5):1558-64. doi:10.1128/JVI.62.5.1558-1564.1988
343. Karpowicz RJ, Jr., Haney CM, Mihaila TS, Sandler RM, Petersson EJ, Lee VM. Selective imaging of internalized proteopathic alpha-synuclein seeds in primary neurons reveals mechanistic insight into transmission of synucleinopathies. *J Biol Chem*. Aug 11 2017;292(32):13482-13497. doi:10.1074/jbc.M117.780296
344. Petsch B, Muller-Schiffmann A, Lehle A, et al. Biological effects and use of PrPSc- and PrP-specific antibodies generated by immunization with purified full-length native mouse prions. *J Virol*. May 2011;85(9):4538-46. doi:10.1128/JVI.02467-10
345. Novak M, Jakes R, Edwards PC, Milstein C, Wischik CM. Difference between the tau protein of Alzheimer paired helical filament core and normal tau revealed by epitope analysis of monoclonal antibodies 423 and 7.51. *Proc Natl Acad Sci U S A*. Jul 1 1991;88(13):5837-41. doi:10.1073/pnas.88.13.5837
346. Arshad H, Patel Z, Mehrabian M, et al. The aminoglycoside G418 hinders de novo prion infection in cultured cells. *J Biol Chem*. Sep 2021;297(3):101073. doi:10.1016/j.jbc.2021.101073
347. Bolder SG, Sagis LM, Venema P, van der Linden E. Thioflavin T and birefringence assays to determine the conversion of proteins into fibrils. *Langmuir*. Apr 10 2007;23(8):4144-7. doi:10.1021/la063048k
348. Iba M, Guo JL, McBride JD, Zhang B, Trojanowski JQ, Lee VM. Synthetic tau fibrils mediate transmission of neurofibrillary tangles in a transgenic mouse model of Alzheimer's-like tauopathy. *J Neurosci*. Jan 16 2013;33(3):1024-37. doi:10.1523/JNEUROSCI.2642-12.2013

349. Falcon B, Cavallini A, Angers R, et al. Conformation determines the seeding potencies of native and recombinant Tau aggregates. *J Biol Chem*. Jan 9 2015;290(2):1049-65. doi:10.1074/jbc.M114.589309
350. Kolay S, Diamond MI. Alzheimer's disease risk modifier genes do not affect tau aggregate uptake, seeding or maintenance in cell models. *FEBS Open Bio*. Sep 2020;10(9):1912-1920. doi:10.1002/2211-5463.12928
351. Seglen PO, Gordon PB. 3-Methyladenine: specific inhibitor of autophagic/lysosomal protein degradation in isolated rat hepatocytes. *Proc Natl Acad Sci U S A*. Mar 1982;79(6):1889-92. doi:10.1073/pnas.79.6.1889
352. Petiot A, Ogier-Denis E, Blommaart EF, Meijer AJ, Codogno P. Distinct classes of phosphatidylinositol 3'-kinases are involved in signaling pathways that control macroautophagy in HT-29 cells. *J Biol Chem*. Jan 14 2000;275(2):992-8. doi:10.1074/jbc.275.2.992
353. Yoshimori T, Yamamoto A, Moriyama Y, Futai M, Tashiro Y. Bafilomycin A1, a specific inhibitor of vacuolar-type H(+)-ATPase, inhibits acidification and protein degradation in lysosomes of cultured cells. *J Biol Chem*. Sep 15 1991;266(26):17707-12.
354. Homewood CA, Warhurst DC, Peters W, Baggaley VC. Lysosomes, pH and the anti-malarial action of chloroquine. *Nature*. Jan 7 1972;235(5332):50-2. doi:10.1038/235050a0
355. Han YH, Moon HJ, You BR, Park WH. The effect of MG132, a proteasome inhibitor on HeLa cells in relation to cell growth, reactive oxygen species and GSH. *Oncol Rep*. Jul 2009;22(1):215-21.
356. Tanida I, Ueno T, Kominami E. LC3 and Autophagy. *Methods Mol Biol*. 2008;445:77-88. doi:10.1007/978-1-59745-157-4_4
357. Yamasaki T, Suzuki A, Hasebe R, Horiuchi M. Comparison of the anti-prion mechanism of four different anti-prion compounds, anti-PrP monoclonal antibody 44B1, pentosan polysulfate, chlorpromazine, and U18666A, in prion-infected mouse neuroblastoma cells. *PLoS One*. 2014;9(9):e106516. doi:10.1371/journal.pone.0106516
358. Kim CL, Karino A, Ishiguro N, Shinagawa M, Sato M, Horiuchi M. Cell-surface retention of PrPC by anti-PrP antibody prevents protease-resistant PrP formation. *J Gen Virol*. Nov 2004;85(Pt 11):3473-3482. doi:10.1099/vir.0.80113-0
359. Vey M, Pilkuhn S, Wille H, et al. Subcellular colocalization of the cellular and scrapie prion proteins in caveolae-like membranous domains. *Proc Natl Acad Sci U S A*. Dec 10 1996;93(25):14945-9. doi:10.1073/pnas.93.25.14945
360. Robinson JL, Lee EB, Xie SX, et al. Neurodegenerative disease concomitant proteinopathies are prevalent, age-related and APOE4-associated. *Brain*. Jul 1 2018;141(7):2181-2193. doi:10.1093/brain/awy146
361. Woodard JS. Concentric hyaline inclusion body formation in mental disease analysis of twenty-seven cases. *J Neuropathol Exp Neurol*. Jul 1962;21:442-9. doi:10.1097/00005072-196207000-00012
362. Popescu A, Lippa CF, Lee VM, Trojanowski JQ. Lewy bodies in the amygdala: increase of alpha-synuclein aggregates in neurodegenerative diseases with tau-based inclusions. *Arch Neurol*. Dec 2004;61(12):1915-9. doi:10.1001/archneur.61.12.1915
363. Dickson DW, Feany MB, Yen SH, Mattiace LA, Davies P. Cytoskeletal pathology in non-Alzheimer degenerative dementia: new lesions in diffuse Lewy body disease, Pick's disease, and corticobasal degeneration. *J Neural Transm Suppl*. 1996;47:31-46. doi:10.1007/978-3-7091-6892-9_2
364. Sengupta U, Guerrero-Munoz MJ, Castillo-Carranza DL, et al. Pathological interface between oligomeric alpha-synuclein and tau in synucleinopathies. *Biol Psychiatry*. Nov 15 2015;78(10):672-83. doi:10.1016/j.biopsych.2014.12.019
365. Jensen PH, Hager H, Nielsen MS, Hojrup P, Gliemann J, Jakes R. alpha-synuclein binds to Tau and stimulates the protein kinase A-catalyzed tau phosphorylation of serine residues 262 and 356. *J Biol Chem*. Sep 3 1999;274(36):25481-9. doi:10.1074/jbc.274.36.25481
366. Guo JP, Arai T, Miklossy J, McGeer PL. Abeta and tau form soluble complexes that may promote self aggregation of both into the insoluble forms observed in Alzheimer's disease. *Proc Natl Acad Sci U S A*. Feb 7 2006;103(6):1953-8. doi:10.1073/pnas.0509386103
367. Giasson BI, Forman MS, Higuchi M, et al. Initiation and synergistic fibrillization of tau and alpha-synuclein. *Science*. Apr 25 2003;300(5619):636-40. doi:10.1126/science.1082324

368. Ono K, Takahashi R, Ikeda T, Yamada M. Cross-seeding effects of amyloid beta-protein and alpha-synuclein. *J Neurochem*. Sep 2012;122(5):883-90. doi:10.1111/j.1471-4159.2012.07847.x
369. Chen DD, Gao LP, Wu YZ, et al. Accumulation of Prion and Abnormal Prion Protein Induces Hyperphosphorylation of alpha-Synuclein in the Brain Tissues from Prion Diseases and in the Cultured Cells. *ACS Chem Neurosci*. Oct 20 2021;12(20):3838-3854. doi:10.1021/acschemneuro.1c00240
370. Guerrero-Ferreira R, Taylor NM, Arteni AA, et al. Two new polymorphic structures of human full-length alpha-synuclein fibrils solved by cryo-electron microscopy. *Elife*. Dec 9 2019;8doi:10.7554/eLife.48907
371. Soto C, Castano EM. The conformation of Alzheimer's beta peptide determines the rate of amyloid formation and its resistance to proteolysis. *Biochem J*. Mar 1 1996;314 (Pt 2):701-7. doi:10.1042/bj3140701
372. Morozova OA, March ZM, Robinson AS, Colby DW. Conformational features of tau fibrils from Alzheimer's disease brain are faithfully propagated by unmodified recombinant protein. *Biochemistry*. Oct 8 2013;52(40):6960-7. doi:10.1021/bi400866w
373. Tomoda H, Kishimoto Y, Lee YC. Temperature effect on endocytosis and exocytosis by rabbit alveolar macrophages. *J Biol Chem*. Sep 15 1989;264(26):15445-50.
374. McKinley MP, Taraboulos A, Kenaga L, et al. Ultrastructural localization of scrapie prion proteins in cytoplasmic vesicles of infected cultured cells. *Lab Invest*. Dec 1991;65(6):622-30.